



LUND UNIVERSITY

Temperature - Time Curves of Complete Process of Fire Development

Magnusson, Sven Erik; Thelandersson, Sven

1970

[Link to publication](#)

Citation for published version (APA):

Magnusson, S. E., & Thelandersson, S. (1970). *Temperature - Time Curves of Complete Process of Fire Development*. (Bulletin of Division of Structural Mechanics and Concrete Construction, Bulletin 16; Vol. Bulletin 16). Lund Institute of Technology.

Total number of authors:

2

General rights

Unless other specific re-use rights are stated the following general rights apply:

Copyright and moral rights for the publications made accessible in the public portal are retained by the authors and/or other copyright owners and it is a condition of accessing publications that users recognise and abide by the legal requirements associated with these rights.

- Users may download and print one copy of any publication from the public portal for the purpose of private study or research.
- You may not further distribute the material or use it for any profit-making activity or commercial gain
- You may freely distribute the URL identifying the publication in the public portal

Read more about Creative commons licenses: <https://creativecommons.org/licenses/>

Take down policy

If you believe that this document breaches copyright please contact us providing details, and we will remove access to the work immediately and investigate your claim.

LUND UNIVERSITY

PO Box 117
221 00 Lund
+46 46-222 00 00

BYGGNADSSTATIK

REFERENS

S. E. MAGNUSSON and S. THELANDERSSON

**TEMPERATURE-TIME CURVES OF COMPLETE
PROCESS OF FIRE DEVELOPMENT**

Ci 65

UDC 614.841.4

ACTA POLYTECHNICA SCANDINAVICA

CIVIL ENGINEERING AND BUILDING CONSTRUCTION SERIES
No. 65

Temperature—Time Curves of Complete Process of Fire Development

Theoretical Study of Wood Fuel Fires in Enclosed Spaces

S. E. MAGNUSSON and S. THELANDERSSON

Division of Structural Mechanics and
Concrete Construction
Lund Institute of Technology
Lund, Sweden

STOCKHOLM 1970

Printed in Sweden by
Elanders Boktryckeri AB Göteborg 1970

Table of contents

Principal notations	5
1. Introduction	8
2. Equation of heat balance of process of fire development	17
3. Study of combustion gas flow and heat flow through openings in enclosed spaces	27
Flow conditions in vertical rectangular opening in enclosed space	28
Deduction of maximum rate of combustion determined by rate of air supply in accordance with [5]	30
Determination of quantity of heat, I_L , withdrawn per unit time through openings in enclosed space during the whole process of fire development	31
Modification of treatment in cases where enclosed spaces are provided with several openings which differ in height	34
Modification of treatment in cases where enclosed spaces are provided with horizontal openings in roofs	34
4. Description of programme for digital computer	39
5. Calculation of time graphs of rate of combustion for some full-scale tests described in literature	42
Test Series A. Tests carried out by Sjölin. Calculation of time graphs of rate of combustion	44
Test Series B. Tests made by Kawagoe [5]. Calculation of time graphs of rate of combustion	46
Test Series C. Tests published by Ödeen [18]. Calculation of time graphs of rate of combustion	48
Test Series D. Tests made at the National Swedish Institute for Materials Testing. Calculation of time graphs of rate of combustion	55
Summary	57
6. Determination of general time graphs of quantity of energy released per unit time during different phases of process of fire development	61
7. Calculation of time graphs of temperature of combustion gases for characteristic types of enclosed spaces	64
8. Summary	76

Acknowledgements	79
References	80
Appendix 1. Time graphs of energy released per unit time and corresponding theoretically calculated time graphs of temperature of combustion gases. Test Series A	84
Appendix 2. Time graphs of energy released per unit time and corresponding theoretically calculated time graphs of temperature of combustion gases. Test Series B	89
Appendix 3. Time graphs of energy released per unit time and corresponding theoretically calculated time graphs of temperature of combustion gases. Test Series C	91
Appendix 4. Time graphs of energy released per unit time and corresponding theoretically calculated time graphs of temperature of combustion gases. Test Series D	100
Appendix 5. Calculated time graphs of temperature of combustion gases for seven types of enclosed spaces differing in opening factor and in bounding structures	103
Appendix 6. Calculated time graphs of temperature of combustion gases represented in tabular form for seven types of enclosed spaces differing in opening factor and in bounding structures	129

Principal notations

A	Area of vertical openings in the enclosed space	m^2
A_h	Area of horizontal openings in the enclosed space	m^2
A_t	Total bounding surface area of the enclosed space	m^2
$(A \cdot \sqrt{H})$	Air flow factor (Ventilation factor)	$m^{5/2}$
$(A \cdot \sqrt{H}/A_t)$	Opening factor	$m^{1/2}$
B	Width of an opening in the enclosed space	m
G	Volume of combustion gases produced per unit weight of fuel	$m^3 \cdot kg^{-1}$
G_0	Volume of combustion gases (expressed in Nm^3) produced per unit weight of fuel	$Nm^3 \cdot kg^{-1}$
H	Height of vertical opening in the enclosed space	m
H'	Height of vertical opening below the neutral zone level in the enclosed space	m
H''	Height of vertical opening above the neutral zone level in the enclosed space	m
I	Enthalpy	$kcal \cdot m^{-3}$
I_C	Heat energy released per unit time during combustion	$kcal \cdot h^{-1}$
I_B	Heat energy stored per unit time in the gas volume which is contained in the enclosed space	$kcal \cdot h^{-1}$
I_L	Heat energy withdrawn per unit time from the enclosed space owing to the replacement of hot gases by cold air	$kcal \cdot h^{-1}$
I_R	Heat energy withdrawn per unit time from the enclosed space by radiation through openings in the enclosed space	$kcal \cdot h^{-1}$

I_w	Heat energy withdrawn per unit time from the enclosed space through wall, roof or ceiling, and floor structures	$\text{kcal} \cdot \text{h}^{-1}$
L	Quantity of air consumed per unit weight of fuel during combustion	$\text{Nm}^3 \cdot \text{kg}^{-1}$
M	Quantity of combustible material	kg
P	Static pressure	$\text{kg} \cdot \text{m}^{-2}$
Q_{out}	Rate of flow of the outgoing gases through a vertical opening in the enclosed space	$\text{kg} \cdot \text{h}^{-1}$
Q_{in}	Rate of flow of the incoming air through a vertical opening in the enclosed space	$\text{kg} \cdot \text{h}^{-1}$
Q_h	Rate of flow of the outgoing gases through a horizontal opening in the enclosed space	$\text{kg} \cdot \text{h}^{-1}$
Q	Rate of flow of air supplied to the enclosed space by means of fans	$\text{m}^3 \cdot \text{s}^{-1}$
R	Rate of combustion	$\text{kg of wood per unit time}$
R_{max}	Maximum rate of combustion determined by the rate of air supply	$\text{kg of wood per unit time}$
T	Duration of the fire defined as the duration of the flame phase	h
W	Heat value of the fuel	$\text{kcal} \cdot \text{kg}^{-1}$
c	Specific heat	$\text{kcal} \cdot \text{m}^{-3} \cdot ^\circ\text{C}^{-1}$
c_p	Specific heat of the combustion gases	$\text{kcal} \cdot \text{m}^{-3} \cdot ^\circ\text{C}^{-1}$
g	Acceleration of gravity	$\text{m} \cdot \text{s}^{-2}$
h	Difference in level between the centre of a vertical opening and a horizontal opening	m
h'	Difference in level between the neutral zone and a horizontal opening	m
q	Fire load	$\text{Mcal} \cdot \text{m}^{-2}$ of bounding surface area
r	Hydraulic radius	cm
v_y, v_z	Velocity of flow	$\text{m} \cdot \text{h}^{-1}$
v_h	Velocity of flow through a horizontal opening in the enclosed space	$\text{m} \cdot \text{h}^{-1}$
t	Time co-ordinate	h
x	Position co-ordinate	m
α_i	Coefficient of heat transfer at a surface exposed to fire (internal surface)	$\text{kcal} \cdot \text{m}^{-2} \cdot \text{h}^{-1} \cdot ^\circ\text{C}^{-1}$

α_u	Coefficient of heat transfer at a surface not exposed to fire (external surface)	$\text{kcal} \cdot \text{m}^{-2} \cdot \text{h}^{-1} \cdot \text{°C}^{-1}$
γ	Weight per unit volume	$\text{kg} \cdot \text{m}^{-3}$
ε_{res}	Resultant emissivity for radiation between flames, combustion gases, and a surface exposed to fire (internal surface)	
ε_{fl}	Emissivity of flames	
ε_i	Emissivity of a surface exposed to fire	
ϑ	Temperature	°C
ϑ_o	Temperature of the outside air	°C
ϑ_g	Temperature of the combustion gases	°C
ϑ_i	Temperature of a surface exposed to fire (internal surface)	°C
ϑ_u	Temperature of a surface not exposed to fire (external surface)	°C
$\Delta\vartheta$	Temperature difference between the combustion gases and the outside air	°C
λ	Thermal conductivity	$\text{kcal} \cdot \text{m}^{-1} \cdot \text{h}^{-1} \cdot \text{°C}^{-1}$
μ	Coefficient of contraction	
ρ	Density	$\text{kg} \cdot \text{m}^{-3}$
ρ_o	Density of the outside air	$\text{kg} \cdot \text{m}^{-3}$
ρ_g	Density of the combustion gases	$\text{kg} \cdot \text{m}^{-3}$

1. Introduction

The efforts made during the past decade in the field of structural fire engineering research have paved the way for differentiated, functionally correct structural fire engineering design carried out on the basis of theoretical calculations. This was rendered possible by investigations which can on the whole be classified in one or several of the main groups enumerated below. At the same time, these groups may be regarded as the essential stages or steps in an appropriate procedure for fire engineering design of load-bearing and separating structures [1].

(a) Determination of the characteristics of the fire load in an enclosed space under exposure to fire.

(b) Study of the variations in the development of energy, in the requisite air supply, and in the evolution of gases, with the time in the course of a fire. Determination of the temperature of the combustion gases in the enclosed space as a function of the time.

(c) Determination of the thermal properties of the materials used for structures in the temperature range which is of interest in connection with fires.

(d) Determination of the non-stationary temperature fields which are produced in a fire-exposed structure on the assumption that the temperature-time curve for the combustion gases is given, cf. (b).

(e) Determination of the structural behaviour and the load-bearing capacity of a fire-exposed structure on the basis of the temperature fields defined under (d), and with the help of the available information on those changes in the strength and deformation characteristics of the materials which take place under such conditions.

The object of the present investigation is to make a close study of the stage (b) in order to determine the complete temperature-time curve for the gaseous products of combustion under different conditions, and in particular the temperature-time curve in the cooling phase,¹⁾ for fires of the wood fuel type in enclosed spaces.

¹⁾ The characteristics of the different phases of the process of fire development are represented in Fig. 1. The term "cooling phase" will be used in this publication to designate the smoulder phase and the cooling phase taken together.

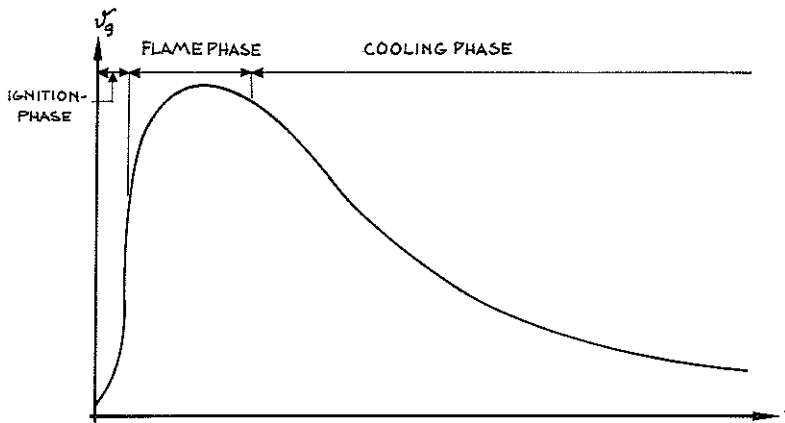


Fig. 1. Phases of the process of fire development as defined in the present publication. The definition in [1] distinguishes between a smoulder phase and a cooling phase, which are here regarded as a single phase designated by the term "cooling phase".

The present state of research in this field is clearly reflected in the sections dealing with fire protection in the Swedish Building Regulations 1967 (abbreviated SBR 67) and in the Draft Specification "Aluminium Structures". In comparison with the relevant regulations which are in force in most other countries, the Swedish rules represent substantial progress on the road to judicious structural fire engineering design. This is primarily due to the fact, that, when the designer has to choose that temperature-time curve which characterises the process of fire development, and which must serve as a basis for all theoretical structural fire engineering design, these rules enables the designer to be guided by all the results, which have been obtained from research in this field during recent years.

On an international plane, it is found that standard temperature-time curves for the process of fire development have been adopted in several countries [1]. If the fuel supply is unlimited, then the agreement between these curves is relatively close, see Fig. 2 a. Under practical conditions, when the fuel supply is limited, the standard specifications used in various countries stipulate that the variation in the temperature with the time shall be in conformity with the standard curve during a certain definite period of time, which is designated by the term "duration of the fire", T , and is defined as the duration of the flame phase. A comparison of the relations between the duration of the fire and the fire load which are employed in various countries is represented in Fig. 2 b [1]. This comparison shows very great differences in an assumption which is fundamental for structural fire engineering design. The wide dispersion between the curves reproduced in Fig. 2 b indicates that there exists no univalued relation between the fire load and the duration of the fire. Concerning

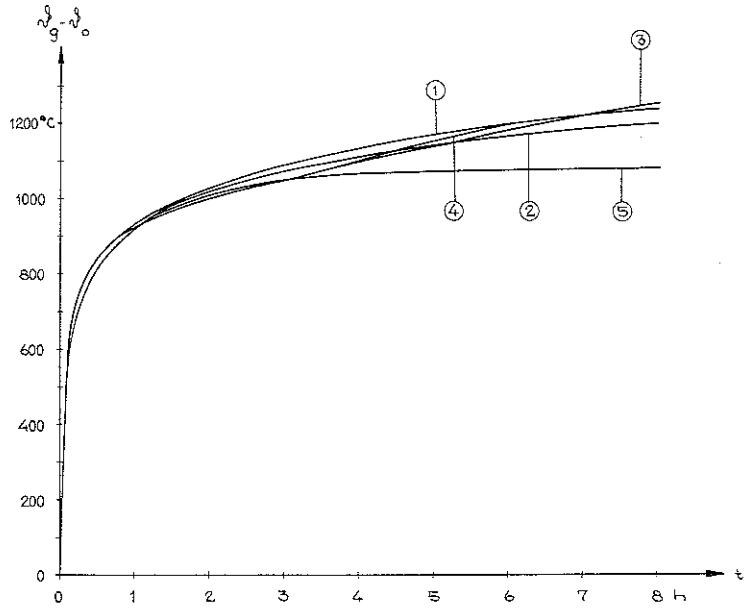


Fig. 2a. Standard curves used in some countries to represent the variation in the temperature, ϑ , in an enclosed space exposed to fire with the time, t . The symbol ϑ_0 denotes the temperature in the enclosed space at the time $t=0$.

1. ISO/TC 92; INSTA 28/2; DIN 4102-62.
2. EMPA, Switzerland.
3. ASTM 119 (1953), USA.
4. V 1076 (1955), Netherlands; BS 476 (1953), United Kingdom.
5. A 1304, Japan.

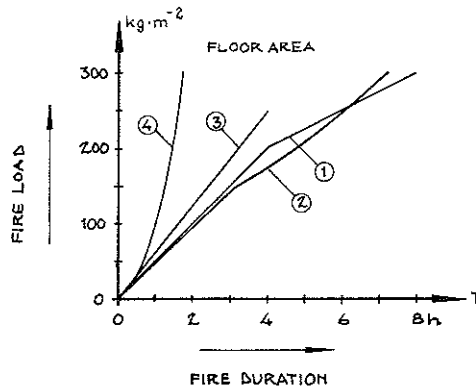


Fig. 2b. Relations between the fire load, in kg of wood per m^2 of floor area, and the duration of the fire, in h, which are stipulated in the standard specifications used in Sweden (Curve 1), United States of America (Curve 2), and United Kingdom (Curve 3), as well as in a Swiss draft standard specification (Curve 4).

the cooling phase of the process of fire development, it should be noted that it is as a rule completely disregarded.

The relevant Swedish standard specifications provide the designer with three alternative methods of design. Just as in other countries, it is permissible to carry out the design in a roughly simplified and stereotyped manner by using Curve 1 in Fig. 2 a as a point of departure. For the flame phase, this curve gives the temperature of the combustion gases, ϑ_g , in the enclosed space in accordance with the equation

$$\vartheta_g - \vartheta_0 = 1325 - 430 e^{-0.2t} - 270 e^{-1.7t} - 635 e^{-19t} \quad (1.1)$$

where t is the time, in hours, and ϑ_0 is the temperature in the enclosed space at the time $t=0$. The differences in the combustion characteristics of various fuels, or the fact that the rate of combustion varies within wide limits with the dimensions of the openings in the enclosed space, are not taken into account in this equation. The above-mentioned curve is closely in agreement with that temperature-time curve which is recommended by the ISO for fire tests on building components.

Alternatively, for certain definite types of fire loads and enclosed spaces, the designer may use a method which is simplified, but is nevertheless more differentiated, in comparison with the design procedure outlined in the above. The applicability of this alternative method presupposes that it is possible to comply with the two necessary conditions which are stated in what follows. In the first place, it is required to demonstrate that the characteristics of the fire load in respect of rate of combustion and radiation are approximately in accordance with those which apply in the case of wood fuel. In the second place, it is stipulated that the opening factor of the enclosed space, which is given by the expression $A\sqrt{H}/A_t$, where A is the total opening area of windows and doors, in m^2 , H is a weighted average of the vertical dimensions of these openings, in m , and A_t is the total area of the surfaces bounding the enclosed space, in m^2 , shall be known during all phases of the process of fire development. If these two conditions are satisfied, then it is allowed to carry out the design on the basis of a specific curve representing the variation in the temperature of the combustion gases in the enclosed space, ϑ_g , with the time. For the flame phase, this curve is determined by the opening factor, see Fig. 2 c, in the course of the duration of the fire, T , which is defined by the equation

$$T = qA_t / (25A\sqrt{H}) \quad \text{min} \quad (1.2)$$

where q is the fire load, in $\text{Mcal} \cdot \text{m}^{-2}$ of bounding surface area. The dash-line curve represents the INSTA curve expressed by Eq. (1.1).

Finally, and generally, in the cases where the quantities of combustible materials which constitute the fire load, as well as the rate of combustion, are accurately known, the above-mentioned two Swedish specifications allow

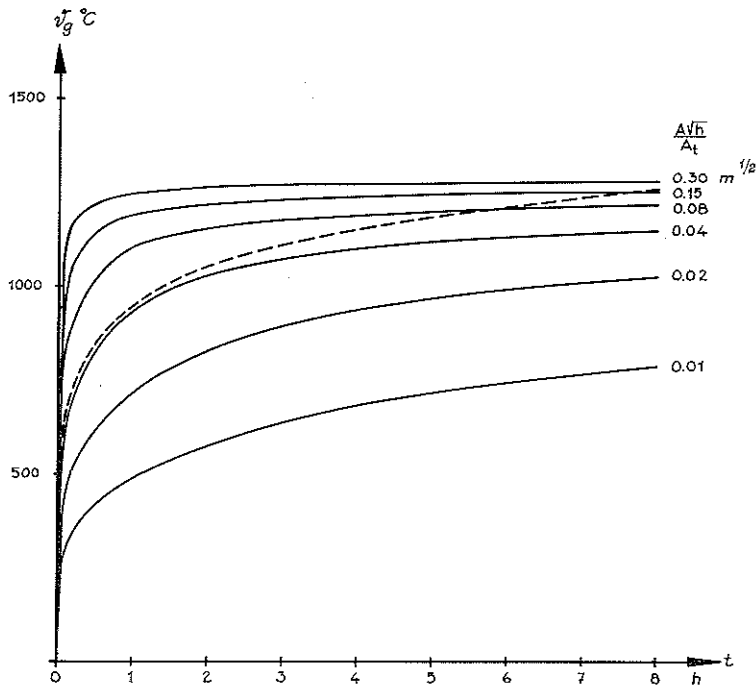


Fig. 2c. Variation in the temperature of the combustion gases, ϑ_g , with the time, t , at different values of the opening factor, $A \cdot \sqrt{H}/A_t$. Curves published in the Swedish Building Regulations 1967 (SBR 67) and in the Swedish draft specification "Aluminium Structures". The dash-line curve is the standard curve calculated by means of Eq. (1.1).

the fire resistance of a building component to be determined on the basis of the variation in the temperature of the combustion gases with the time, calculated with the help of the formula which is known as the equation of heat balance. This equation, which constitutes a fundamental description of the energy balance of the process of fire development, and hence also serves as a basis for Eq. (1.2), will be discussed at some length in Chapter 2.

What has been said up to this point relates only to the ignition and flame phases of the process of fire development. As regards the cooling phase, it is stipulated in a summary manner merely that the time graph of the temperature of the combustion gases shall be chosen so as to be linear, and that the rate of decrease in the gas temperature shall be taken to be $10^\circ\text{C} \cdot \text{min}^{-1}$, unless other assumptions can be demonstrated to be more correct. If the design is carried out by means of the second or third alternative method, each of which is functionally realistic, then this implies that two phases of the same continuous process are represented in such a way that their descriptions are entirely different in the degree of accuracy as well as in the extent to which the actual conditions are taken into account. It is obvious that this gives

rise to a considerable unbalance in the basis for design. To show how important it is that the cooling phase should also be described in a differentiated manner, it may be useful to give two examples of structural members which are characterised by low and high thermal inertia, respectively.

For an enclosed space, where the fire load is $q = 12 \text{ Mcal} \cdot \text{m}^{-2}$ of bounding surface area, and the opening factor is $A\sqrt{H}/A_t = 0.08 \text{ m}^{0.5}$, Fig. 3 represents a calculated temperature-time curve for a steel column exposed to fire and characterized by the ratio $F_s/V_s = 100 \text{ m}^{-1}$ and by $\epsilon_r = 0.5$, where F_s is the total bounding surface area of the column, which is equal to its fire-exposed area, in m^2 , V_s is the steel volume of the column, in m^3 , and ϵ_r is the resultant emissivity for heat transfer from the flames and the combustion gases to the

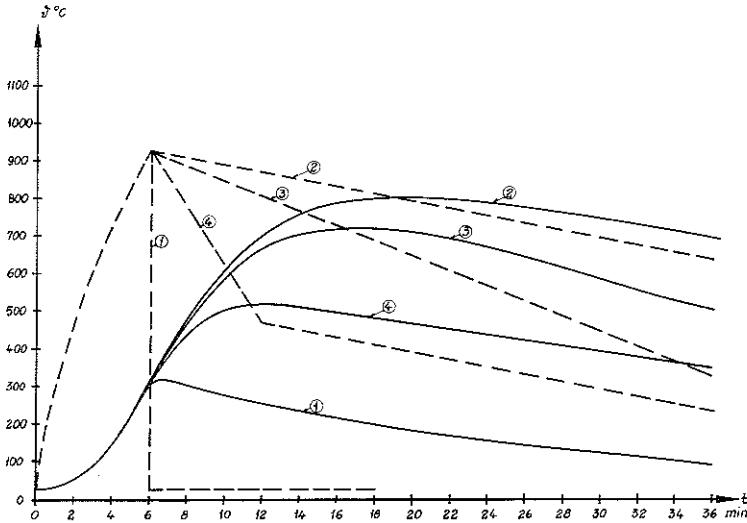


Fig. 3. Variation in the temperature, ϑ_s , of a steel column with the time, t , calculated on the basis of temperature-time curves, which differ in shape during the cooling phase (dash-line curves).

F_s/V_s = Ratio, in m^{-1} , of the fire-exposed surface area, i.e. the total bounding surface area, of the column to the steel volume of the column.

ϵ_r = Resultant emissivity.

— ϑ_s

----- ϑ_g at $A\sqrt{H}/A_t = 0.08 \text{ m}^{1/2}$.

$q = 12 \text{ Mcal} \cdot \text{m}^2$.

1. Instantaneous cooling. Rate of decrease in temperature $\infty^\circ\text{C} \cdot \text{h}^{-1}$.

2. Linear rate of decrease in temperature, $600^\circ\text{C} \cdot \text{h}^{-1}$.

3. Linear rate of decrease in temperature, $1200^\circ\text{C} \cdot \text{h}^{-1}$.

4. Linear rate of decrease in temperature, $6 \text{ min} \leq t \leq 12 \text{ min}$, $4600^\circ\text{C} \cdot \text{h}^{-1}$; $t \geq 12 \text{ min}$, $600^\circ\text{C} \cdot \text{h}^{-1}$.

$F_s/V_s = 100 \text{ m}^{-1}$ $\epsilon_r = 0.5$.

steel column. The characteristics of the flame phase for the temperature-time curve of the enclosed space have been chosen in conformity with the Swedish Building Regulations 1967. In Fig. 3, the full-line curves represent the temperature of the steel, ϑ_s , and the dash-line curves show the temperature of the combustion gases, ϑ_g , on the basis of the four alternative assumptions concerning the cooling phase of the process of fire development which are stated in what follows.

(1) After the duration of the fire $T = qA_i / (25A\sqrt{H}) = 6$ min, the temperature of the combustion gases drops instantaneously to ordinary room temperature.

(2) The temperature of the combustion gases decreases in accordance with the Swedish Building Regulations 1967 at a linear rate of $10^\circ\text{C} \cdot \text{min}^{-1}$.

(3) The temperature of the combustion gases decreases at a linear rate of $20^\circ\text{C} \cdot \text{min}^{-1}$.

(4) The temperature of the combustion gases is assumed to vary in a more realistic manner, that is to say, it drops to half their maximum temperature during the first 6 min of the cooling phase, and then decreases at a linear rate of $10^\circ\text{C} \cdot \text{min}^{-1}$.

At the end of the flame phase, the temperature of the steel is 303°C . After that, the temperature of the steel continues to increase during the cooling phase of the process of fire development to its respective maximum values corresponding to the four alternative assumptions, viz., 303 , 799 , 719 , and 518°C .

Fig. 4 shows the effects on the load-bearing capacity of a reinforced concrete slab which are produced by different slopes of the linear cooling phase of the time-temperature curves. Each T -value on the horizontal axis corresponds to a specific time-temperature curve. T is the duration of the flame phase, and depends on the fire load. The distance from the centre lines of the reinforcing bars to the fire-exposed surface of the slab, is assumed to be 2 cm. The emissivity of the flames is taken to be 0.7. The temperature in the enclosed space is supposed to vary with the time during the flame phase in accordance with Eq. (1.1). The temperature of the combustion gases is assumed to decrease at linear rates of 5, 10, and $20^\circ\text{C} \cdot \text{min}^{-1}$, or to drop instantaneously to ordinary room temperature ($\infty^\circ\text{C} \cdot \text{h}^{-1}$). For a static load which causes failure at a temperature of the reinforcing bars $\vartheta_{scr} = 450^\circ\text{C}$, we obtain a fire resistance period, t_{fr} , which varies from 0.52 to 0.82 h, and for $\vartheta_{scr} = 500^\circ\text{C}$, the corresponding variation in the fire resistance period ranges from 0.72 to 1.01 h.

These examples show that it is necessary to calculate the fire resistance period of a building component so as to take account of that reduction in its load-bearing capacity, or in its separating capacity, which occurs during the cooling phase. Moreover, they indicate that those temperature-time curves for enclosed spaces which are to serve as a basis for such calculations should also be differentiated and as realistic as possible in the cooling phase.

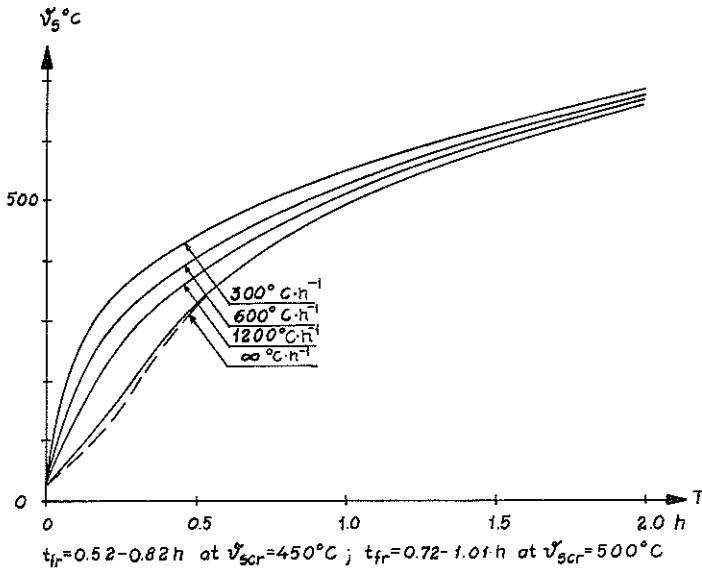


Fig. 4. Relation between the calculated *maximum* temperature, ϑ_s , of the reinforcing steel in a concrete slab, 18 cm in thickness, exposed to fire on one side, and the duration, T , of the flame phase of the process of fire development. This relation is represented for different values of the fire load and for different slopes of the linear cooling phase of the temperature-time curve.

————— Cooling phase taken into account.

----- Cooling phase not taken into account.

Concrete cover 2 cm.

ε_{fl} = Emissivity of the flames = 0.7.

t_{fr} = Fire resistance period.

ϑ_{scr} = Critical temperature of the steel, i.e. the temperature at which the reinforcement fails.

$t_{fr} = 0.52$ to 0.82 h at $\vartheta_{scr} = 450^\circ\text{C}$.

$t_{fr} = 0.72$ to 1.01 h at $\vartheta_{scr} = 500^\circ\text{C}$.

The object of the present investigation is therefore to evolve a method which shall be applicable to different combinations of the values of the air flow factor (ventilation factor), $A\sqrt{H}$, and the fire load, as well as the type of material of the structures bounding the enclosed space under exposure to fire of the wood fuel type. This shall enable that the temperature-time curves for the enclosed space to be calculated by means of a theoretical procedure so as to cover the whole process of fire development, and shall thus make it possible to carry out judicious structural fire engineering design on the basis of the variation in the temperature with the time during all phases of the fire.

In connection with a general treatment of the equation of heat balance, Chapter 2 deals with the problems which are met with when a theoretical calculation of the temperature-time curve for the combustion gases is extended so as to comprise the cooling phase. Chapter 3 describes the methods which

have been used to tackle these problems, and the modifications of the equation of heat balance which have been necessary for this purpose. In Chapter 4, an account is given of the computer programme which has been prepared for the calculations, and which is represented in the form of a flow chart. In Chapter 5, the full-scale tests which have served as a basis for the present investigation are subjected to comparative theoretical analysis. The time graphs of the rate of combustion which have been determined with the help of these theoretical analyses are presented in Chapter 6. Finally, in Chapter 7, these graphs are used as a basis for the calculation of complete temperature-time curves for combustion gases in enclosed spaces which vary in the values of the opening factor and the fire load, as well as in type of material employed in the structures bounding the enclosed space.

2. Equation of heat balance of process of fire development

The papers published by *Kawagoe* and *Sekine* [2], as well as by *Ödeen* [3], in the early 1960ies have made it possible to carry out theoretical calculations of temperature-time curves for combustion gases in the flame phase of the process of fire development to a degree of accuracy that is sufficient for practical purposes. These three authors have studied the energy balance during the process of fire development. The quantity of energy released per unit time, just as the volume of combustion gases evolved, during combustion were assumed to be known. With the help of the calculation of the quantity of energy which was lost per unit time by conduction and radiation from the enclosed space through its bounding structures, it was possible to deduce an equation of heat balance, and to solve it so as to obtain the temperature of the combustion gases. The treatment of this problem was based on the simplified assumptions which are reproduced in what follows.

(a) The temperature in the interior of the whole enclosed space is uniform at any given instant.

(b) The coefficient of heat transfer to the interior bounding surfaces of the enclosed space is uniform at every point.

(c) The heat flow through the bounding structures of the enclosed space is one-dimensional and, except for the window and door openings, if any, uniformly distributed.

Kawagoe and *Sekine*, as well as *Ödeen*, confined themselves throughout their papers to a study of the flame phase of the process of fire development, and the equation which they have deduced cannot be applied directly to the cooling phase. Primarily, the calculation of the temperature-time curve for the combustion gases during the cooling period requires an analytical investigation of two fundamental sub-problems, which have been but little studied up to the present time. In the first place, it is necessary to determine the quantity of energy liberated per unit time when this quantity, as is the case in the cooling phase, is no longer determined by the rate of air supply. In the second place, it is required to investigate the thermodynamic conditions which are encountered when the rate of combustion is no longer limited by the dimensions of the openings in the enclosed space. The equation of energy balance which has been deduced by *Kawagoe* and *Sekine* and by *Ödeen*, as

well as that extension of the theory which is required for the calculation of the temperature-time curve in the cooling phase of the process of fire development, will be dealt with in what follows.

The above-mentioned equation expresses for any given instant t , the balance between the respective quantities of heat energy generated and lost per unit time in the enclosed space under consideration. In its complete form, this equation is

$$I_C = I_L + I_W + I_R + I_B \quad (2.1)$$

where

- I_C = the heat energy released per unit time during combustion,
- I_L = the heat energy withdrawn per unit time from the enclosed space owing to the replacement of hot gases by cold air,
- I_W = the heat energy withdrawn per unit time from the enclosed space through wall, roof or ceiling, and floor structures,
- I_R = the heat energy withdrawn per unit time from the enclosed space by radiation through the openings in the enclosed space,
- I_B = the heat energy stored per unit time in the gas volume which is contained in the enclosed space.

The terms entering into the above equation are schematically illustrated in Fig. 5.

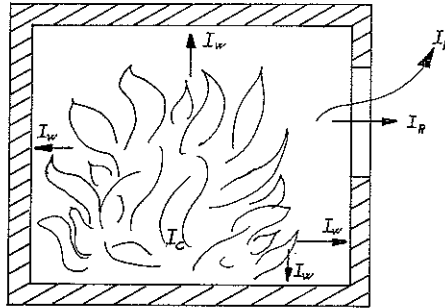


Fig. 5. Schematic illustration of the terms entering into the equation of heat balance.

Term I_B

In comparison with the quantities of energy which are involved in fires, the quantity of energy which can be stored in the gas volume contained in the enclosed space is of minor importance. Therefore, the term I_B can to a close approximation be put equal to zero.

Term I_C

In the case of fires of the wood fuel type, the term I_C , which expresses the quantity of heat released per unit time during combustion, is a factor which is difficult to determine in the equation of heat balance. In order to obtain this term, Kawagoe and Sekine, as well as Ödeen, chose as a point of departure the rate of combustion, expressed in terms of kilogrammes of wood per unit time, which they multiplied by a heat value.

This gives the equation

$$I_C = R \cdot W \quad \text{kcal} \cdot \text{h}^{-1} \quad (2.2)$$

where

R = the rate of combustion, in kg of wood per h,

W = the heat value, in kcal per kg of wood.

With the exception of a small number of calculations which were based on a triangular variation in the rate of combustion, R , with the time, Ödeen assumed that R is constant, and is arbitrarily chosen, and that the quantity of heat, W , released during the flame phase is 4120 kcal per kg of wood. Thus, the heat energy liberated per unit time during combustion, I_C , is supposed to remain constant until the fuel has burnt up, and the cooling phase is characterized by the fact that no additional energy is supplied to the enclosed space. This description of the quantity of energy developed per unit time is applicable to burning of liquid fuels, but does not take account of the real combustion characteristics of wood fuels. As a rule, these fuels give off 30 to 50 per cent of the total quantity of energy after the end of the flame phase.

The investigation made by Kawagoe and Sekine is more differentiated in respect of the characterization of the process of fire development. As Kawagoe had shown in an earlier paper [5], during that period of the fire when the rate of combustion reaches a maximum, i.e. during the flame phase, the rate of air supply to the enclosed space, and hence also the maximum rate of combustion, R_{\max} , are proportional to the air flow factor, $A\sqrt{H}$.

If the areas are expressed in m^2 , and the maximum rate of combustion, R_{\max} , is expressed in kg of wood per min, then we have the approximate relation

$$R_{\max} = 5.5 \cdot A\sqrt{H} \quad \text{kg of wood per min} \quad (2.3)$$

Furthermore, in the papers published by Kawagoe and Sekine, the quantity of heat liberated during the flame phase, W , is stated to be 2575 kcal per kg of wood. This value was obtained by reducing the nominal heat value of wood so as to take account of the degree of incomplete combustion. The degree of incomplete combustion was estimated with the help of those analyses of the composition of the combustion gases which were carried out during fire

tests [5]. As regards the cooling phase, Kawagoe and Sekine had made a few isolated comparative calculations based on a polygon-shaped time graph of the rate of combustion, and then found that the temperatures obtained when the cooling phase was characterized by a linear decrease in temperature at a rate of 7 or $10^{\circ}\text{C} \cdot \text{min}^{-1}$ were much too high.

Accordingly, if the results of the investigations made by Ödeen, as well as by Kawagoe and Sekine, are to be applied to fires where the fuel is of the wood type, then the calculations have to be confined to the flame phase of the process of fire development.

When the treatment of this problem is extended so as to comprise the cooling phase of the process of fire development, Eq. (2.3) is not generally applicable. For the quantity of energy released per unit time during combustion, Eq. (2.3), in combination with Eq. (2.2), gives only the theoretical upper limit, which is determined by the available rate of air supply. During the cooling phase, the energy liberated per unit time will be governed by other factors. For this reason, and since no systematic investigation has so far been made in order to determine the relations between the three quantities which are of interest in this connection, viz., the reduction in the weight of fuel, the quantity of energy developed per unit weight of fuel, and the requisite rate of air supply, the quantity of energy released per unit time during the cooling phase of the process of fire development had to be determined by means of the method described in what follows. The procedure in calculation for the solution of the equation of heat balance was programmed for a CD 3600 computer. A study of the literature was carried out in order to examine the available publications on full-scale tests. A number of these tests were selected in the cases where the reported data were so complete as to enable numerical treatment. After that, the computer was used to calculate the temperature-time curve on the basis of an assumed form of the time graph of the rate of combustion for the complete process of fire development. The time graph of the rate of combustion was then varied until the agreement between the experimental and theoretical temperature-time curves was as close as possible. The only absolute requirement to be fulfilled in this connection was that the total quantity of energy liberated during the whole process of fire development should be equal to the total energy of combustion of the fuel. When an adequate range of variation in the opening factor and in the fire load was considered to have been covered, the time graphs of the rate of combustion obtained in this way were systematized. For a given fire load and a given opening factor, it was then possible to assume that the curve showing the variation in the rate of combustion with the time was known on the basis of this systematization. The investigation referred to in the above is described in Chapter 5, and its results, expressed in terms of time graphs of the rate of combustion in a dimensionless form, are presented in Chapter 6.

In connection with the treatment of the term I_C , it should be pointed out that the fire load must be described in combustion engineering terms in such a way that it may be associated with the equation of heat balance, Eq. (2.1).

In most countries, the fire load is expressed in terms of the quantity of wood that is equivalent to it in heat value per unit *floor area*. This characterization must be replaced by a parameter which has a physical significance when it is treated in calculations. This has been done in the Swedish Building Regulations 1967 and in the Draft Specification "Aluminium Structures", which stipulate that the fire load shall be stated as that total quantity of heat, q , in $\text{Mcal} \cdot \text{m}^{-2}$ of total bounding surface area of the enclosed space exposed to fire, which is liberated on the assumption of complete combustion of all the combustible material contained in the enclosed space. A still more refined description of the fire load, which should take into account the variation with the time in the quantity of energy released by combustion, as well as the emissivities of the flames and the combustion gases, is an urgently recommended subject for research in this field.

Term I_L

The term I_L in the equation of heat balance expresses that quantity of heat which is withdrawn per unit time from the enclosed space owing to the replacement of hot gases by cold air through the openings in the enclosed space. For the determination of I_L , Ödeen, as well as Kawagoe and Sekine, used the equation

$$I_L = R \cdot G_0 \cdot (\vartheta_g - \vartheta_0) \cdot c_p \quad (2.4)$$

where

R = the rate of combustion, in kg of wood per h,

G_0 = the volume of combustion gases produced by the fire, in $\text{Nm}^3 \cdot \text{kg}^{-1}$ of fuel,¹⁾

c_p = the specific heat of the combustion gases, in $\text{kcal} \cdot \text{Nm}^{-3} \cdot ^\circ\text{C}^{-1}$,

ϑ_g = the temperature of the combustion gases, in $^\circ\text{C}$,

ϑ_0 = the temperature of the air outside the enclosed space, in $^\circ\text{C}$.

Eq. (2.4) states that the term I_L is put equal to the heat content of the combustion gases produced by the fire with reference to that of the outside air. On account of the difference in density between the cold outside air and the hot gases in the interior of the enclosed space, an exchange of heat by convection takes place in the openings of the enclosed space. The rate of this heat exchange determines the maximum value of the rate of combustion so far as the supply of oxygen is concerned. Therefore, Eq. (2.4) can be used as an expression for I_L when the rate of combustion is determined by the rate

¹⁾ Nm^3 = normal cubic metre = the quantity of a gas which occupies a volume of 1 cubic metre at 0°C and 760 mm barometric pressure.

of air supply, in spite of the fact that this equation in itself does not describe I_L , but expresses the heat content of the combustion gases produced by the fire. However, if the rate of combustion is limited by factors other than the rate of air supply, e.g. by the available quantity of fuel, or if the combustion is completed, then it is obvious that Eq. (2.4) does not hold good. Accordingly, a theoretical treatment of the cooling phase of the process of fire development requires an expression for I_L which is more generally applicable, and which is based on the rate of air exchange. This problem has been studied in a thesis for degree of Master of Engineering prepared by *Ahlquist* and *Thelandersson* [6], in the Division of Structural Mechanics and Concrete Construction, Lund Institute of Technology, Lund, Sweden. These authors based their study on the assumption that the static pressure distribution in the enclosed space varies linearly from the floor to the ceiling or roof, and that there exists a level (the neutral layer) at which the pressure in the enclosed space is equal to the pressure outside the enclosed space. This simplified model has been used by several authors, e.g. by *Kawagoe* [5] in the theoretical deduction of Eq. (2.3), and by *Thomas* [7] in studies which dealt with venting in the course of fires. In this connection, *Kawagoe* showed by means of a number of tests that the assumed pressure was actually applicable to a close approximation. On the assumption that the openings in the enclosed space are vertical only, *Kawagoe* used Bernoulli's equation to determine the quantities of outgoing combustion gases and incoming cold air as functions of the difference in temperature and the position of the neutral layer. On the basis of the condition that the difference between the quantities of gases flowing into and out of the enclosed space shall be equal to the difference between the quantities of gases produced and consumed by combustion, *Ahlquist* and *Thelandersson* calculated the position of the neutral layer as a function of the temperature and the rate of combustion. In this calculation, it was assumed that the rate of combustion may vary from zero to a maximum value, which is dependent on the dimensions of the openings. Furthermore, it was assumed that the liberation of a certain definite quantity of energy is associated with the consumption of the same quantity of air and the production of the same quantity of combustion gases, irrespective of the rate of combustion.

After the position of the neutral layer had been determined in this way, it was possible to obtain an expression for I_L at different values of the temperature and the rate of combustion. In the above-mentioned thesis [6], the treatment was also extended so as to comprise the modifications which are necessary when the enclosed space is provided with a vent. The deduction of the equations which are required for this purpose is reproduced in its main features in Chapter 3 of the present publication. Moreover, this chapter also contains a summary treatment of the case where the roof of the enclosed space is provided with horizontal openings.

Term I_W

The term I_W denotes the quantity of heat which is withdrawn per unit time from the enclosed space through the structures bounding this space. The term I_W is determined by solving the general equation of heat conduction in the one-dimensional case under non-steady flow conditions so as to take into account those thermal properties of the materials which are dependent on the temperature, the evaporation of occluded water, and the possible structural transformations in the materials entering into the bounding structures. This equation is

$$c \cdot \gamma \cdot \frac{\partial \vartheta}{\partial t} = \frac{\partial}{\partial x} \left(\lambda_x \cdot \frac{\partial \vartheta}{\partial x} \right) \quad (2.5)$$

where

- c = the specific heat of the wall material,
- γ = the weight per unit volume of the wall material,
- λ_x = the thermal conductivity of the wall material,
- ϑ = the temperature in the interior of the wall material,
- t = the time,
- x = the position co-ordinate.

The above equation is solved by means of a numerical procedure which had been described by *Odemark* [8], among others, and which has subsequently been further developed by *Ödeen*, and others, [9]. The walls, ceiling, roof, and floor structures which bound the enclosed space are divided into n layers having the thickness Δx_k each, and the equation of heat balance is written for each one of these layers. If the temperature at the centre of the layer k at the time t is denoted by ϑ_k , and that at the time $t + \Delta t$ is designated by $\vartheta_k + \Delta \vartheta_k$, then the application of this procedure gives the relations

$$\left. \begin{aligned} \varphi_1 \cdot \frac{\Delta \vartheta_1}{\Delta t} &= \psi_1(\vartheta_g - \vartheta_1) - \psi_2(\vartheta_1 - \vartheta_2) \\ &\vdots \\ \varphi_k \cdot \frac{\Delta \vartheta_k}{\Delta t} &= \psi_k(\vartheta_{k-1} - \vartheta_k) - \psi_{k+1}(\vartheta_k - \vartheta_{k+1}) \\ &\vdots \\ \varphi_n \cdot \frac{\Delta \vartheta_n}{\Delta t} &= \psi_n(\vartheta_{n-1} - \vartheta_n) - \psi_{n+1}(\vartheta_n - \vartheta_0) \end{aligned} \right\} \quad (2.6)$$

where

ϑ_g = the temperature of the gases in the enclosed space,

ϑ_o = the temperature of the outside air,

$\varphi_k = \Delta x_k \cdot c(x, \vartheta) \cdot \gamma$

$$\psi_1 = \frac{1}{\frac{1}{\alpha_i(\vartheta)} + \frac{\Delta x_1}{2 \cdot \lambda(x, \vartheta)}}$$

·
·
·

$$\psi_k = \frac{1}{\frac{\Delta x_{k-1}}{2 \cdot \lambda(x, \vartheta)} + \frac{\Delta x_k}{2 \cdot \lambda(x, \vartheta)}}$$

·
·
·

$$\psi_{n+1} = \frac{1}{\frac{\Delta x_n}{2 \cdot \lambda(x, \vartheta)} + \frac{1}{\alpha_u(\vartheta)}}$$

where

$\alpha_i(\vartheta)$ = the coefficient of heat transfer at the internal surface,

$\alpha_u(\vartheta)$ = the coefficient of heat transfer at the external surface,

$\lambda(x, \vartheta)$ = the thermal conductivity at the section x ,

$c(x, \vartheta)$ = the specific heat at the section x ,

γ = the weight per unit volume at the section x .

The coefficient of heat transfer, α_i , at the internal surface exposed to fire may be supposed to consist of two components, viz., first, a radiation component, which is markedly predominant at the high temperatures in question, and second, a convection component, which can be chosen with adequate accuracy so as to be constant, and to be equal to $20 \text{ kcal} \cdot \text{m}^{-2} \cdot \text{h}^{-1} \cdot \text{°C}^{-1}$ [9]. By applying the Stefan-Boltzmann law, this gives, for α_i , the relation

$$\alpha_i = \frac{4.96 \cdot \varepsilon_{res}}{\vartheta_g - \vartheta_i} \left[\left(\frac{\vartheta_g + 273}{100} \right)^4 - \left(\frac{\vartheta_i + 273}{100} \right)^4 \right] + 20 \text{ kcal} \cdot \text{m}^{-2} \cdot \text{h}^{-1} \cdot \text{°C}^{-1} \quad (2.7a)$$

where

ϑ_i = the temperature of the internal surface,

ε_{res} = the resultant emissivity for radiation between flames, combustion gases, and the internal surface.

The resultant emissivity, ε_{res} , is determined from the formula

$$\frac{1}{\varepsilon_{res}} = \frac{1}{\varepsilon_{fl}} + \frac{1}{\varepsilon_i} - 1 \quad (2.7b)$$

where

ε_{fl} = the emissivity of the flames,

ε_i = the emissivity of the surface exposed to fire.

Properly speaking, Eq. (2.7b) represents the emissivity for radiation between two parallel surfaces, but it was considered to be the best available approximation in the case of radiation between flames and a surface exposed to fire.

According to [9], the coefficient of heat transfer, α_u , at the external surface, which is not exposed to fire, can be represented by the approximate expression

$$\alpha_u = 7.5 + 0.028 \cdot \vartheta_u \quad \text{kcal} \cdot \text{m}^{-2} \cdot \text{h}^{-1} \cdot \text{°C}^{-1} \quad (2.8)$$

where

ϑ_u = the temperature of the external surface.

The system of differential equations of the first order, Eq. (2.6), is solved numerically (see Chapter 4), and then the term I_W is given by the relation

$$I_W = A_t \cdot \psi_1 \cdot (\vartheta_g - \vartheta_1) \quad (2.9)$$

where

A_t = the total area of the surfaces bounding the enclosed space.

If the structures bounding the enclosed space consist of different materials, or if they differ in thickness, as is usually the case in practice, then the above-mentioned operations are carried out separately for each type of structure, and after that the term I_W is obtained from the expression

$$I_W = \sum_j I_{W,j} = \sum_j A_j \cdot \psi_{1,j} \cdot (\vartheta_g - \vartheta_{1,j}) \quad (2.10)$$

The present section, which deals with the term I_W , is based in its entirety on the publications of Kawagoe and Sekine as well as Ödeen referred to in the above.

Term I_R

Kawagoe and Sekine calculated the term I_R from the following formula, which is a generalization of the Stefan-Boltzmann law:

$$I_R = A \cdot (E_g - E_0) \quad (2.11)$$

where

A = the area of the opening,

$$E_g = 4.96 \cdot \left(\frac{g_g + 273}{100} \right)^4$$

$$E_o = 4.96 \cdot \left(\frac{g_o + 273}{100} \right)^4$$

This formula is applicable to the whole duration of the process of fire development, and is used in its unchanged form for the calculations in the present publication.

3. Study of combustion gas flow and heat flow through openings in enclosed spaces

As has been shown in the section dealing with the term I_L in Chapter 2, the expression given by Eq. (2.4) is applicable only during the flame phase of the process of fire development. In that section, the term I_L was determined on the basis of a maximum rate of combustion. If this expression is to be extended so as to be valid for the cooling phase of the fire also, then this requires that the rates of gas and air flow through the openings in the enclosed space shall be determined directly, and that these rates shall then be used as a point of departure for determining the quantity of heat which is withdrawn per unit time from the enclosed space. Similar problems, which were defined in thermodynamic terms, and which related to fires in enclosed spaces, have been treated by *Kawagoe* [5], among others. The primary prerequisites to such a treatment are the assumptions that the pressure distribution in a vertical direction is linear, and that there exists a neutral layer or zone, i.e. a level at which the static pressure in the interior of the enclosed space is equal to the atmospheric pressure outside the enclosed space. From these assumptions, *Kawagoe* deduced the expression for the maximum rate of combustion, R_{max} , which is given by Eq. (2.3). On the assumption that the position of the neutral zone is the unknown variable, he used the Bernoulli equation to calculate the respective quantities of gases and air which flow out of and into the enclosed space per unit time. After that, he determined the position of the neutral zone from the condition that the rate of flow of the incoming gases shall be equal to the rate of flow of the gases which are consumed by combustion, and that the rate of flow of the outgoing gases shall be equal to the rate of flow of the gases which are produced by combustion. Finally, on the assumption that the quantity of air consumed per unit weight of fuel is known, he calculated the maximum rate of combustion, R_{max} .

In this chapter, a similar analysis will be carried out in what follows. The purpose of this analysis is to determine the term I_L by an expression which is more general than that given by Eq. (2.4). A detailed deduction will be presented for the case where the enclosed space is provided with one or several vertical openings which are equal in height. After that, we shall deal with the modifications which are required in the applications which involve openings of other types.

Flow conditions in vertical rectangular opening in enclosed space

The interchange between the gaseous products of combustion and the combustion air takes place because the density of the hot gases is lower than that of the cold air outside the enclosed space. On the assumption that the temperature in the whole enclosed space is uniform, and that there exists a neutral zone, the velocities of gas and air flow can be determined theoretically. After that, if the dimensions of the opening are known, it is possible to calculate the respective rates of flow, i.e. the masses of the outgoing gases and the incoming air per unit time.

The velocity distribution in a vertical rectangular opening is schematically represented in Fig. 6.

The difference in static pressure between the outside and the inside is equal to zero at the level of the neutral zone. Accordingly, if use is made of the notations given in Fig. 6, the pressure difference, P_y , above the neutral zone is

$$P_y = (\rho_0 - \rho_g) \cdot y \quad (3.1 a)$$

and the pressure difference, P_z , below the neutral zone is

$$P_z = -(\rho_0 - \rho_g) \cdot z \quad (3.1 b)$$

where

ρ_0 = density of the outside air,

ρ_g = density of the combustion gases.

The density of the gaseous products of combustion is assumed to be equal to the density of the air at the same temperature [10].

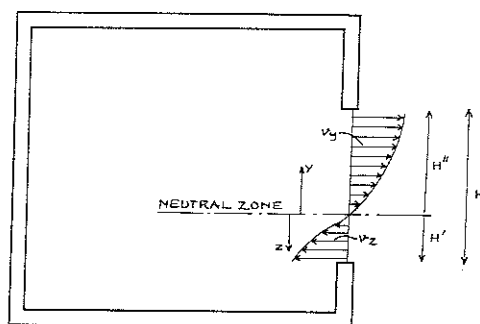


Fig. 6. Gas flow in an enclosed space provided with a vertical opening.

A = Area of the vertical opening in the enclosed space.

H = Height of the vertical opening in the enclosed space.

H'' = Height of the vertical opening above the neutral zone level.

H' = Height of the vertical opening below the neutral zone level.

v_y = Velocity of gas flow above the neutral zone level.

v_z = Velocity of gas flow below the neutral zone level.

From Bernoulli's theorem we obtain the following expressions for the variation in the velocity of flow with the distance from the neutral zone

$$v_y = \sqrt{2g \cdot y \cdot \frac{\rho_0 - \rho_g}{\rho_g}} \quad (3.2a)$$

and

$$v_z = \sqrt{2g \cdot z \cdot \frac{\rho_0 - \rho_g}{\rho_0}} \quad (3.2b)$$

Then the rate of flow of the outgoing gases is

$$Q_{out} = \mu \cdot B \cdot \rho_g \cdot \int_0^{H''} v_y \cdot dy \quad (3.3a)$$

and the rate of flow of the incoming air is

$$Q_{in} = \mu \cdot B \cdot \rho_0 \cdot \int_0^{H'} v_z \cdot dz \quad (3.3b)$$

where

μ = the coefficient of contraction,
 B = the width of the opening.

By substituting Eqs. (3.2a) and (3.2b) in Eqs. (3.3a) and (3.3b), respectively, we can directly calculate Q_{out} and Q_{in} . We find

$$Q_{out} = \frac{2}{3} \cdot \mu \cdot B \cdot (H'')^{3/2} \cdot \sqrt{2g \cdot \rho_g \cdot (\rho_0 - \rho_g)} \quad (3.4a)$$

and

$$Q_{in} = \frac{2}{3} \cdot \mu \cdot B \cdot (H')^{3/2} \cdot \sqrt{2g \cdot \rho_0 \cdot (\rho_0 - \rho_g)} \quad (3.4b)$$

The position of the neutral zone is determined by the equation of gas interchange in the enclosed space. This equation states that the difference between the rates of flow of the outgoing gases and the incoming air shall be equal to the difference between the rates of flow of the gases which are produced and consumed by combustion.

The mass of air contained in the enclosed space is assumed to be constant during the whole period of time under consideration. That total error, referred to the whole duration of the process of fire development, which is caused by this assumption in the calculation of heat flow is not greater than the heat content of the volume of air in the enclosed space. In comparison with the quantities of heat which are associated with fires, and in view of the other approximations which have been made in connection with the application of Eq. (2.1), this error may be regarded as negligible.

Deduction of maximum rate of combustion determined by rate of air supply in accordance with [5]

On the assumption that the rate of combustion, R , is determined by the rate of air supply ($R=R_{\max}$), we have

$$Q_{\text{out}} = R_{\max} \cdot G_0 \cdot \rho_0 \quad (3.5a)$$

and

$$Q_{\text{in}} = R_{\max} \cdot L \cdot \rho_0 \quad (3.5b)$$

where

G_0 = the volume of combustion gases, in Nm^3 , produced by the combustion of 1 kg of fuel,

L = the volume of air, in Nm^3 , consumed by the combustion of 1 kg of fuel.

By substituting Eqs. (3.4a) and (3.4b) in Eqs. (3.5a) and (3.5b), respectively, we can calculate the position of the neutral zone, i.e. H' and H'' . After that, by substituting H' in Eq. (3.5b), we obtain, for R_{\max} , the expression

$$R_{\max} = \kappa(\Delta\vartheta) \cdot A \cdot \sqrt{H} \quad (3.6)$$

where

$\kappa(\Delta\vartheta)$ is a coefficient, which depends on $\Delta\vartheta$

and

$$\Delta\vartheta = \vartheta_g - \vartheta_0$$

The values of $\kappa(\Delta\vartheta)$ is calculated for two fuels. First, for fires of the wood fuel type, which are most characteristic of actual fires, because wood usually constitutes the predominant fire load. Second, for fires, where the fuel consists of alcohol. The numerical values used in these calculations are given in what follows [10].

$$\mu = 0.7$$

$$G_0 = 4.86 \text{ Nm}^3 \cdot \text{kg}^{-1} \text{ for wood} \\ 6.22 \text{ Nm}^3 \cdot \text{kg}^{-1} \text{ for alcohol}$$

$$L = 3.98 \text{ Nm}^3 \cdot \text{kg}^{-1} \text{ for wood} \\ 5.23 \text{ Nm}^3 \cdot \text{kg}^{-1} \text{ for alcohol}$$

The relation between κ and $\Delta\vartheta$ is represented in Fig. 7. This graph shows that the variation in the value of κ with the temperature is very slight in the temperature range which is met with in fires. For practical applications, Kawagoe put the value of κ for wood fires equal to $330 \text{ kg} \cdot \text{h}^{-1} \cdot \text{m}^{-5/2}$, irrespective of the temperature. The value in question was used in deducing Eq. (2.3). This equation has been verified experimentally by several authors in model tests as well as in full-scale tests, see [5]. Eqs. (3.6) and (2.3) are applicable only to one or several openings of equal height, H . In these equations, A denotes the sum of the areas of the individual openings.

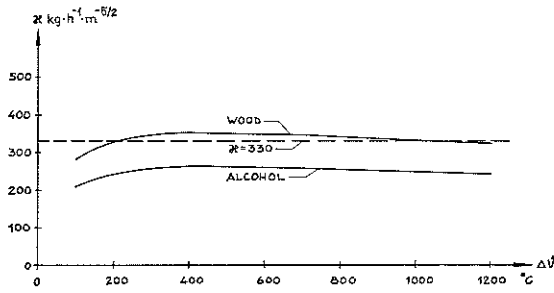


Fig. 7. Relation between the coefficient z in the equation $R_{\max} = zA\sqrt{H}$ and the temperature difference, $\Delta\theta$, between the combustion gases and the outside air.
Wood fires and alcohol fires.

Determination of quantity of heat, I_L , withdrawn per unit time through openings in enclosed space during the whole process of fire development

In order that an expression may be valid throughout the duration of the process of fire development, it is necessary to presuppose that the rate of combustion, R , may assume all values in the interval extending from zero to the maximum value which is given by Eq. (2.3). Therefore, R can be written

$$R = a \cdot 330 \cdot A \cdot \sqrt{H} \quad \text{kg} \cdot \text{h}^{-1}$$

where

$$0 \leq a \leq 1$$

The balance between the respective rates of flow of the outgoing gases and the incoming air is given by the relation

$$Q_{\text{out}} - Q_{\text{in}} = G_0 \cdot R \cdot \rho_0 - L \cdot R \cdot \rho_0 \quad (3.8)$$

After substitution of Q_{out} and Q_{in} from Eqs. (3.4a) and (3.4b), respectively, and after simplification, we obtain

$$\begin{aligned} \left(\frac{H''}{H}\right)^{3/2} \cdot \sqrt{\rho_g(\rho_0 - \rho_g)} - \left(1 - \frac{H''}{H}\right)^{3/2} \cdot \sqrt{\rho_0(\rho_0 - \rho_g)} &= \\ = \frac{(G_0 - L) \cdot \rho_0 \cdot 330a}{\frac{2}{3}\mu \cdot \sqrt{2g}} & \quad (3.9) \end{aligned}$$

With the help of Gay-Lussac's law of volumes for gases

$$\rho_0 = \rho_g \left(1 + \frac{\Delta\theta}{273}\right) \quad (3.10)$$

the ratio H''/H can be determined for different values of a and $\Delta\theta$ from Eq. (3.9).

The quantity of heat which is withdrawn per unit time from the enclosed space can be written

$$I_L = Q_{\text{out}} \cdot c_p \cdot \frac{\Delta \vartheta}{\rho_0} \quad (3.11a)$$

where

c_p = the specific heat of the outgoing gases, in $\text{kcal} \cdot \text{m}^{-3} \cdot ^\circ\text{C}^{-1}$.

By substituting Eq. (3.4a) in Eq. (3.11a), we get

$$I_L = \varphi(\Delta \vartheta) \cdot c_p \cdot \Delta \vartheta \cdot A \cdot \sqrt{H} \quad (3.11b)$$

where

$$\varphi(\Delta \vartheta) = \frac{3}{2} \mu \sqrt{2g} \frac{\sqrt{\frac{\Delta \vartheta}{273}}}{1 + \frac{\Delta \vartheta}{273}} \cdot \left(\frac{H''}{H} \right)^{3/2} \quad (3.11c)$$

If the ratio H''/H is determined from Eq. (3.9), then Eq. (3.11c) yields $\varphi(\Delta \vartheta)$ for different values of a and $\Delta \vartheta$. For combustion of wood fuel, this relation is represented in Fig. 8, which is based on the values of μ , G_0 , and L given on p. 30. It is seen from this graph that the family of curves in question

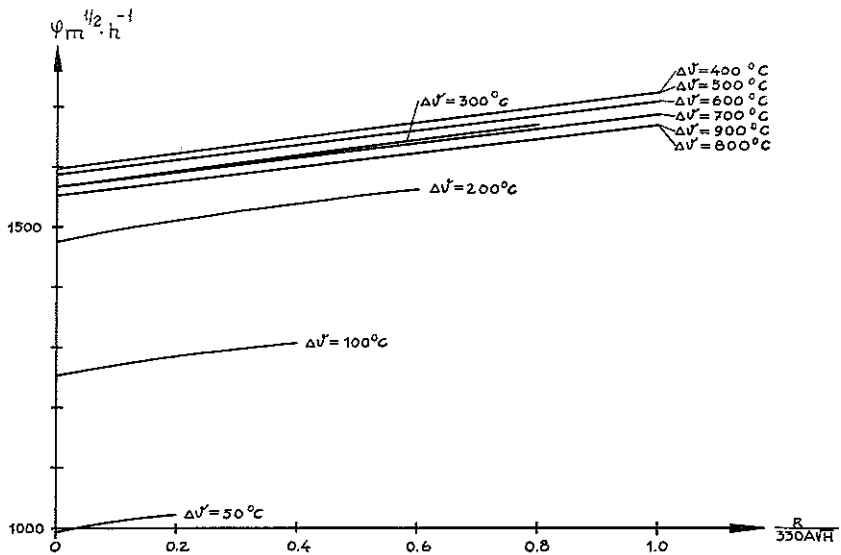


Fig. 8. Relation between the coefficient φ in the equation $I_L = \varphi \cdot c_p \cdot \Delta \vartheta \cdot A \cdot \sqrt{H}$ and the ratio $a = \frac{R}{330 \cdot A \cdot \sqrt{H}}$ for various values of the temperature difference $\Delta \vartheta$.

consists of approximately parallel straight lines. Therefore, we can write

$$\varphi = \varphi_0 + 120 \cdot a \quad (3.12)$$

where

φ_0 is the value of φ for $a=0$.

Table 1 gives φ_0 for various values of $\Delta\vartheta$.

For $\Delta\vartheta > 300^\circ\text{C}$, the value of φ_0 is nearly independent of the temperature, and may be assumed to range from 1500 to 1600.

If the rate of combustion, and hence the factor a , are known, then I_L can be calculated for any instant, t , during the process of fire development. The assumptions which have been chosen for the deduction of the expression for the term I_L will be briefly discussed in what follows.

In spite of the fact that steady-state conditions have been assumed in the calculation of the flow through the opening, the results obtained from this calculation can also be applied under non-steady-state conditions, because a change in a position of equilibrium almost immediately gives rise to the establishment of a new position of equilibrium [7].

Table 1. Relation between φ_0 and $\Delta\vartheta$.

$\Delta\vartheta, ^\circ\text{C}$	$\varphi_0,$ $\text{m}^{1/2} \cdot \text{h}^{-1}$	$\Delta\vartheta, ^\circ\text{C}$	$\varphi_0,$ $\text{m}^{1/2} \cdot \text{h}^{-1}$
10	515	500	1597
50	991	600	1587
100	1254	700	1567
200	1476	800	1551
300	1567	900	1552
400	1595	1000	1510

The calculation of I_L requires that the specific heat of the outgoing gases shall be known. The air content of these gases is dependent on the rate of combustion. When $a=0$, the outgoing gases consist of air alone, and when $a=1$, they consist of gaseous products of combustion only. However, the difference in the specific heat between the air and the combustion gases is very slight, and the specific heat may therefore to a close approximation be regarded as independent of the rate of combustion.

Furthermore, in the calculation of φ , it is assumed that the values of G_0 and L remain constant during the whole process of fire development, irrespective of the rate of combustion. This assumption has not been verified by any physical considerations, but if we examine the right-hand member of Eq. (3.9), then we find that the effect produced by an error in the difference between G_0 and L on the value of φ is comparable to that of an error in a , that is to say, this effect is very slight.

In his treatment which relates to the flame phase only, Kawagoe has assumed that the temperature is uniform in the whole enclosed space. In the present publication, this assumption has been extended so as to be applicable during the whole process of fire development. The assumption that the variation in temperature in a vertical direction is relatively slight when the intensity of the fire decreases has been confirmed by the full-scale tests which are described in Chapter 5 of this publication. In most of these tests, the dispersion in the temperature measured at different points in the enclosed space during the cooling phase was found to be smaller than during the flame phase.

Modification of treatment in cases where enclosed spaces are provided with several openings which differ in height

The deduction carried out in the preceding section is applicable only in the cases where the air is supplied to the enclosed space through one or several openings which are equal in height, and which have a common neutral zone. If the enclosed space is provided with several openings which differ in height, then a corresponding deduction can be made in each individual case. For the determination of the maximum rate of combustion, R_{\max} , Yokoi [13] has described an approximate method. It consists in the determination of a fictitious air flow factor, which is used in the original formula, Eq. (2.3). The fictitious air flow factor is determined from the expression

$$(A \cdot \sqrt{H})_{\text{fict}} = \sum_i A_i \cdot \sqrt{H_i} \quad (3.13)$$

For some cases, Kawagoe [14] has compared the values of R_{\max} which were obtained from Eq. (3.13) with those which were determined by means of accurate calculations. He found that Eq. (3.13) gives values which are sufficiently accurate for practical uses when the differences in the height and in the vertical position of the openings are not too great. The Swedish Building Regulations 1967 recommended another acceptable approximation, namely, that a weighted average of the heights of the individual openings should be used as a value of H in the calculation of the air flow factor.

After a fictitious value of the air flow factor has been determined from Eq. (3.13), this value can be used instead of $A \cdot \sqrt{H}$ in Eq. (3.11b) where the factor φ is calculated from Eq. (3.12) as before.

Modification of treatment in cases where enclosed spaces are provided with horizontal openings in roofs

In the preceding two sections, it was assumed that all openings in the enclosed space are vertical. In the present section, we shall expound a more general theory which makes it possible to take account of the presence of

horizontal openings in the roof of the enclosed space. We suppose the enclosed space to be in conformity with Fig. 9.

We assume that there exists a neutral zone in the enclosed space, and that the level of this zone is not higher than the upper edge of the vertical opening, and not lower than its lower edge. A condition which is prerequisite to this assumption will be stated further on in the present section. For the vertical opening, the rate of flow of the outgoing gases, Q_{out} , is obtained from Eq. (3.4a), and the rate of flow of the incoming air, Q_{in} , is computed from Eq. (3.4b). The velocity of the gases which flow out through the horizontal opening is (Bernoulli's theorem)

$$v_h = \sqrt{2gh' \cdot \frac{\rho_o - \rho_g}{\rho_g}} \quad (3.14)$$

This formula has been verified experimentally in connection with studies of venting fires [7]. The rate flow of the outgoing gases through the horizontal opening is

$$Q_h = \mu \cdot A_h \cdot v_h \cdot \rho_g \quad (3.15)$$

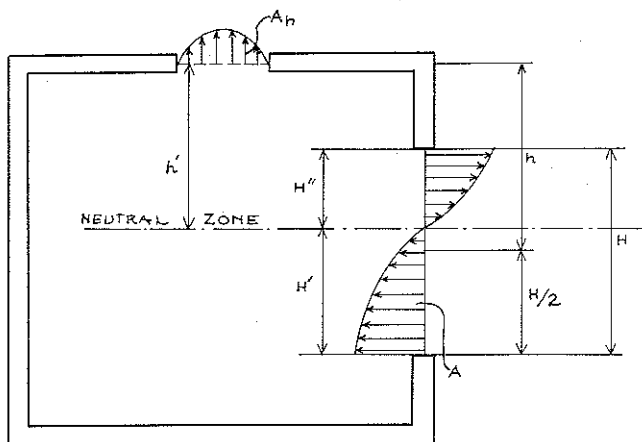


Fig. 9. Gas flow in an enclosed space provided with a vertical opening and a horizontal opening.

- A = Area of the vertical opening.
- A_h = Area of the horizontal opening.
- H = Height of the vertical opening.
- H'' = Height of the vertical opening above the neutral zone level.
- H' = Height of the vertical opening below the neutral zone level.
- h = Vertical distance from the centre of the vertical opening to the level of the horizontal opening.
- h' = Vertical distance from the neutral zone to the level of the horizontal opening.

At a maximum rate of combustion, $R = R_{\max}$, the equation of mass balance of gases requires that

$$\left. \begin{aligned} Q_{\text{out}} + Q_h &= G_0 \cdot R_{\max} \cdot \rho_0 \\ Q_{\text{in}} &= L \cdot R_{\max} \cdot \rho_0 \end{aligned} \right\} \quad (3.16)$$

These two relations can be used to determine the position of the neutral zone which is modified in view of the presence of the horizontal opening, and then the maximum rate of combustion, R_{\max} , can be calculated. R_{\max} is a function of the term $\frac{A_h \cdot \sqrt{h^3}}{A \cdot \sqrt{H}}$ at a given temperature. The value of R_{\max} varies slightly with the temperature. If we write

$$R_{\max} = 330 \cdot (A \cdot \sqrt{H})_{\text{fict}} \quad (3.17)$$

then $(A \cdot \sqrt{H})_{\text{fict}}$ can be determined from the alignment chart in Fig. 10, which is entered at the value of $A_h \cdot \sqrt{h^3} / A \cdot \sqrt{H}$.

It is to be expected that the value of $(A \cdot \sqrt{H})_{\text{fict}}$ determined in this manner may be used to an adequate degree of accuracy in the same way as the air flow factor, $A \cdot \sqrt{H}$, to characterize a fire. Accordingly, for an enclosed space with horizontal openings in the roof, the opening factor is given by the expression $(A \cdot \sqrt{H})_{\text{fict}} / A_t$, where $(A \cdot \sqrt{H})_{\text{fict}}$ is determined from the alignment chart in Fig. 10. The term I_L in the equation of heat balance, Eq. (2.1), of the process of fire development is obtained by analogy with Eq. (3.11 b) from

$$I_L = \varphi(\Delta\vartheta) \cdot c_p \cdot \Delta\vartheta \cdot (A \cdot \sqrt{H})_{\text{fict}} \quad (3.18)$$

where $\varphi(\Delta\vartheta)$ is given by Eq. (3.12).

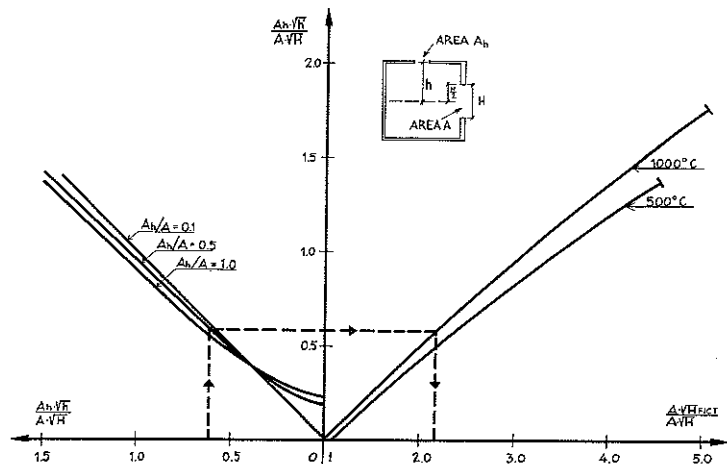


Fig. 10. Alignment chart for the calculation of the value of the modified air flow factor, $(A\sqrt{H})_{\text{fict}}$, on the basis of known geometrical data. For notations, see Fig. 9.

This procedure presupposes that the flow through the horizontal opening in the roof is not predominant. Consequently, the factor $A_h \cdot \sqrt{h'} / A \cdot \sqrt{H}$ has an upper limit at which the above model of the flow conditions ceases to be relevant. This upper limit is

$$\frac{A_h \cdot \sqrt{h'}}{A \cdot \sqrt{H}} = \begin{cases} 1.76 & \text{at } 1000^\circ\text{C} \\ 1.37 & \text{at } 500^\circ\text{C} \end{cases}$$

At this limit, the neutral zone is on a level with the upper edge of the vertical opening, and then h' is identical with the vertical distance from the level of the horizontal opening in the roof to the upper edge of the vertical opening. Tests [7] have indicated that the model used is relevant up to this upper limit. For values of $A_h \cdot \sqrt{h'} / A \cdot \sqrt{H}$ which are higher than this limit, all gaseous products of combustion will be vented through the horizontal opening in the roof. This is sometimes intentional if it is desired that the spread of fire to adjoining rooms should be prevented by venting the fire [15]. If the air and the combustion gases flow in the main through horizontal openings, then the flow becomes unstable, and it is difficult to represent it by a simple theoretical model [16].

Example showing how to use alignment chart in Fig. 10

Calculate the maximum rate of combustion, R_{\max} , during the flame phase at 1000°C in the enclosed space characterized by the following data:

$$A=2 \text{ m}^2, \quad H=1 \text{ m}, \quad A_h=1 \text{ m}^2, \quad h=1.5 \text{ m}.$$

$$\frac{A_h \cdot \sqrt{h}}{A \cdot \sqrt{H}} = \frac{1 \cdot \sqrt{1.5}}{2 \cdot \sqrt{1}} = 0.61; \quad \frac{A_h}{A} = 0.5$$

The dash line in the alignment chart gives

$$(A \cdot \sqrt{H})_{\text{fict}} = 2.18 \cdot A \cdot \sqrt{H} = 4.36 \text{ m}^{5/2}$$

$$R_{\max} = 330 \cdot 4.36 \text{ kg} \cdot \text{h}^{-1} = 1440 \text{ kg} \cdot \text{h}^{-1}$$

This alignment chart can also be used for enclosed spaces where the horizontal opening in the roof is replaced by a ventilation duct. In such cases, the height h is replaced by the height of the gas column (the static head), with the reduction of the losses due to friction, which can be expressed in terms of the equivalent loss in static head. In an ordinary flat or office equipped with common ventilators made of non-combustible materials, the effect of the ventilation ducts is usually negligible.

If the enclosed space is ventilated through air inlets and outlets by means of a fan installation, then the corresponding fictitious air flow factor can be calculated in an analogous manner. If the quantity of gases exhausted per

unit time is Q_{out}^v , in $\text{kg} \cdot \text{h}^{-1}$, and the quantity of air supplied per unit time is Q_{in}^v , in $\text{kg} \cdot \text{h}^{-1}$, then, for $R=R_{\text{max}}$, we have the conditions

$$\left. \begin{aligned} Q_{\text{out}} + Q_{\text{out}}^v &= G_0 \cdot R_{\text{max}} \cdot \rho_0 \\ Q_{\text{in}} + Q_{\text{in}}^v &= L \cdot R_{\text{max}} \cdot \rho_0 \end{aligned} \right\} \quad (3.19)$$

from which R_{max} and $(A \cdot \sqrt{H})_{\text{fict}}$ can be determined by analogy with the above.

4. Description of programme for digital computer

The integration of the system of equations given by Eq. (2.6) was carried out by using the Runge-Kutta method in a modified form which has been suggested by Merson [22]. This modified method enables the computer to choose that interval of integration, Δt , which is required in order to ensure a certain definite degree of accuracy. To integrate the above-mentioned system of equations in the time interval from t to $t + \Delta t$, this system was evaluated in five individual operations. A determination of the temperature of the combustion gases is required for each one of these operations. According to Eqs. (2.1), (2.10), (2.11), and (3.11), the equation of heat balance of the process of fire development can be written

$$I_C = I_L + I_W + I_R \quad (4.1)$$

where

$$I_L = \varphi(\Delta \vartheta) \cdot c_p \cdot A \sqrt{H} (\vartheta_g - \vartheta_0)$$

$$I_W = \sum_j I_{W,j} = \sum_j A_j \psi_{1,j} (\vartheta_g - \vartheta_{1,j})$$

$$I_R = A \cdot (E_g - E_0)$$

If I_R , φ and c_p are calculated on the basis of that value of the temperature of the combustion gases which has been obtained from the next preceding determination, then Eq. (4.1) can be solved for the temperature of the combustion gases, ϑ_g , in an explicit form

$$\vartheta_g = \frac{I_C + \varphi(\Delta \vartheta) \cdot A \sqrt{H} \cdot \vartheta_0 + \sum_j A_j \cdot \psi_{1,j} \cdot \vartheta_{1,j} - I_R}{\varphi(\Delta \vartheta) \cdot c_p \cdot A \sqrt{H} + \sum_j A_j \psi_{1,j}} \quad (4.2)$$

which can be substituted in the system of equations represented by Eq. (2.6).

The programme for the computer has been prepared in such a way as to be applicable to enclosed spaces bounded by structures which were assumed to be of up to three different types. Two of these structures were supposed to be homogeneous, whereas the third might be divided into two or three layers consisting of different materials, e.g. plasterboard panels, mineral wool, and brick.

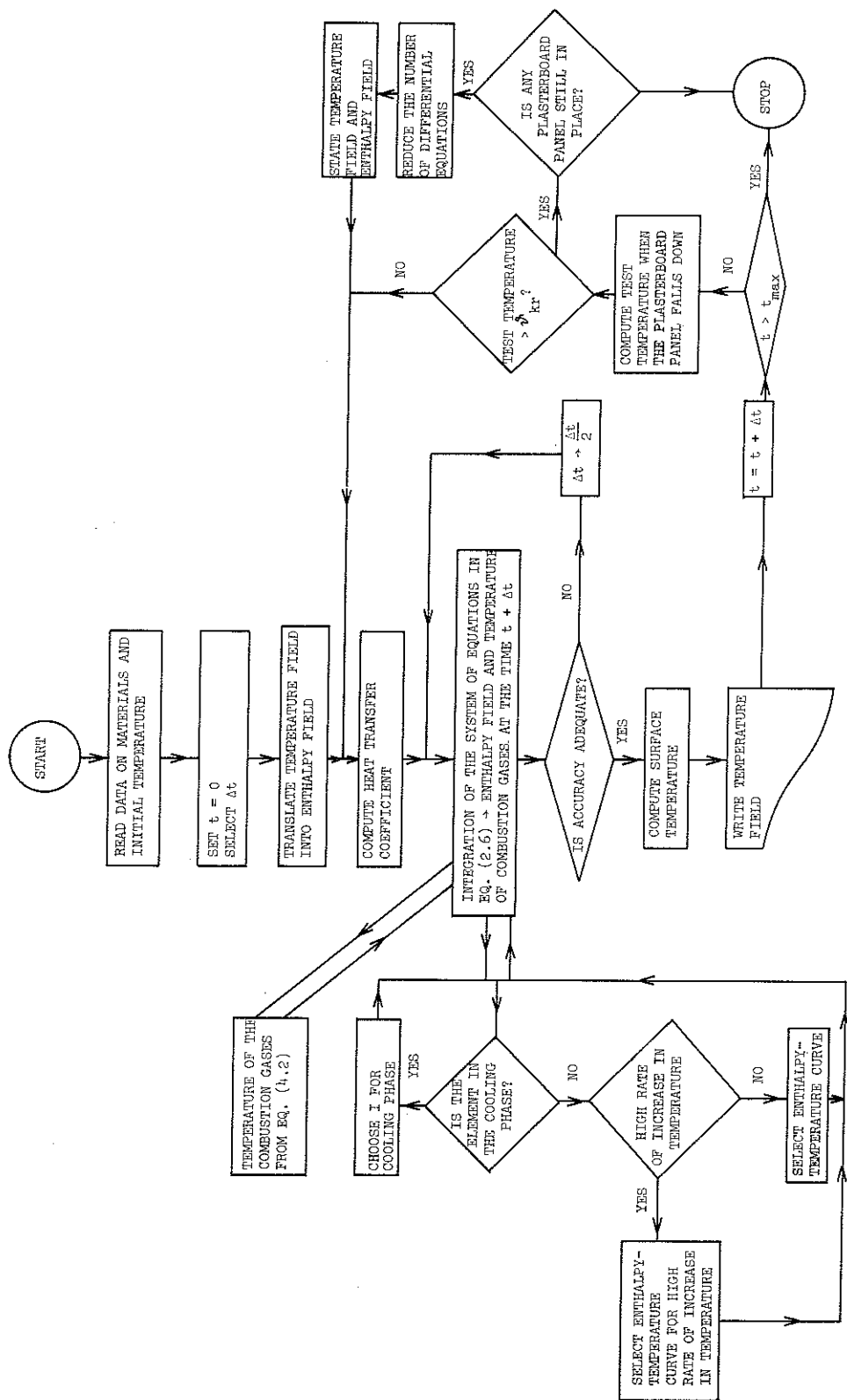


Fig. 11. Flow chart for the calculation of the temperature-time curve of the process of fire development in an enclosed space. The structures which bound the enclosed space are supposed to comprise, first, a roof or/and ceiling and a floor made of homogeneous material, and second, partitions which consist of a load-bearing frame made of steel studs and covered on the outside as well as on the inside with two plasterboard panels, 13 mm in thickness each.

The specific heat of most structural materials, e.g. concrete having a non-negligible moisture content or plasterboard panels, varies discontinuously with the temperature when these materials are subjected to physical or chemical transformations. Therefore the programme used the enthalpy I , in $\text{kcal} \cdot \text{m}^{-3}$, of the different materials as a dependent variable in the calculation of the temperature fields.

Fig. 11 represents a schematic flow chart which shows the programming procedure in the calculation of the combustion gases in an enclosed space where the floor and the roof or/and ceiling are made of concrete, while all the walls consist of a lightweight frame built of steel which are covered on the inside as well as on the outside with two plasterboard panels, 13 mm in thickness each. This type of wall exhibits two characteristic features, viz., first, experiments have shown that a plasterboard panel exposed to fire disintegrates when the temperature of the panel has reached a certain definite value, and second, the relation between the temperature and the enthalpy is dependent on the rate of temperature rise. Furthermore, it was necessary to choose different enthalpy-temperature curves depending on whether the temperature of the plasterboard panel in question was assumed to be increasing or decreasing. For further particulars, reference is made to the description of the calculations for the Type G enclosed space in Chapter 7.

5. Calculation of time graphs of rate of combustion for some full-scale tests described in literature

As has been mentioned in Chapter 2, the present chapter will deal with the comparative calculations which have led to a determination of the variation in the rate of combustion, expressed in $\text{kcal} \cdot \text{h}^{-1}$, with the time. The method of successive approximations employed for this purpose consisted in making calculations which were based on different forms of the time graph of the rate of combustion. These calculations were repeated until they resulted in that curve which corresponded to the closest agreement between experimental and calculated curves representing the variation in the temperature of the combustion gases with the time. This method required a certain systematization of the description which represents the variation in the quantity of energy released by combustion with the time. What can be assumed to be known to a sufficient degree of accuracy in this connection is solely the total quantity of energy that can be liberated during the whole process of fire development, i.e. the fire load. Furthermore, it can be assumed that Eq. (2.3)

$$R_{\max} = 330A\sqrt{H} \text{ kg of wood per h}$$

expresses the maximum rate of combustion, in kg of wood per h. In order that a theoretical determination of the temperature of the combustion gases may be possible, it is moreover necessary to determine the relation between released energy and weight loss of fuel, W , in

$$I_C = R \cdot W \text{ kcal} \cdot \text{h}^{-1}$$

This determination is rendered difficult by the fact that the combustion of the gases formed by pyrolysis and that of solid wood fuel constitute a complicated process which involves a series of chemical reactions in different phases, see [4]. In respect of energy conditions, some of these reactions are endothermic, others exothermic. So far as the Authors know, no systematic investigation has been made up to now in order to carry out a quantitative analysis of the liberation of energy during the individual phases of the process of fire development.

These considerations have necessitated certain assumptions which concern the form of the curve showing the variation in the rate of combustion with the time. These assumptions are stated in what follows. The quantity of energy

liberated per unit time during the ignition phase was supposed to increase according to a polygonal function of the time to a level which corresponds to the rate of combustion during the flame phase. The determination of this level was based on Eq. (2.3), $R_{\max} = 330A\sqrt{H}$ kg of wood per h. When the quantity of energy released per kg of wood fuel during the flame phase was assumed to range from 2500 to 2800 kcal, it was found that the calculated temperature-time curves were closely in agreement with the results of the full-scale tests in respect of the maximum temperature and the duration of the flame phase. In order to adapt these assumptions to the temperature-time curves which have been published in the Swedish Building Regulations 1967 and in the Draft Specification "Aluminium Structures", and which are used in Sweden as a basis for calculations of the fire endurance of structural components in conformity with standard specifications, the quantity of heat evolved during the flame phase was supposed to be 2575 kcal · kg⁻¹ of wood, since this value had been employed for calculating the above-mentioned temperature-time curves. Cf. Chapter 2. The value in question has originally been stated by Kawagoe, who used it as a measure of the quantity of energy that is liberated by incomplete combustion of 1 kg of wood. By analysing the composition of the combustion gases in fire tests, see e.g. [5], it has been found that they contain considerable quantities of carbon monoxide, and this indicates that the combustion is not complete. It seems that the analysis of the combustion gases was performed during the flame phase, and the value 2575 therefore applies to this phase only. During the cooling phase, the weight loss of fuel per liberated energy unit is considerably less than during the flame phase. This means, that, when the whole process of fire is considered, the energy released by the combustion of 1 kg of wood must be higher than 2575 kcal even if the combustion is incomplete. As a rule, there was scant basis for an accurate prediction of how the rate of completeness of combustion varied during the different phases. Consequently, in our comparative analysis the nominal heat value of wood, ranging from 3500 to 4500 kcal · kg⁻¹, was used as the energy liberated during the whole course of fire. This means that combustion is assumed to be complete throughout the present publication. The resulting time-temperature curves for the combustion gases therefore as a rule are found to be more in agreement with the maximum temperature curves than with the mean temperature curves obtained in the full scale tests.

Consequently, during the flame phase, the value of the rate of combustion will be constant, $330 \cdot A\sqrt{H} \cdot 2575$ kcal · h⁻¹. The cooling phase is characterized by a rate of combustion which decreases in conformity with a polygonal time graph in such a way that the slope of each individual side of the polygon is dependent on the duration of the flame phase. In every case, the area between the rate of combustion curve and the time axis must equal the fire load, expressed in energy units. The use of a polygonal time graph of the rate of

combustion makes it easier to check the agreement between the total quantity of energy liberated during the process of fire development and the fire load which is given from the outset.

The factors which must be taken into account in a comparative theoretical calculation of the temperature of the combustion gases in fire tests are enumerated in what follows.

(1) Characteristics of fuel: Quantity, moisture content, porosity factor (hydraulic radius), distribution in the enclosed space.

(2) Geometric characteristics of the enclosed space: Opening factor and its variation with the time (e.g. in the case where the fire burns through a door), shape of openings, cross-sectional area of ventilation ducts (if any).

(3) Characteristics of the structures bounding the enclosed space: Structural design, thermal properties and temperatures of disintegration (if any) of the materials entering into the structures, emissivity characteristics of the surfaces.

By studying the available literature on full-scale wood fire tests, it was found, first, that the number of published tests is relatively small, and second, that those data which are so detailed as to render possible a comparative theoretical calculation have been stated only for a few tests out of this number. For this reason, it was necessary to confine the comparative calculations to only four test series reported in the literature or in other sources.¹ These test series are enumerated below.

(1) Test series A. Tests carried out by *Sjölin*, and dealt with in a thesis for a L. Techn. degree, [17].

(2) Test series B. Tests made by *Kawagoe*, and published in [5].

(3) Test series C. Tests performed by *Ödeen* at the Royal Institute of Technology, Stockholm, and described in his doctoral thesis [18].

(4) Test series D. Tests directed by *Pettersson* and *Ödeen*, which were carried out in a test house of the Atomic Energy Co., Ltd. (AB Atomenergi) at Studsvik, Sweden.

Test series A. Tests carried out by *Sjölin*. Calculation of time graphs of rate of combustion

The tests made by *Sjölin* were undertaken in order to study the spread of fire, and the process of fire development, in rooms and combinations of rooms exposed to ignition at a single point by heat radiation emitted by an explosion of nuclear weapons. The fire tests were carried out in a test house which was provided with concrete floor structures and concrete or lightweight concrete

¹ Not until too late in the publication of this paper did the authors learn about the full scale fire tests carried out at Fire Research Station, Boreham Hood, London [11, 12].

This is the more regrettable as these experiments make an excellent basis for comparative theoretical calculations.

walls. The test house was designed in such a way that various enclosed spaces might be formed by individual rooms, or by several rooms connected together. The available model scales were 1 to 1, 1 to 2, and 1 to 4. The variables recorded in these tests were expressed as functions of the time, and comprised the temperature and the velocity of gas flow at characteristic points, the intensity of radiation, the composition of the gases, and the rate of combustion, which was determined by continuous weighing of the quantity of fuel in the enclosed space.

The fire load in all these tests consisted of authentic furniture. This was an extraordinarily valuable feature of the tests, seeing that all the other full-scale tests which are dealt with in the present publication were made by using fire loads of the wood crib type.

Seven of the fire tests included in this test series were found to be suited for the present theoretical study. In the other tests, the ignition did not cause the fuel to take fire. Table 2 shows the scope of the seven tests under consideration.

Table 2. Test series A.

Test No.	Type of room	Window area, m ²	Opening factor, $\frac{A \cdot \sqrt{H}}{A_t}$ m ^{1/2}	Fire load, kg · m ⁻² of bounding surface area	Remarks
1	<i>B</i>	1.16	0.0237–0.06	3.5	The fire burnt through a door, 1.6 m ² in area, during the time interval from <i>t</i> =0 min. to <i>t</i> =6 min.
2	<i>B</i>	1.16	0.0237–0.06	4.4	
3	<i>L</i>	1.16	0.0160–0.0356	4.9	The fire burnt through a door, 1.6 m ² in area, during the time interval from <i>t</i> =8 min. to <i>t</i> =12 min.
4	<i>L</i>	1.88	0.0278–0.0486	5.6	
5	<i>L</i>	1.88	0.0548	5.0	
6	<i>L</i>	2.95	0.068	5.7	
7	<i>B+L</i>	3.20	0.040	8.1	

B = Furnished two-person bedroom, 10.4 m² in floor area.

L = Furnished living room, 18.8 m² in floor area.

B+L = Combination of *B* and *L*.

The curves representing the variation in the temperature of the combustion gases with the time in the above-mentioned seven tests, as well as the corresponding curves obtained by calculations with the help of automatic computer, are reproduced in Appendix 1. In the test No. 7, the enclosed space consisted of two contiguous rooms, which communicated through an open door. The partition between these two rooms was considered in the theoretical calculations to be an enclosed structure which possessed a heat-absorbing capacity.

For this test, the curves representing the temperature of the combustion gases as a function of the time are shown separately for the bedroom and the living-room.

All the fires in these tests were characterized by a protracted process of ignition, which was followed by a rapid transition to the flame phase. For the calculated curves, the time was put equal to zero at the instant when the flame phase began, i.e. when the fuel took fire, in the actual fire tests. The time graphs of the rate of combustion which were finally obtained from the calculations are also reproduced in the respective diagrams. In the tests Nos. 1 to 4, the opening factor was changed during the process of fire development because the fire had burnt through a door. This change was taken into account in the calculations, and constituted the cause of the somewhat unusual shape of the time graphs of the rate of combustion which refer to these four tests. In these cases, the curves were plotted in such a way as to relate the rate of combustion to that value of the opening factor which was obtained after the fire had burnt through the door. In the test No. 3, the fact that the fire has burnt through a door is reflected very clearly in the curve, which shows that the temperature of the combustion gases remained constant at 500 to 600°C, and then rapidly rose to about 800°C when the fire burnt through the door.

Since the calculations were based on the opening factor and on the total energy content of the fuel, it was possible to choose the time graphs of the rate of combustion in such a manner that the agreement between the observed and calculated time graphs of the temperature of the combustion gases was very close in all the tests except the test No. 7. In the test No. 7, the calculated time graph of the combustion gas temperature was compared with the corresponding observed curves for the living-room as well as for the bedroom. The agreement between these curves was relatively close in the second case, but not in the first, where the curve is slightly displaced in time with reference to the curve for the bedroom. Moreover, when use was made of the opening factor which was determined geometrically, the temperatures obtained for the flame phase were found to be somewhat too low. However, it is not correct to regard the above-mentioned two rooms as a single enclosed space, since there existed quite a considerable difference in temperature between these rooms. Nor are the two rooms in question to be regarded as two separate enclosed spaces, since a certain heat exchange took place between these rooms.

Test series B. Tests made by Kawagoe [5]. Calculation of time graphs of rate of combustion

In [5], *Kawagoe* has described a large number of fire tests which had been carried out in Japan. In this investigation, he primarily studied the relation between the reduction in the weight of fuel per unit time and the dimensions

of the openings in the enclosed space. Among other things, he also deduced the equation which is reproduced in Eq. (2.3) in the present publication. The variables measured in these tests were the reduction in the weight of fuel, the temperature of the combustion gases, the composition of the combustion gases, the gas velocities, the intensity of radiation, and the pressure distribution in the window openings. On account of the above-mentioned main purpose of Kawagoe's investigation, it is only in three of these tests that the results of measurements, the geometric data, and the data on the materials entering into the structures which bounded the enclosed space are presented in such a way as to make it possible to carry out theoretical calculations of the type under consideration. These three tests were performed in a test house which was provided with walls made of hollow concrete blocks and with concrete floor and roof structures. The other test data are given in Table 3.

Table 3. Test series B.

Test No.	Fire load, kg of wood	Bounding surface area, m ²	Window dimensions, width × height, m × m	Opening factor, $\frac{A \cdot \sqrt{H}}{A_t}$ or, m ^{1/2}
1	400	48	0.93 × 1.8	0.0467
2	900	48	0.93 × 1.8	0.0467
3	1000	48	0.93 × 1.8	0.0467

Each hollow concrete block used for the walls comprised a single large cavity, without any subdivisions. The volume of the cavity was estimated at 30 to 40 per cent of the total volume of the block. In the calculations, the walls were considered to be composed of two different structures. One of them consisted of concrete alone, while the other comprised three layers, viz., concrete, air-filled cavity, and concrete, respectively. The second structure represented that part of the wall surface which corresponded to the cavities of the hollow concrete blocks, while the first structure was equivalent to the remaining part of the wall surface.

The observed and calculated temperature-time curves, as well as the time graphs of the rate of combustion used in the calculations, are reproduced in Appendix 2. The fire loads in the tests Nos. 2 and 3 were relatively high and the duration of the fires in these tests was therefore long. In order that the calculated values should agree with the values observed in these tests, it was necessary to choose a comparatively flat slope for the ascending branch of the time graph of the rate of combustion.

The data on the cooling phases in the tests Nos. 2 and 3 reported in [5] are not complete, and this is the reason why the curves relating to these tests break off at such an early stage.

Test series C. Tests published by Ödeen [18]. Calculation of time graphs of rate of combustion

The tests described by Ödeen in [18] were carried out in a tunnel building of an approximately semi-circular shape, which had been specially constructed for this purpose. It was provided with a concrete wall, 20 cm in thickness, its total bounding surface area was 75 m², and its total enclosed volume was 46 m³. A fan system made it possible to regulate and to measure the quantity of air which was supplied per unit time of the fire. In addition, a vent, 0.5 m² in cross-sectional area, for conveying the combustion gases to the outside air was provided in the upper part of each end wall of the tunnel.

A series of fire tests using fir wood as fuel has been carried out in this test building. A study was made of the effects produced on the process of fire development by the factors which are enumerated in what follows.

- (1) The volume of air supplied per unit time to the tunnel, Q , in m³ · s⁻¹.
- (2) The quantity of combustible material (fire load), M , in kg of wood.
- (3) The hydraulic radius of the fuel, r , in cm. This factor expresses the ratio of the total volume of the fuel to its total bounding surface area.

The scope of the test series using wood fuel is shown in Table 4, which was extracted from [18].

In order that the results of these tests may be compared by means of calculations with those of fire tests in ordinary enclosed spaces, where the rate

Table 4. Test series C.

Test No.	Fire load, M , kg of wood	Rate of air supply, Q , m ³ · s ⁻¹	Hydraulic radius, r , cm	Moisture content of fuel, per cent	Energy content of fuel, Mcal
1	270	1.0	—	9	1129
2	675	2.0	1.0	17	2565
3	675	1.0	1.0	17	2565
4	675	0.7	1.0	22	2468
5	675	1.5	1.0	22	2468
6	675	MIN	1.0	21	2501
7	675	1.0	1.7	21	2501
8	675	0.7	1.7	21	2501
9	675	1.0	0.6	21	2501
10	270	0.7	1.0	21	1000
11	405	0.7	1.0	22	1481
12	405	0.7	2.4	28	1440
13	135	0.7	1.0	28	481
14	945	1.0	1.6	16	3659
15	1350	2.0	1.4	17	5130
16	405	0.7	0.4	17	1539

of air supply is determined by the openings in the enclosed space, the quantity of air supplied per unit time, Q , must be converted into an air flow factor, $A\sqrt{H}$, or into an opening factor, $A\sqrt{H}/A_t$. In this connection, it is necessary to take account of the air flow which may possibly enter into the tunnel through the outlets for combustion gases at low values of Q , and may therefore increase the value of the air flow factor.

In an ordinary enclosed space provided with a vertical opening, the rate of flow of the incoming air, Q_{in} , is given according to Eq. (3.4b), by the relation

$$Q_{in} = 2/3 \mu B (H')^{3/2} \sqrt{2g \cdot \frac{(\rho_0 - \rho_g)}{\rho_0}} \text{ m}^3 \cdot \text{s}^{-1} =$$

$$= 2/3 \cdot 0.7 \cdot A\sqrt{H} \sqrt{2g} (H'/H)^{3/2} \left(\frac{\frac{\Delta\vartheta}{273}}{1 + \frac{\Delta\vartheta}{273}} \right)^{1/2} \text{ m}^3 \cdot \text{s}^{-1} \quad (5.1)$$

The notations used in Eq. (5.1) have been explained in Chapter 3.

With the help of Eqs. (3.9) and (3.10), we obtain, for $a=1$, the relation between H''/H and $\Delta\vartheta$ shown in Table 5.

Table 5. Relation between H''/H and $\Delta\vartheta$.

$\Delta\vartheta$	H''/H	$\Delta\vartheta$	H''/H
400	0.61	800	0.64
500	0.62	900	0.65
600	0.63	1000	0.66

Since $H' = H - H''$, we can substitute H''/H in Eq. (5.1). For different values of the temperature $\vartheta_g = \vartheta_0 + \Delta\vartheta$, this yields the simplified expression

$$Q_{in} = K \cdot A\sqrt{H} \quad (5.2a)$$

where K varies with the temperature of the combustion gases, ϑ_g , in conformity with Table 6, where ϑ_0 was put equal to zero.

Table 6. Relation between K and ϑ_g .

ϑ_g	K	ϑ_g	K
400	0.40	900	0.38
500	0.40	1000	0.38
600	0.40	1100	0.37
700	0.39	1200	0.37
800	0.39		

In the case under consideration, the rate of flow of the incoming air, Q_{in} , was equal to the quantity of air supplied per unit time by the fan system. Hence it follows that this quantity of air can be replaced by a fictitious air flow factor, $(A\sqrt{H})_{fict}$, by means of Eq. (5.2a).

If the constant K is put equal to its value at 600°C, then we obtain

$$Q = 0.40(A\sqrt{H})_{fict} \quad (5.2b)$$

By substituting $A_t = 75 \text{ m}^2$, we get

$$(A\sqrt{H}/A_t)_{fict} = 0.033Q \quad (5.3)$$

This relation between the fictitious opening factor, $(A\sqrt{H}/A_t)_{fict}$, and the rate of air flow, Q , shall include the effect of the air which may possibly enter into the tunnel through the paraboliform outlets for combustion gases, 0.5 m² in cross-sectional area each. In the calculations, these outlets were assumed to be replaced by two rectangular openings having a base $B = 1.13 \text{ m}$ and a height $H = 0.44 \text{ m}$ each.

If the rate of flow of the incoming air through these openings is put equal to Q_{in} , then Q_{in} at a maximum rate of combustion is given by the equation

$$Q_{in} + Q\rho_0 = LR_{max}\rho_0$$

For notations in this equation, see Chapter 3.

By substituting Q_{in} from Eq. (3.4b), we find

$$2/3 \sqrt{2gH' \frac{\rho_0 - \rho_g}{\rho_0}} \mu B \cdot H' \rho_0 + Q\rho_0 = LR_{max}\rho_0 \quad (5.4)$$

where R_{max} is determined from Eq. (3.5a).

$$Q_{out} = G_0 \cdot \rho_0 \cdot R_{max}$$

or

$$2/3 \cdot \sqrt{2gH'' \frac{\rho_0 - \rho_g}{\rho_g}} \cdot \mu \cdot B \cdot H'' \cdot \rho_g = G_0 \cdot \rho_0 \cdot R_{max} \quad (5.5)$$

By substituting $B = 1.13 \text{ m}$, $H = 0.44 \text{ m}$, $\mu = 0.7$, $G_0 = 4.86 \text{ Nm}^3 \cdot \text{kg}^{-1}$, $L = 3.98 \text{ Nm}^3 \cdot \text{kg}^{-1}$ and R_{max} from Eq. (5.5) into Eq. (5.4) we obtain

$$0.83(H'/H)^{3/2} + 0.722Q = 0.38(H''/H)^{3/2} \quad (5.6)$$

In the calculation of ρ_g , the temperature of the combustion gases was assumed to be 600°C.

For those values of Q which are of interest in this connection, i.e. $Q \geq 0.7 \text{ m}^3 \cdot \text{s}^{-1}$ in conformity with Table 4, Eq. (5.6) has no solution in the interval $0 \leq H'/H \leq 1$. This means that the flow is possible in an outward direction only.

In the test No. 6, the fans were switched off, and the exchange of air took place through the outlets for combustion gases alone. If these outlets are supposed, as before, to be approximately represented by rectangular openings having a base of 1.13 m and a height of 0.44 m each, then we obtain an opening factor $A\sqrt{H}/A_t = 0.0088 \text{ m}^{1/2}$, which corresponds to a rate of air flow $Q_{\min} = 0.26 \text{ m}^3 \cdot \text{s}^{-1}$ according to Eq. (5.3). Cf. the average value of the rate of air flow, $0.19 \text{ m}^3 \cdot \text{s}^{-1}$, which has been computed by Ödeen for the whole process of fire development.

Thus, in the tests under consideration, the fictitious opening factor, $(A\sqrt{H}/A_t)_{\text{fict}}$, and hence the maximum rate of combustion, are determined approximately in conformity with the above from Eq. (5.3).

For the 16 tests comprised in this series, Table 7 gives, first, the opening factor calculated by means of the above relations, and second, the opening factor, $(A \cdot \sqrt{H}/A_t)_{\text{exp}}$, that has proved to give theoretical results which are in agreement with the experimental values. The test results, the theoretical results, and the time graphs of the rate of combustion are shown in Appendix 3. As regards the time graphs of the combustion gas temperature, it is to be noted that the six full-line curves represent the temperatures at different

Table 7. Theoretical and experimental values of the opening factor.
Test series C [18].

Test No.	Fire load, M , kg of wood	Hydraulic radius, r , cm	Rate of air supply, Q , $\text{m}^3 \cdot \text{s}^{-1}$	Opening factor, theoretical value, $(A\sqrt{H}/A_t)_{\text{theor}}$ calculated from the formula $A\sqrt{H}/A_t = 0.0334 \cdot Q$	Opening factor, experimental value, $(A\sqrt{H}/A_t)_{\text{exp}}$	$\frac{(A\sqrt{H}/A_t)_{\text{exp}}}{(A\sqrt{H}/A_t)_{\text{theor}}}$
4	675	1.0	0.7	0.023	0.035	1.52
8	675	1.7	0.7	0.023	0.015	0.65
10	270	1.0	0.7	0.023	0.015	0.65
11	405	1.0	0.7	0.023	0.020	0.87
12	405	2.4	0.7	0.023	0.012	0.52
13	135	1.0	0.7	0.023	0.005	0.22
16	405	0.4	0.7	0.023	0.060	2.60
1	270	—	1.0	0.033	0.023	0.70
3	675	1.0	1.0	0.033	0.043	1.30
7	675	1.7	1.0	0.033	0.037	1.12
9	675	0.6	1.0	0.033	0.051	1.54
14	945	1.6	1.0	0.033	0.037	1.12
5	675	1.0	1.5	0.050	0.055	1.10
2	675	1.0	2.0	0.067	0.060	0.90
15	1350	1.4	2.0	0.067	0.060	0.90
6	675	1.0	about 0.25	0.009	0.010	1.11

points in the enclosed space. The fine dash-line curve summarises the values recorded in the radiation measurements, and the heavy dash-line curve is the calculated curve. The variation in the rate of combustion with the time, I_c , is represented in terms of $330 \cdot (A\sqrt{H})_{\text{exp}} \cdot 2575 \text{ kcal} \cdot \text{h}^{-1}$ put equal to unity. The rate of flow of the incoming air, Q , conveyed by the fan system was constant during the whole process of fire development. The radiation measurements have provided certain indications for choosing the instant at which the rate of combustion had decreased to zero. The difference between the temperature at the level of the floor surface and the average temperature in the other parts of the enclosed space has been taken into account. In the test series under review, this difference in temperature has probably been increased owing to the fact that air was supplied to the enclosed space by means of fans at the floor surface level. The temperature difference was taken into consideration by assuming that the coefficient of heat transfer at the floor surface was equal to 80 per cent of the corresponding coefficient for the other surfaces. In all cases when the rate of burning was controlled by the fuel bed and not by the ventilation it was taken into account that heat energy was withdrawn from the enclosed space by that part of the incoming air which did not take part in the combustion.

As may be seen from Table 7, the positive as well as negative differences between the value of the opening factor, $(A\sqrt{H}/A_d)_{\text{exp}}$, determined from the test results, i.e. the actual maximum values of the rate of combustion, and the corresponding values obtained on the assumption that the rate of combustion is limited by the rate of air supply, were found to be great in some tests. However, the calculated curves were as a rule closely in agreement with the observed values. The agreement between the maximum temperature and the duration of the flame phase indicates that those values of the quantity of energy released per unit time which were used for the theoretical calculations were on the whole correct.

Furthermore, Table 7 shows two other factors among those which, in addition to the air flow factor, determine the rate of combustion. These factors are the hydraulic radius and the amount of fuel (the fire load). The effect of the first-mentioned factor can be demonstrated, for instance, by a comparison between the tests. Nos 16 and 12. The values of the air flow factor, as well as those of the fire load, in these two tests were equal, whereas the respective values of the hydraulic radius were 0.4 and 2.4 cm. In consequence of the difference in the hydraulic radius, the actual maximum rate of combustion in the test No. 16 was about 5 times as high as in the test No. 12. This may roughly be explained by the simplified study of the mechanism of combustion in what follows.

In a wood fuel consisting of comparatively large pieces of wood, pyrolysis takes place in several forms at the same time. In a certain definite inner zone

of the wood, where the temperature is relatively low, say, below about 250°C, the reactions are endothermic, whereas in the outer zones, where the temperature is higher, the reactions are exothermic, and in certain cases, e.g. in the secondary pyrolysis of tar products, markedly exothermic. The combustion of the products of pyrolysis generates heat, which increases the temperature of the fuel by conduction, and hence renders possible an exothermic decomposition in the inner zone. In the test No. 16, the wood fuel consisted of concrete form timber, for which the ratio of the volume to the exposed surface was 0.4 cm. Accordingly, if the width, the length, and the thickness of a piece of wood are denoted by b , l , and t , respectively, then we have

$$r = 0.4 \text{ cm} = \frac{b \cdot l \cdot t}{2l(b+t)}$$

If we put $b = t$ (square cross section), then we obtain a thickness of 1.6 cm, and if we set $b \gg t$, then we get a thickness of 0.8 cm. In view of the small thickness, in combination with the mechanism of heat return to the fuel described in the above, it is probable that a few minutes after the fuel has taken fire the whole quantity of fuel is in a state of active exothermic pyrolysis. Tests [23] have shown that the progression of the charred layer on a wooden beam exposed to fire is about $0.6 \text{ mm} \cdot \text{min}^{-1}$. This value is applicable to a firwood beam exposed to fire in conformity with a standard temperature-time curve. The variation in the rate of carbonization with the intensity of the process of fire development is a problem which appears to be wholly unexplored at the present time. But if the above-mentioned value, $0.6 \text{ mm} \cdot \text{min}^{-1}$, is assumed to be correct, then this implies that the whole amount of fuel would be charred in the course of 5 to 10 min. Since from one half to two thirds of the total quantity of energy is liberated during the flame phase, this can explain the intense release of energy immediately after the fuel has taken fire.

The test No. 12 shows that when the fire-exposed surface area diminishes below a certain definite limit, the quantity of energy which can be developed per unit time is determined by the rate of progression of the charred layer, and not by the air flow factor. In this test, the hydraulic radius was 2.4 cm. If the above-mentioned value, $0.6 \text{ mm} \cdot \text{min}^{-1}$, which is probably too high in view of the low temperature during the process of fire development in this case, is used as a measure of the progression of the charred layer, then this corresponds to a maximum rate of combustion of $405 \cdot 0.6 \cdot 10^{-2} / 0.24 = 10.1 \text{ kg} \cdot \text{min}^{-1}$. The value of the maximum rate of combustion computed from the formula $R = 5.5A\sqrt{H}$ is $9.7 \text{ kg} \cdot \text{min}^{-1}$, and this implies that the quantity of energy released per unit time during a fire is determined by the surface area exposed to fire, and not by the rate of air supply, at least during certain phases of the fire.

Furthermore, a closer study of Table 7 also demonstrates the marked effect produced by the amount of fuel on the rate of combustion. This can likewise be explained by means of the mechanism of return of the heat evolved by combustion which has been outlined in the above. In the tests Nos. 13, 10, 11, and 4, the values of the hydraulic radius, r , were equal, just as those of the rate of air supply Q , whereas the fire load, M , was varied. For the values of the fire load $M=135, 270, 405,$ and 675 kg, which approximately corresponded to 7, 15, 20, and 35 Mcal \cdot m⁻² of bounding surface area of the enclosed space, the respective values of the maximum rate of combustion calculated from the test results were found to be equal to 0.22, 0.65, 0.87, and 1.5 times the rate of combustion which was computed on the basis of the air flow factor. In [18], it is stated that the flame phase was slightly developed in the tests Nos. 10 and 11, whereas the fuel did not take fire at all in the test No. 13.

Moreover, it is seen from Table 7 that the variation in the rate of combustion with the hydraulic radius seems to decrease as the opening factor or the fire load increases.

Finally, it may be useful to touch on the question to what extent these analytic fire tests, which were carried out under conditions that were idealized so far as possible, and which exhibited characteristics of combustion that in several tests markedly differed from those predicted by the theory, can be utilized as a basis for predicting the behaviour of more conventional fires. An ordinary fire in an enclosed space is governed to a varying degree by two feed-back mechanisms. In the first place, the lower density of the combustion gases forces unconsumed air by natural convection towards the flames, and hence increases the rate of combustion, as well as the evolution of combustion gases. In the second place, part of the heat generated by combustion returns to the fuel, and increases the rate of energy release. So long as these mechanisms are negative, the combustion remains stable. Cf. e.g. the test No. 13. An essential difference between Ödeen's tests described in [18] and an ordinary fire is that the return mechanism which governs the rate of air supply was eliminated in the tests. The effect of this circumstance is difficult to determine, but it may be mentioned for comparison that all the theoretical and experimental results in the test series (A, B, and D) where the exchange of air was self-regulated were found to be closely in agreement if the rate of combustion was assumed to be determined by the rate of air supply. However, a comparison of the time graphs of the rate of combustion for the test series A to D shows that, in the cases where differences were present, the results obtained from the test series C deviated from those of the other test series only in respect of the maximum quantity of energy released per unit time. If the time graphs of the rate of combustion are represented in terms of $330 \cdot (A\sqrt{H})_{\text{exp}} \cdot 2575$ kcal \cdot h⁻¹ put equal to unity, then the curves for this test series are found

to be closely in agreement with those for the test series A, B, and D when the fire load and the opening factor are given. All the same, since a dispersion in the values of the quantity of energy liberated per unit time has been observed in the test series C even when the tests were identical in respect of the rate of air supply and the wall material, it should be noted that this dispersion indicates the need for determining the factors which, in addition to those mentioned in the above, govern the rate of release of energy.

Test series D. Tests made at the National Swedish Institute for Materials Testing. Calculation of time graphs of rate of combustion

Under the direction of the Fire Engineering Laboratory of the National Swedish Institute for Materials Testing, a test house for model-scale and full-scale fire studies has been erected at the Studsvik Test Station of the Atomic Energy Co., Ltd. The primary object of the investigations carried out in this house was to study the spread of fire and smoke along the exterior walls and along the ventilation ducts in the case of fire in an individual enclosed space in a multi-storeyed building. Extensive measurements of the reduction in the weight of fuel, the temperature, the intensity of radiation, the gas flow, and the composition of combustion gases were made in these tests, and the test results are therefore well suited for theoretical comparisons.

Fig. 12 shows the test house, which was three storeys high, and which consisted of a load-bearing steel frame clad with lightweight concrete elements. The results of the tests carried out up to now have not yet been published, but the test programme and the test equipment are described in [20] and [21]. The Authors of the present publication were afforded an opportunity to acquaint themselves with the results of the first four full-scale tests. The data for these tests are reproduced in Table 8.

The fires were initiated in the lowermost storey, which was connected with the outside air by means of a vertical ventilation duct by-passing the storeys

Table 8. Test series D.

Test No.	Fire load, kg of wood	Window dimensions, width \times height m \times m	Bounding surface area, m ²	Air flow factor, $A \cdot \sqrt{H}$, m ^{5/2}	Air flow factor, fictitious value, $(A\sqrt{H})_{\text{fict}}$ m ^{5/2}	Moisture content of fuel, per cent	Moisture content of lightweight concrete, per cent
1	350	1.3 \times 1.3	75	1.93	2.10	7.7	4.0
2	200	1 \times 1	75	1.00	1.10	8.8	3.1
3	115	0.8 \times 0.8	75	0.57	0.69	7.4	2.1
4	1150	2 \times 2	75	5.63	5.65	9.7	2.3

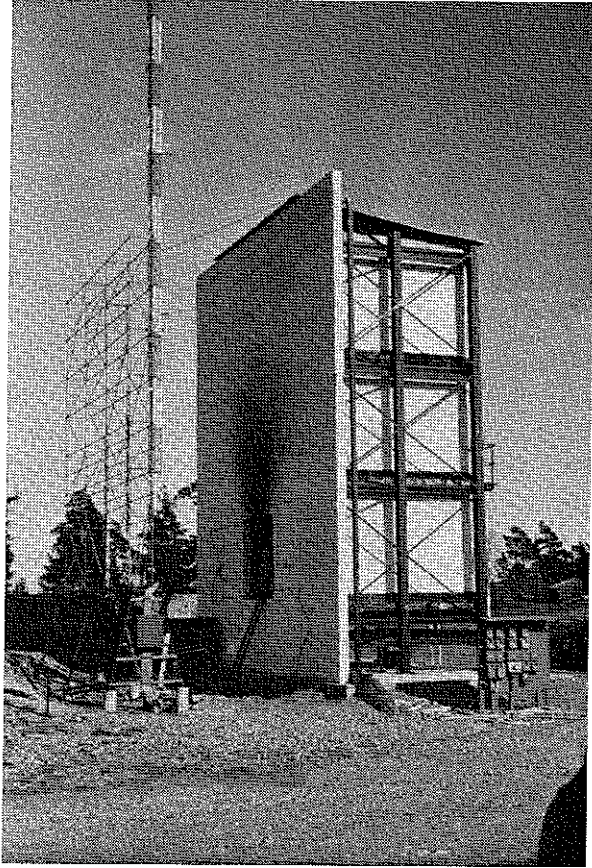


Fig. 12. Photograph of the test house used in the test series D to study the spread of fire and smoke along the external walls and through a vertical ventilation duct in the case of fire in a certain definite storey in a multi-storey building.

situated above. Calculations showed that the effect of the ventilation duct on the air flow factor was not to be disregarded, and a fictitious air flow factor, $(A\sqrt{H})_{\text{fict}}$, was therefore computed in accordance with the principles stated in Chapter 3. The magnitude of the corresponding correction can be seen from Table 8. The time graphs of the temperature of the combustion gases which were obtained from these tests, and which are expressed in terms of the mean value of the temperatures observed during the tests at 21 points in the enclosed space, are reproduced in Appendix 4. In order to give an idea of the dispersion about this mean value, the diagram relating to the test No. 2 shows the temperature-time curves for a point situated 45 cm above the floor and a point located 45 cm below the ceiling. Furthermore, the four diagrams in Appendix 4 also comprise the calculated curves which represent the varia-

tion in the temperature of the combustion gases with the time, as well as the time graphs of the rate of combustion in a dimensionless form which were used in the calculations.

It proved possible to bring the calculated and observed curves into close agreement by choosing the time graphs of the rate of combustion which were similar in shape in all the tests, and were based on a maximum rate of combustion $I_c = 330 \cdot A\sqrt{H} \cdot 2575 \text{ kcal} \cdot \text{h}^{-1}$. The value of the air flow factor used in the calculations was the value $(A\sqrt{H})_{\text{fict}}$, which was corrected so as to take account of the effect of the ventilation duct.

Summary

All the comparative calculations dealt with in the present chapter were based on the assumption that the energy conditions during the process of combustion can be characterized by an ignition phase in which the quantity of energy released per unit time increases from a zero value in accordance with a polygonal function of the time to a value that is given by the air flow factor. This phase is followed by a flame phase, during which the rate of combustion was supposed to be constant. After that the rate of combustion decreases to zero as a polygonal function of the time in the course of the cooling phase, during which the slopes of the individual sides of the polygon vary in a marked manner with the fire load. The higher the fire load, the slower the decrease in the rate of combustion. Of course, these assumptions give a simplified picture of the variation in the liberation of energy per unit time during the process of fire development. Thus, for most types of fire loads, it is to be expected that the plane part of the curve which represents the rate of combustion during the flame phase is rather to be regarded as the mean value of the quantity of energy released per unit time. This is illustrated in Fig. 13, which represents the variations in the observed rate of combustion (expressed in terms of the rate of reduction in the weight of fuel) and in the oxygen content of the combustion gases during the test No. 1 in the test series A. On account of technical difficulties in measurements, the values of the rate of reduction in the weight of fuel were somewhat uncertain immediately after the fuel had taken fire, as the rate of combustion was then liable to very wide variations. However, these values were confirmed by the fact that the oxygen content of the combustion gases in the enclosed space exhibited corresponding variations. Even when the curve which represents the variation in the rate of reduction in the weight of fuel with the time is known, our present knowledge of the relation between the rate of reduction in the weight of fuel and the rate of release of energy during the different phases of the process of fire development does not make it possible to determine the quantity of energy liberated per unit time during combustion. For the test No. 3 in the test series D, Fig. 14 shows three theoretical temperature-time curves calculated on the basis

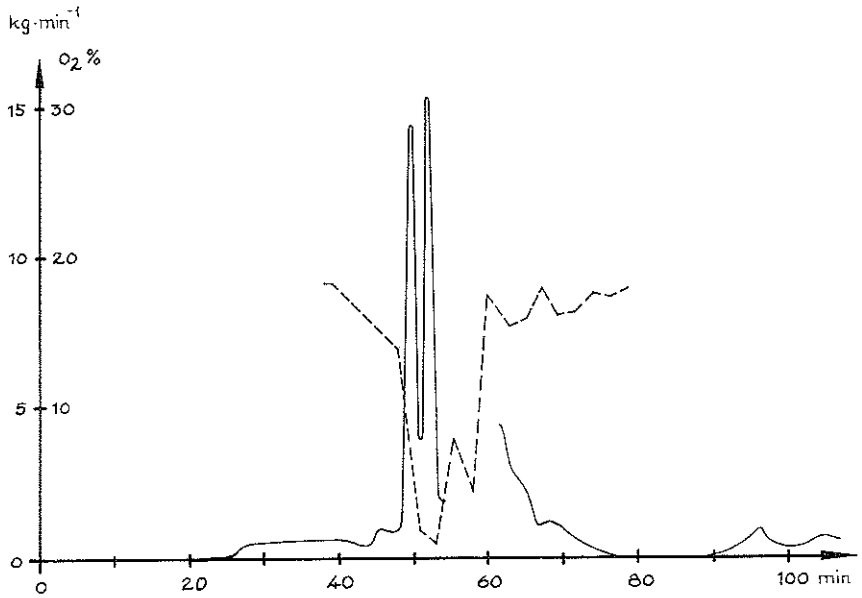


Fig. 13. Variation in the rate of combustion, in $\text{kg} \cdot \text{min}^{-1}$, with the time, t , determined by measuring the reduction in the weight of fuel in one of the tests comprised in the test series A, see Chapter 5. Furthermore, this figure also shows the time graph of the oxygen content of the combustion gases in the same test (dash-line curve). During the interval from the 55th to the 60th minute, the weighing of the fuel was disturbed by the fact that parts of the ceiling of the enclosed space fell down.

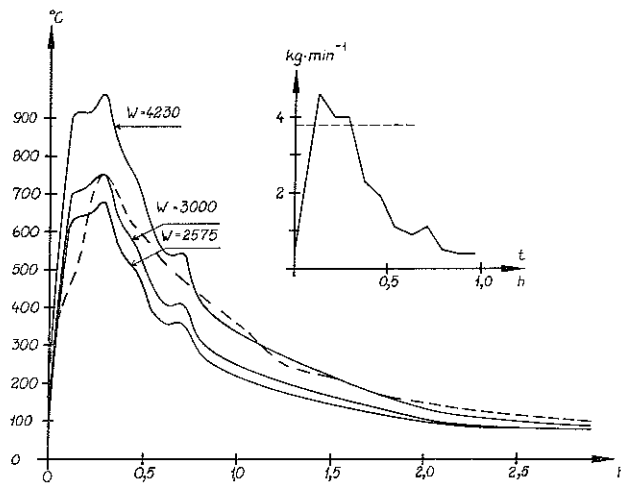


Fig. 14. Time graphs of the temperature of the combustion gases calculated for three different heat values of the fuel, viz., $W=2575$, 3000 , and $4230 \text{ kcal} \cdot \text{kg}^{-1}$ of wood, on the basis of an observed time graph of weight loss of fuel (inset). An experimental temperature-time curve is represented by the dash-line curve.

of a measured rate of weight loss. It was assumed that the heat value W corresponding to 1 kg of weight loss was constant during the whole process of fire development and equal to 2575, 3000 and 4230 kcal, respectively. The dash line curve represents the values observed in the test. The observed rate of reduction in the weight of fuel is represented in a separate diagram in fig. 14. As seen from this diagram, the maximum rate of reduction in the weight of fuel is closely in agreement with the theoretical value $R = 5.5 \times A/\bar{H} = 3.80 \text{ kg} \cdot \text{min}^{-1}$ (horizontal dash line). It is also seen from fig. 14 that the assumption of a constant value of W obviously is incorrect. A comparison between the curves indicates that the quantity of energy released per unit weight of fuel, at least during the first part of the cooling phase is greater than that during the flame phase.

Accordingly, the relative values of the rate of combustion obtained from the above comparative calculations cannot be directly expressed in terms of the rate of reduction in the weight of fuel, in $\text{kg} \cdot \text{min}^{-1}$. If the quantity of energy liberated per unit time is expressed directly in $\text{kcal} \cdot \text{min}^{-1}$, then this obviates the difficulty of determining the heat of combustion of the wood fuel during the various phases of the process of fire development.

A prerequisite in most of the calculations has been that the fire process is controlled by ventilation. This condition is far from being generally realized when it comes to actual fires. As a rule, a combination of small ventilation area and high fire load gives a process of fire development where the rate of burning is proportional to the air flow factor. If the fire load is low and the ventilation area large, the combustion will proceed as if in the open. This means that the rate of burning depends on the fire load density (fire exposed surface) and that an increase in ventilation will not result in a corresponding increase in rate of burning.

It is, however, impossible to say in advance if the process of fire development will be ventilation controlled or not even if the air flow factor and the fire load are known. The orientation and the distribution of the fuel in the enclosed space and the thickness or the porosity of the fuel will be a decisive factor in each particular case. An assumption that the rate of burning is determined by the air flow factor ought to give time-temperature curves which are on the safe side in practically every case. If such an assumption is made and the combustion in spite of this happens as in the open, i.e. is fuel bed controlled, the result will be a fire process of lower maximum temperature and, at least in some cases, of longer duration. The longer duration will not increase the severity of the fire to a corresponding degree. This is due to the fact that part of energy released by the combustion will be withdrawn from the enclosed space by the surplus air. In this way the temperature of the combustion gases will be lower compared to the case when the duration is the same but the process controlled by the ventilation.

To sum up, a comparative theoretical analysis of the results obtained from some thirty full-scale fire tests of the wood fuel type has been carried out in Chapter 5. The calculations made for this purpose covered relatively wide variations in fire load, opening factor, and hydraulic radius, as well as in the thermal properties of the structures bounding the enclosed space. As a result of these calculations, the time graph of the quantity of energy released per unit time may be assumed to be known within this range of variation.

6. Determination of general time graphs of quantity of energy released per unit time during different phases of process of fire development

In order to afford a basis for the calculation of the curve which represents the variation in the temperature of the combustion gases with the time during the process of fire development under varying conditions, it is necessary to systematize the time graphs of the rate of combustion which have been obtained in Chapter 5. A detailed investigation has been made of these graphs in order to find out how they vary with the fire load and with the opening factor. This investigation indicated the possibility of the simplification outlined in what follows.

If the ratio of the fire load, which is given from the outset, to the air flow factor, $A\sqrt{H}$, is constant, that is to say, if the duration of the fire is constant, then the time graph of the rate of combustion, expressed in a relative form in terms of the maximum rate of combustion, $330 \cdot A\sqrt{H} \cdot 2575 \text{ kcal} \cdot \text{h}^{-1}$, put equal to unity, is independent of the opening factor. This implies, for instance, that an enclosed space where the opening factor is $A\sqrt{H}/A_t = 0.01 \text{ m}^{1/2}$ and the fire load is $q = 5 \text{ Mcal} \cdot \text{m}^{-2}$ can be characterized by the same graph of the rate of combustion as an enclosed space where the opening factor is $0.04 \text{ m}^{1/2}$ and the fire load is $20 \text{ Mcal} \cdot \text{m}^{-2}$. Accordingly, the results of the calculations in Chapter 5, which show how the quantity of energy released per unit time varies with the time, can be represented by a graph which comprises a separate curve for each value of the ratio $qA_t/A\sqrt{H}$. In this connection, it is convenient to introduce the duration of the fire, T , defined as the duration of the flame phase, cf. Eq. (1.2),

$$T = qA_t / (1500A \cdot \sqrt{H}) \text{ h}$$

as the variable at which the graph shall be entered. In this formula for calculating the duration of the flame phase, the product of the constant 330 in the expression $R = 330 \cdot A\sqrt{H} \text{ kg} \cdot \text{h}^{-1}$ and the heat value of the wood fuel, i.e. $4.5 \text{ Mcal} \cdot \text{kg}^{-1}$, has been put equal to 1500. For the values of the duration of the fire defined in this way, $T = 0.1, 0.2, 0.3, 0.5, 0.75, 1.0, 1.5$ and 2.0 h , which correspond to the respective fire loads $(150, 300, 450, 750, 1125, 1500, 2250, \text{ and } 3000) \cdot A\sqrt{H}/A_t \text{ Mcal} \cdot \text{m}^{-2}$ of the total surface area bounding

the enclosed space, Fig. 15 shows the variation in the rate of combustion with the time.

In order to make it easier to check the agreement between the total quantity of energy liberated during the process of fire development and the fire load, which is given from the beginning, and since a more accurate representation would be illusory, considering the character of the available data, the curve form has been assumed to be polygonal, just as in the comparative calculations in Chapter 5. In Fig. 15, $330A\sqrt{H} \cdot 2575 \text{ kcal} \cdot \text{h}^{-1}$ has been put equal to unity. The respective areas between the above-mentioned curves and the axis of time shall therefore be $\frac{1}{330 \times 2575}$ (150, 300, 450, 750, 1125, 1500, 2250, and 3000) area units. In the relevant Swedish regulations, the quantity T , determined by the relation

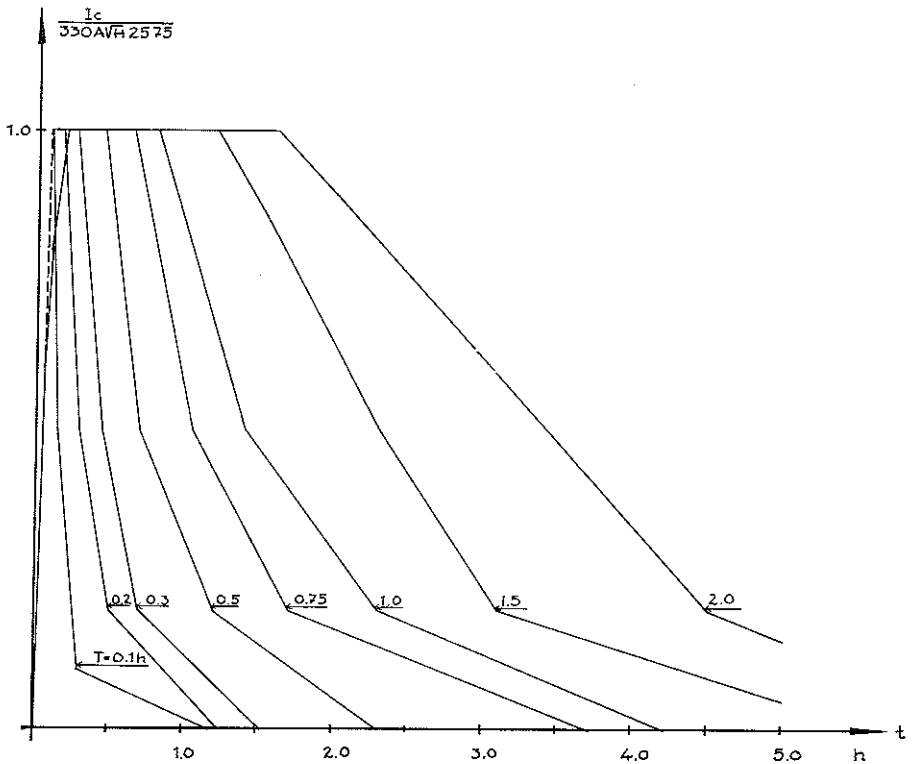


Fig. 15. Time graphs of the energy released per unit time in the process of combustion, I_c , expressed in a relative form by putting $330 \cdot 2575 \cdot A\sqrt{H}$ equal to unity. The eight curves shown in this figure correspond to different values of the duration of the fire defined as the duration of the flame phase by the expression $T=q \cdot A_f / (1500 \cdot A \cdot \sqrt{H})$. The dash-line portion of the curve for the ignition phase belongs to the curves relating to the lowest four values of the duration of the fire.

$$T = qA_i / (25A\sqrt{H}) \quad \text{min}$$

designates the instant which marks the end of the flame phase and the beginning of the linear cooling phase. On the basis of the experiences derived from the comparative theoretical analyses, the instant at which the rate of combustion begins to decrease has been chosen so as to be slightly anterior to the instant defined by T . For the values of the duration of the fire $T=6, 12, 18,$ and 30 min, the time graphs of the rate of combustion during the ignition phase have been given a slightly different shape, which implies that the fuel takes fire within a shorter period of time.

7. Calculation of time graphs of temperature of combustion gases for characteristic types of enclosed spaces varying in opening factor and in fire load

The time graphs of the rate of combustion represented in a relative form in Fig. 15 for fires of the wood fuel type in enclosed spaces are utilized in the present chapter as a basis for the calculation of complete time graphs of the temperature of the combustion gases. This is done for varying values of the opening factor and the fire load in enclosed spaces of the seven types dealt with in what follows, which differ in respect of the bounding structures.

Type A enclosed space

Bounding structures.

All the surfaces which bound the enclosed space are supposed to consist of a material, 20 cm in thickness, whose thermal properties are characterized by the average values given below, which apply to structural materials of such types as concrete, brick, and lightweight concrete.

Thermal conductivity, $\lambda = 0.7 \text{ kcal} \cdot \text{m}^{-1} \cdot \text{h}^{-1} \cdot \text{°C}^{-1}$.

Product of the specific heat and the weight per unit volume,

$$c \cdot \gamma = 400 \text{ kcal} \cdot \text{m}^{-3} \cdot \text{°C}^{-1}.$$

The same data on the properties of materials had also been used for the calculation of those temperature-time curves for the flame phase of the process of fire development which have been published in the Swedish Building Regulations 1967 and in the Draft Specification "Aluminium Structures".

Type B enclosed space

Bounding structures.

Concrete, 20 cm in thickness.

Thermal conductivity, $\lambda = 1.4 \cdot e^{-0.001 \cdot s} \text{ kcal} \cdot \text{m}^{-1} \cdot \text{h}^{-1} \cdot \text{°C}^{-1}$ [1].

Enthalpy, I , see Fig. 17.

Type C enclosed space

Bounding structures.

Lightweight concrete, 20 cm in thickness.

Weight per unit volume, $\gamma = 500 \text{ kg} \cdot \text{m}^{-3}$.

Thermal conductivity, λ , see Fig. 16.

Enthalpy, I , see Fig. 17.

The specific heat and the weight per unit volume of the lightweight concrete are assumed to be independent of the temperature. Consequently, the enthalpy-temperature curve is rectilinear. The variation in the thermal conductivity, λ , with the temperature is based on a determination which has been made in connection with the test series D described in Chapter 5.

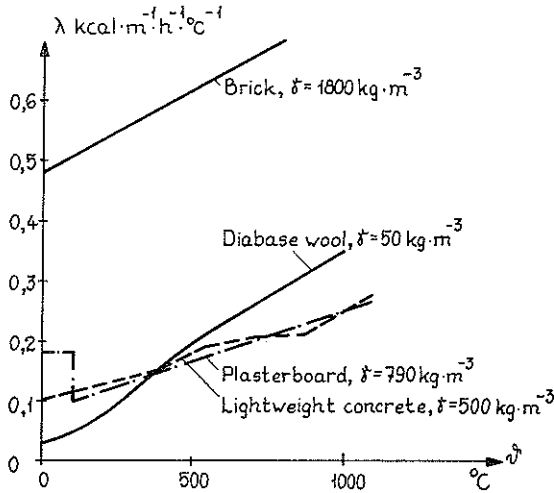


Fig. 16. Relations between the thermal conductivity, λ , and the temperature, θ , used in the calculations for brick, diabase wool, plasterboard, and lightweight concrete.

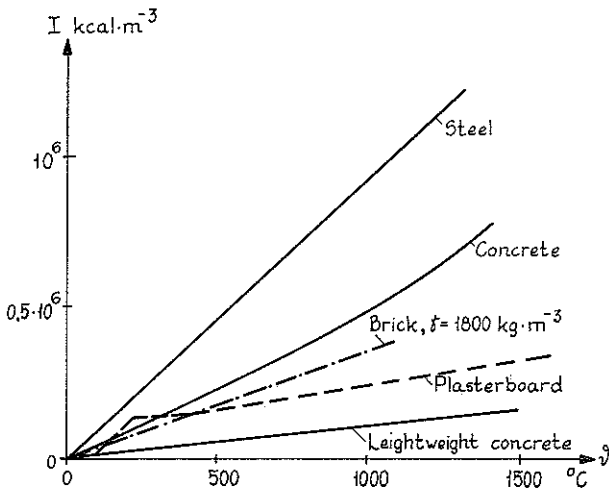


Fig. 17. Relations between the enthalpy, I , and the temperature, θ , used in the calculations for steel, concrete, brick, plasterboard, and lightweight concrete.

Type D enclosed space

Bounding structures.

Concrete, 50 per cent of the total bounding surface area.

Lightweight concrete, 50 per cent of the total bounding surface area.

Thicknesses, weight per unit volume, and thermal properties as in the Type B and Type C enclosed spaces, respectively.

Type E enclosed space

Bounding structures.

Lightweight concrete, 50 per cent of the total bounding surface area.

Thickness, weight per unit volume, and thermal properties as in the Type C enclosed space.

Concrete, 33 per cent of the total bounding surface area.

Thickness and thermal properties as in the Type B enclosed space.

Other structural components, 17 per cent of the total bounding surface area, enumerated in the order from the interior to the exterior:

Plasterboard panel, 13 mm in thickness.

Weight per unit volume, $\gamma = 790 \text{ kg} \cdot \text{m}^{-3}$.

Diabase wool, 10 cm in thickness.

Weight per unit volume, $\gamma = 50 \text{ kg} \cdot \text{m}^{-3}$.

Brickwork, 20 cm in thickness.

Weight per unit volume, $\gamma = 1800 \text{ kg} \cdot \text{m}^{-3}$.

Thermal properties of plasterboard, diabase wool, and brick, see Figs. 16, 17, and 18.

The enthalpy-temperature curve chosen for brick is based on a value of the specific heat which is supposed to be independent of the temperature. In reality, the specific heat of brick slightly varies with the temperature [1]. However, in the present case, the values of the temperature rise in the brickwork, which is most remote from the surface exposed to fire, are so low that

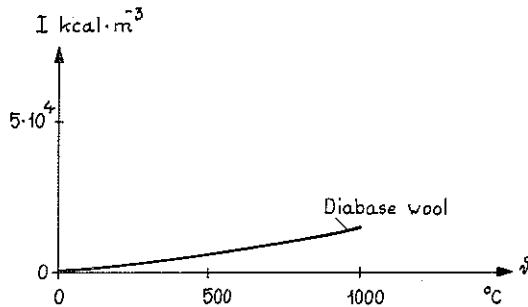


Fig. 18. Relation between the enthalpy, I , and the temperature, ϑ , used in the calculations for diabase wool.

the effect of this variation may be disregarded. The variation in the enthalpy of diabase wool with the temperature is based on that relation between the specific heat and the temperature which was published in [1]. The thermal properties of plasterboard are based on the curves which were published in [19]. It is assumed that the plasterboard panels will not fall down or disintegrate.

The values of the thermal conductivity, λ , of brick and diabase wool were taken from [1].

Type F enclosed space

Bounding structures.

Sheet steel, 2 mm in thickness, 80 per cent of the total bounding surface area.

Concrete, 20 cm in thickness, 20 per cent of the total bounding surface area.

Thermal properties as in the Type B enclosed space.

Curves representing the variations in the enthalpy and in the thermal conductivity of sheet steel with the temperature, see Figs. 17 and 19, respectively.

This type of enclosed space corresponds to a storage space, or the like with a sheet steel roof, sheet steel walls, and a concrete floor.

Type G enclosed space

Bounding structures.

Concrete, 20 per cent of the total bounding surface area.

Thickness and thermal properties as in the Type B enclosed space.

Other structural components, 80 per cent of the total bounding surface area, enumerated in the order from the interior to the exterior:

Two plasterboard panels, 2×13 mm in thickness.

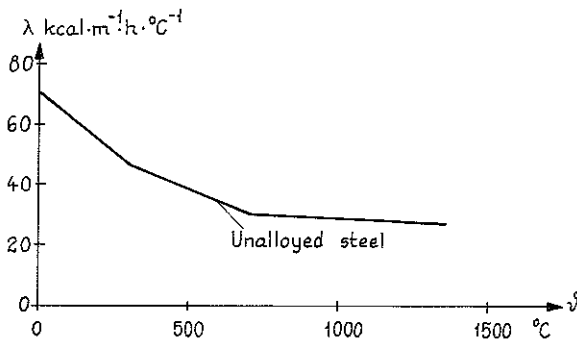


Fig. 19. Relation between the thermal conductivity, λ , and the temperature, θ , used in the calculations for unalloyed steel.

Weight per unit volume, $\gamma = 790 \text{ kg} \cdot \text{m}^{-3}$.

Cavity, 10 cm in width.

Two plasterboard panels, $2 \times 13 \text{ mm}$ in thickness.

Thermal properties of plasterboard, see Figs. 16 and 20.

This structure represents a type of partition which is becoming more and more common, and which consists of two plasterboard panels on each side, supported on steel stud framing. It is assumed that the steel studs have no thermal conductivity and no thermal absorptivity.

The test results published in [19] have shown that plasterboard panels which are not fibre-filled disintegrate when their temperature on the side that is not exposed to fire reaches about 550°C . However, this does not apply to the outermost, i.e. the fourth, plasterboard panel. This panel is in contact with the air, which has a temperature of 20°C . Therefore, this panel never reaches a surface temperature of 550°C . In fact, tests have demonstrated that a plasterboard panel in this position disintegrates when the temperature at its centre rise to about 750°C . These criteria have been used in calculating the time graph of the combustion gas temperature for enclosed spaces of the type in question. The calculations were discontinued when they had been carried out to the instant at which the fire was expected to burn through the wall, that is to say, after all four plasterboard panels had disintegrated.

As may be seen from Fig. 20, which was taken from [19], the variation in the enthalpy of plasterboard with the temperature is dependent on whether

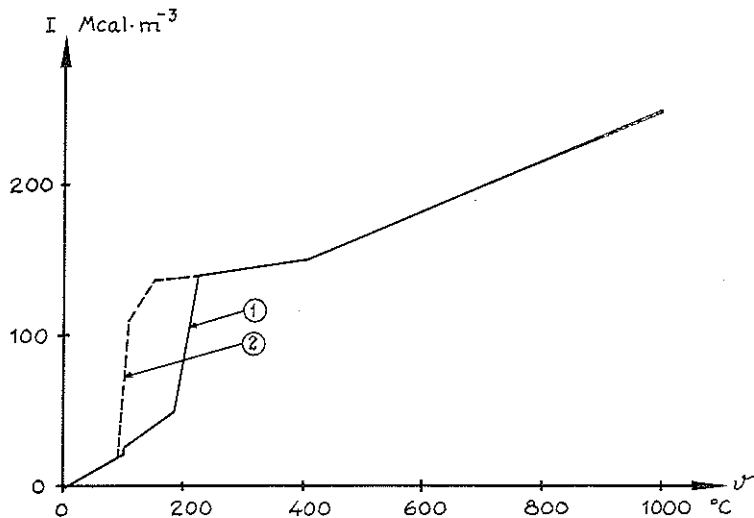


Fig. 20. Relation between the enthalpy, I , and the temperature, θ , used in the calculations for plasterboard. Curve 1: High rate of temperature rise. Curve 2: Low rate of temperature rise.

the rate of temperature rise is high or low. This circumstance was taken into account in the calculations by assuming a high rate of temperature rise for that plasterboard panel which is nearest to the fire and a low rate of temperature rise for all the other plasterboard panels. Since the structural transformations of plasterboard require an additional quantity of heat that cannot be recovered, the enthalpy-temperature curve during the cooling period is not identical with that during the heating period.

In the calculations, it was assumed that the variation in the enthalpy with the temperature during the cooling period is represented by a straight line which corresponds to a constant value of the product $c \cdot \gamma = 200 \text{ kcal} \times \text{m}^{-3} \cdot \text{°C}^{-1}$.

For the surfaces exposed to fire in the enclosed spaces of all the types dealt with in the present chapter, the coefficient of heat transfer, α_i , was calculated by means of Eq. (2.7a), where it was assumed that $\epsilon_{fl} = 0.7$ and $\epsilon_i = 0.8$ for the Type A to the Type E enclosed spaces, and for the Type G enclosed space. These values give $\epsilon_{res} \sim 0.60$. For the Type F enclosed space, the calculations were based on three values of ϵ_i , viz., 0.1, 0.4, and 0.8. Hence, for $\epsilon_{fl} = 0.7$, the respective values of ϵ_{res} were found to be 0.1, 0.35, and 0.6. For the exterior surfaces of the structures bounding the enclosed space, the coefficient of heat transfer, α_u , for the Type A to Type E enclosed spaces, and for the Type G enclosed space, was supposed to vary with the surface temperature, ϑ_u , in accordance with Eq. (2.8), while its value for the Type F enclosed space was supposed to vary in conformity with the relation

$$\alpha_u = 7.5 + \frac{4.96 \cdot \epsilon_{res}}{\vartheta_u - \vartheta_0} \left[\left(\frac{\vartheta_u + 273}{100} \right)^4 - \left(\frac{\vartheta_0 + 273}{100} \right)^4 \right] \text{ kcal} \cdot \text{m}^{-2} \cdot \text{h}^{-1} \cdot \text{°C}^{-1} \quad (7.1)$$

where ϵ_{res} was chosen in the same way as in the above-mentioned calculation of α_i .

The variation in the specific heat, c_p , of the combustion gases with the temperature is shown in Fig. 21 [3]. For the rest, the calculations were based on the principles which have been stated in Chapters 2 and 4.

The input values used in the calculations were only the opening factor $A \cdot \sqrt{H}/A_t$, in $\text{m}^{1/2}$, and the fire load, q , in $\text{Mcal} \cdot \text{m}^{-2}$ of bounding surface area. If the radiation term, I_R , is disregarded, then Eq. (2.1) becomes independent of dimensions. In other words, if the values of $A \cdot \sqrt{H}/A_t$ and q are given, then the result will be independent of the terms A , H , and A_t entering into the opening factor. However, I_R is proportional to the total opening area, A , and, in order that I_R may be taken into account, it is necessary to specify the above-mentioned terms. This has been done in the calculations dealing with test results in Chapter 5. For the determination of the total

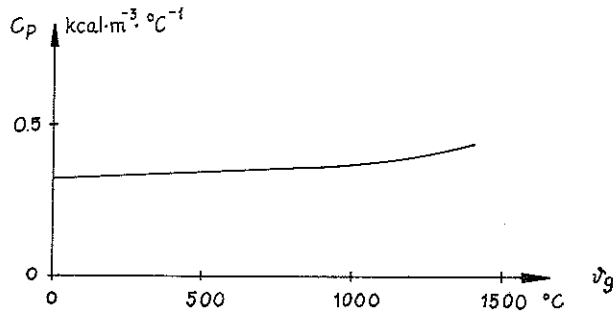


Fig. 21. Relation between the specific heat of the combustion gases, c_p , and their temperature, ϑ_g , used in the calculations.

opening area, A , in the calculations described in the present chapter, it was supposed that the dimensions of the enclosed space were the same as those which had been assumed as a basis for the curves published in the Swedish Building Regulations 1967, viz., a total bounding surface area $A_t=10,000 \text{ m}^2$ and a square opening. Consequently, the ratio of the total opening area to the total bounding surface area, A/A_t , was in all cases lower than those values which can be expected to be met with in ordinary buildings, and all the results will therefore be on the safe side. The value $A_t=10,000 \text{ m}^2$ was used only to determine the value of the ratio A/A_t , which was then substituted in the term I_R in the equation of heat balance. For a value of the opening factor $A \cdot \sqrt{H}/A_t=0.04 \text{ m}^{1/2}$, Table 9 gives the respective values of the ratio A/A_t , which correspond to $A_t=10,000 \text{ m}^2$ and $A_t=1 \text{ m}^2$ on the assumption that the opening is square, or that it has a height $H=1 \text{ m}$.

Table 9. Values of the ratio A/A_t .

	Square opening	$H=1 \text{ m}$
$A_t=1 \text{ m}^2$	0.075	0.04
$A_t=10,000 \text{ m}^2$	0.012	0.04

In order to illustrate the consequence of this variation in the ratio A/A_t , Fig. 22 shows the temperature-time curve for an enclosed space characterized by an opening factor $A \cdot \sqrt{H}/A_t=0.04 \text{ m}^{1/2}$, a fire load $q=30 \text{ Mcal} \cdot \text{m}^{-2}$, as well as by the two extreme values of the ratio A/A_t , i.e. 0.012 and 0.075. As is seen from this graph, the effect of the difference in the value of the ratio A/A_t is practically negligible.

Temperature-time curves have been calculated for each one of the seven enclosed spaces, Types A to G, for varying values of the duration of the fire and the opening factor. As regards the relation between the duration of the fire and the fire load, reference is made to Chapter 6. For the Type A to the

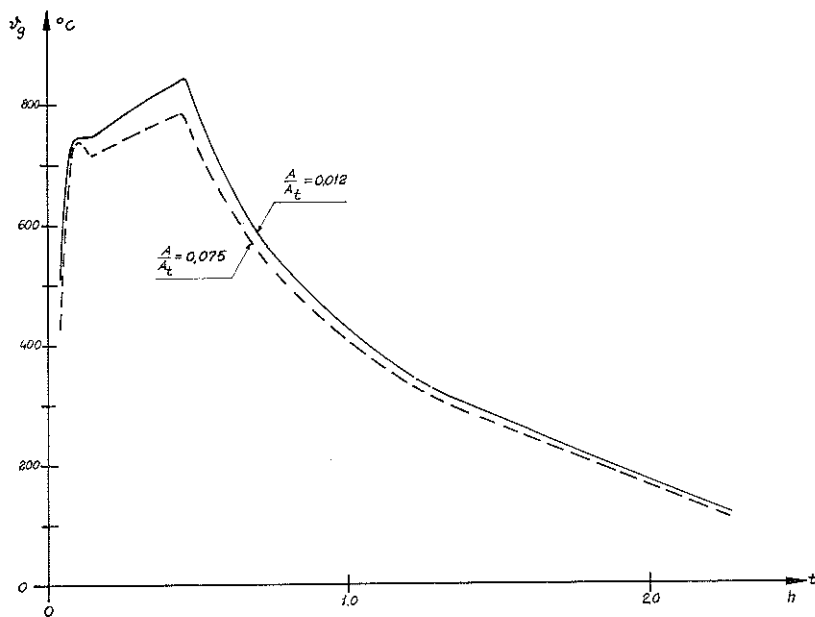


Fig. 22. Calculated temperature-time curves for the Type A enclosed space. Opening factor $A\sqrt{H}/A_t = 0.04 \text{ m}^{1/2}$. Fire load $q = 30 \text{ Mcal} \cdot \text{m}^{-2}$ of bounding surface area. Ratio A/A_t set equal to 0.012 and 0.075, respectively.

Type E enclosed space, as well as for the Type G enclosed space, the temperature-time curves were computed on the basis of 6 different values of the opening factor, viz., $A \cdot \sqrt{H}/A_t = 0.01, 0.02, 0.04, 0.06, 0.08,$ and $0.12 \text{ m}^{1/2}$. For each of these values the curves were computed for 8 different values of the duration of the flame phase of the fire for which the time graphs of the rate of combustion have been constructed in Chapter 6. This means that 48 temperature-time curves have been obtained for each type of enclosed space. In the case of the Type F enclosed space, the calculations were carried out for 3 different values of the resultant emissivity. Furthermore, for each one of these values, use was made of 5 different values of the opening factor, viz., $0.01, 0.02, 0.04, 0.08,$ and $0.12 \text{ m}^{1/2}$. For each one of these combinations of values, the curves were calculated on the basis of 5 different values of the fire load corresponding to 5 different values of the duration of the flame phase, viz., $0.1, 0.3, 0.5, 1.0,$ and 2.0 h , if computed by means of Eq. (2.1). All these curves are shown in Appendix 5. The curves are denoted by the symbols A1 to G6, where the letter A refers to the Type A enclosed space, etc. All these curves are represented in an approximate form after smoothing out the irregularities which were caused by the polygonal shape of the time graphs of the rate of combustion. Furthermore, in order to render the graphs in Appendix 5 more readily legible, that part of each one of the curves which

represents the ignition phase was based on that ascending branch of the time graph of the rate of combustion which corresponds to the lower four values of the fire load. The exact results of the calculations are reproduced in tabular form in Appendix 6. In the case of the Type G enclosed space, where the calculation of the temperature-time curves was carried out with reference to the instants when the plasterboard panels fell down, each one of these instants is marked with a circle on the corresponding curve. When a plasterboard panel falls down, this corresponds in the calculations to an instantaneous temperature drop in the enclosed space, as may be seen from the relevant curves.

In practical design, it should be possible to proceed in three steps, viz., first, to choose that type of enclosed space which is most closely similar in respect of the thermal properties of the bounding structures to the case under consideration; second, to determine the opening factor and the fire load; and third, to interpolate linearly between the values given in the tables in Appendix 6. If, instead of using this procedure, the designer chooses a curve which is determined without interpolation so as to be on the safe side, that is to say, if he chooses the next higher values of the opening factor and the fire load, then this will probably not involve errors which are too great. In order to afford a basis for the choice of the type of enclosed space, the temperature-time curves which correspond to an opening factor $A \cdot \sqrt{H}/A_t = 0.04 \text{ m}^{1/2}$ and to a fire load of $60 \text{ Mcal} \cdot \text{m}^{-2}$ of bounding surface area are represented in Fig. 23 for the Type A to the Type F enclosed spaces. For comparison, this graph also reproduces the standard ISO temperature-time curve and the curve for an opening factor of $0.04 \text{ m}^{1/2}$ published in the Swedish Building Regulations 1967.

A comparison between the temperature-time curves which correspond to the different types of enclosed spaces in Fig. 23 shows that the maximum difference in the maximum temperature amounts to about 400°C . The Type C enclosed space, which is provided with lightweight concrete bounding structures, exhibits markedly higher temperatures than the other types of enclosed spaces comprised in the present calculations. The lowest maximum temperature was obtained in the case of the Type F enclosed space ($\epsilon_{\text{res}} = 0.60$), which is equipped with bounding structures made of sheet steel, 2 mm in thickness. However, it is seen from Fig. 23 that the resultant emissivity for radiation between the flames and a sheet steel surface produces a substantial effect on the magnitude of the maximum temperature. If ϵ_{res} is supposed to change from 0.6 to 0.1, then the corresponding difference in the maximum temperature is slightly over 200°C , other conditions being equal. Therefore, it is important that the heat transfer conditions, and particularly the resultant emissivity, should be accurately determined in the calculation of the temperature-time curve for an enclosed space of this type.

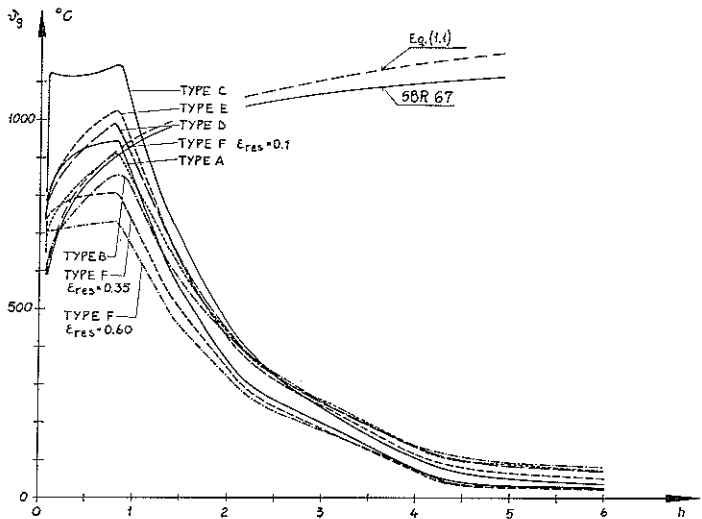


Fig. 23. Temperature-time curves for the Type A to the Type F enclosed spaces. Opening factor $A\sqrt{H}/A_t=0.04 \text{ m}^{1/2}$. Fire load $q=60 \text{ Mcal} \cdot \text{m}^{-2}$ of bounding surface area. Furthermore, this graph also shows the respective temperature-time curves calculated by means of Eq. (1.1) and determined in conformity with the Swedish Building Regulations 1967 (SBR 67) for an opening factor $A\sqrt{H}/A_t=0.04 \text{ m}^{1/2}$.

With the exception of the Type F, it is the Type B enclosed space, which is bounded by concrete walls, that exhibits the lowest maximum temperature. This is due to the relatively high thermal conductivity and the great heat capacity of the concrete. On the other hand, since the large quantity of heat that is stored in the concrete is partly transferred back to the enclosed space during the cooling period, comparatively high temperatures are obtained in the course of the cooling phase.

The temperature-time curves published in the Swedish Building Regulations 1967 and in the Draft Specification "Aluminium Structures" relate to "enclosed spaces bounded by wall, roof or ceiling, and floor structures which are made of brickwork, concrete, or lightweight concrete as a material that is predominant in thermal respects". As has previously been mentioned, these curves had been calculated on the basis of those characteristics of the bounding structures which were used to describe the Type A enclosed space. Moreover, for guidance, the comments on the Draft Specification "Aluminium Structures" also comprise temperature-time curves for an enclosed space which is bounded by walls made of mineral wool. In addition, it is shown how the temperature-time curve is influenced by a concrete wall, 20 cm in thickness, which is situated in the interior of the enclosed space. By examining Fig. 23, it will readily be understood that a further differentiation of the above-mentioned Swedish standard temperature-time curves according to the thermal characteristics of the bounding structures would be desirable.

In order that the temperature-time curves for the cooling phase which have been determined in the present publication might be compared with the corresponding Swedish standard curves, Fig. 24 shows the temperature-time curves for the Type A enclosed space calculated on the basis of an opening factor $A \cdot \sqrt{H}/A_t = 0.04 \text{ m}^2/\text{m}^2$, together with the Swedish standard temperature-time curves for the cooling phase determined on the assumption that the rate of temperature decrease is $10^\circ\text{C} \cdot \text{min}^{-1}$. The ascending branches of the curves are identical because the curves for the Type A enclosed space are based on the same assumptions as the standard curves. The linear temperature-time curves for the cooling phase, which start from the ascending branch at the time T , calculated by means of Eq. (1.2), are represented by dash lines in Fig. 24. As is seen from this graph, the calculated curves result in a rate of cooling which is higher or lower than the standard rate of temperature decrease, $10^\circ\text{C} \cdot \text{min}^{-1}$, according as the duration of the process of fire development is shorter or longer, respectively.

Thus, if the duration of the fire is comparatively short, then an application of the temperature-time curves which have been computed in the present publication gives considerably more favourable results, i.e. lower temperatures, than the standard rules which are at present in force in Sweden. For instance, the temperature-time curve for the cooling phase in fires of short duration is a decisive factor in determining the temperatures of unprotected steel structures, as has already been shown in an example which was adduced under

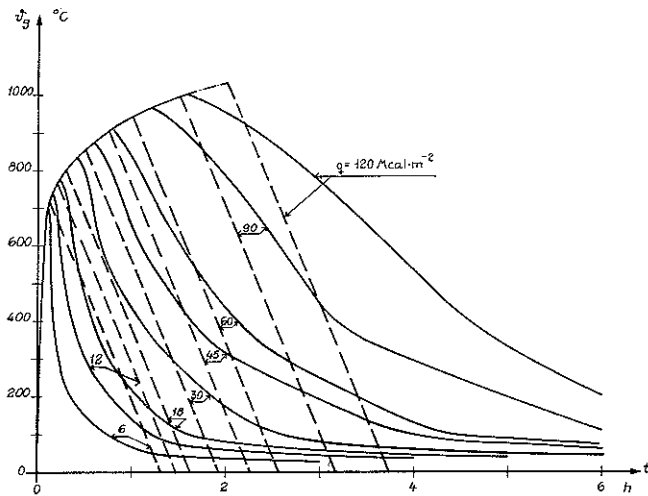


Fig. 24. Temperature-time curves for the Type A enclosed space. Opening factor $A\sqrt{H}/A_t = 0.04 \text{ m}^2/\text{m}^2$. (Full-line curves.) Curves for the cooling phase corresponding to a rate of decrease in temperature of $10^\circ\text{C} \cdot \text{min}^{-1}$ stipulated in the relevant Swedish regulations. (Dash-line curves.)

the heading "Introduction". However, if the duration of the fire is relatively long, then the calculated temperature-time curves are less favourable, i.e. they give higher temperatures, than the curves stipulated in the Swedish regulations. All the same, since a given structure that is exposed to fire has already been subjected to the action of high temperatures for a long time before the beginning of the cooling phase, the difference between these curves in the latter case will have a comparatively slight effect on practical design.

8. Summary

The point of departure of the present investigation was the fact that the results obtained in recent years from research in the field of structural fire engineering had made it possible to carry out reliable calculations of the load bearing and separating capacity in the design of structural components exposed to fire. Such design calculations must be based on the knowledge of the temperature-time curve which covers the whole process of fire development. However, further progress towards realistic structural fire engineering design was impeded by the circumstance that it was not possible to make a theoretical determination of the temperature-time curve for the cooling phase of the process of fire development under known external conditions. Up to now, the research in this field has evolved methods for calculating the variation in the temperature with the time during the flame phase of the process of fire development on the basis of known external conditions, whereas the cooling phase has not been dealt with in this connection.

In consequence of this gap in our knowledge, the methods for determining the temperature-time curves for the flame phase and the cooling phase stipulated in the Swedish Building Regulations 1967 are widely different in degree of accuracy. The determination of the temperature-time curve for the flame phase shall be based on the fire load which characterizes the case under consideration, as well as on the shape and the dimensions of the openings in the enclosed space. For the cooling phase, on the other hand, it is stipulated only that the rate of temperature decrease shall be set equal to $10^{\circ}\text{C} \cdot \text{min}^{-1}$, irrespective of the actual conditions which characterize the case in question. This undifferentiated characterization of the cooling phase is particularly unfavourable to structures which possess a low thermal inertia, e.g. non-insulated or slightly insulated load-bearing steel structures. It was therefore considered to be urgently required to undertake an investigation in order to find out whether a theoretical determination of the temperature-time curve for the cooling phase would be possible.

The theoretical calculations in the present publication are founded on a basic equation of heat balance in an enclosed space which has been deduced by Kawagoe and Sekine, as well as by Ödeen. This equation states that the quantity of heat, I_c , which is released per unit time during the process of combustion is at any instant equal to the sum of the quantities of heat which

are withdrawn per unit time in different ways from the enclosed space. Heat is ordinarily abstracted from the enclosed space by heat transfer through the structures which bound the enclosed space (term I_W in the equation of heat balance), by radiation through the openings in the enclosed space (term I_R), and by the replacement of combustion gases by cold air (term I_L).

In order to extend the range of application of the equation of heat balance so that it might cover the whole process of fire development, it was necessary to solve two fundamental problems. In the first place, the quantity of heat released per unit time had to be determined as a function of the time for the entire process of fire development. In the second place, the expression for I_L which had been deduced previously, and which was applicable to the flame phase only, had to be extended and supplemented.

The study of the last-mentioned problem resulted in an expression for I_L which was based on the magnitude of the heat transfer by convection through the openings in the enclosed space. The rates of gas and air flow involved in this process were calculated in two steps, viz., first by determining the velocity distribution of gas flow in a vertical opening by which two masses of gas differing in density are separated from each other, and second, by satisfying the condition that the net exchange of gases between the enclosed space and its surroundings shall be equal to the difference between the quantity of gas produced and the quantity of air consumed in the process of combustion. After that, it was possible to determine I_L directly as the difference in heat content between the outgoing gases and the incoming air. It was found that I_L was approximately proportional to the temperature of the combustion gases and to the air flow factor $A \cdot \sqrt{H}$.

Since no physical basis is available which could enable the quantity of energy liberated per unit time during the process of fire development to be determined as a function of the time, a study of the literature was carried out with a view to an analysis of full-scale fire tests. For the tests where the external conditions were stated in a sufficiently precise manner, comparative calculations of temperature-time curves were made by means of a computer.

A tentatively chosen time graph of the quantity of energy liberated per unit time was used for this purpose. The time graph in question was varied until the agreement between the observed and calculated temperature-time curves became as close as possible. The only requirement to be fulfilled in this connection was that the total quantity of energy released during the whole process of fire development should be equal to that which was available in the fuel from the outset. When all those tests which were suited for this study had been examined, it was possible to systematize the results of the study in such a way that the time graph of the quantity of energy released per unit time during the process of fire development might generally be assumed to be known.

This procedure was primarily justified by the consideration that an error, if any, could only be involved in the time graph of the quantity of energy liberated per unit time, since the total magnitude of this quantity is determined by the fire load, i.e. by the quantity of energy which is available from the beginning.

The computer programme which was used for the calculation of the temperature-time curves has a far-advanced general validity. One of the features of this programme is that it affords a possibility of taking into account various factors, viz., first, those thermal properties of the materials entering into the structures bounding the enclosed space which are dependent on the temperature, second, the variations in the dimensions of the openings during the process of fire development, third, the moisture content of the bounding structures, and fourth, the effects of heat-absorbing structures in the interior of the enclosed space. This programme can be used for enclosed spaces which are bounded by structures of up to three different types at the same time, and one of these structures may be built of up to three different materials.

Moreover, a modified programme has been prepared for enclosed spaces provided with plasterboard panel walls, which are assumed under certain definite conditions to disintegrate during the fire.

The time graphs of the quantity of energy liberated per unit time which had been obtained by means of the method outlined in the above were used to calculate the time graphs of the temperature of the combustion gases during the process of fire development. The latter time graphs were computed on the assumption of different values of the fire load and the opening factor for seven types of enclosed spaces which differ in respect of the bounding structures. The results of these calculations are represented in graphs as well as in tables.

In carrying out the comparative theoretical analyses, it was possible to discuss to a limited extent the effects produced on the temperature-time curve of the process of fire development by some quantities which do not directly enter into the equation of heat balance, with the result that their effects on this process must be determined in each individual case. In addition to the size and the shape of the openings, the factors which may be expected to be of importance in this connection comprise, among others, the porosity of the fuel and its distribution in the enclosed space, the moisture content of the fuel, and the magnitude of the fire load. For future research in this field, it may be urgently recommended to make a study of the effects produced by these and other parameters on the quantity of energy released per unit time in the process of combustion, and hence also on the temperature-time curve, which is dependent on this quantity.

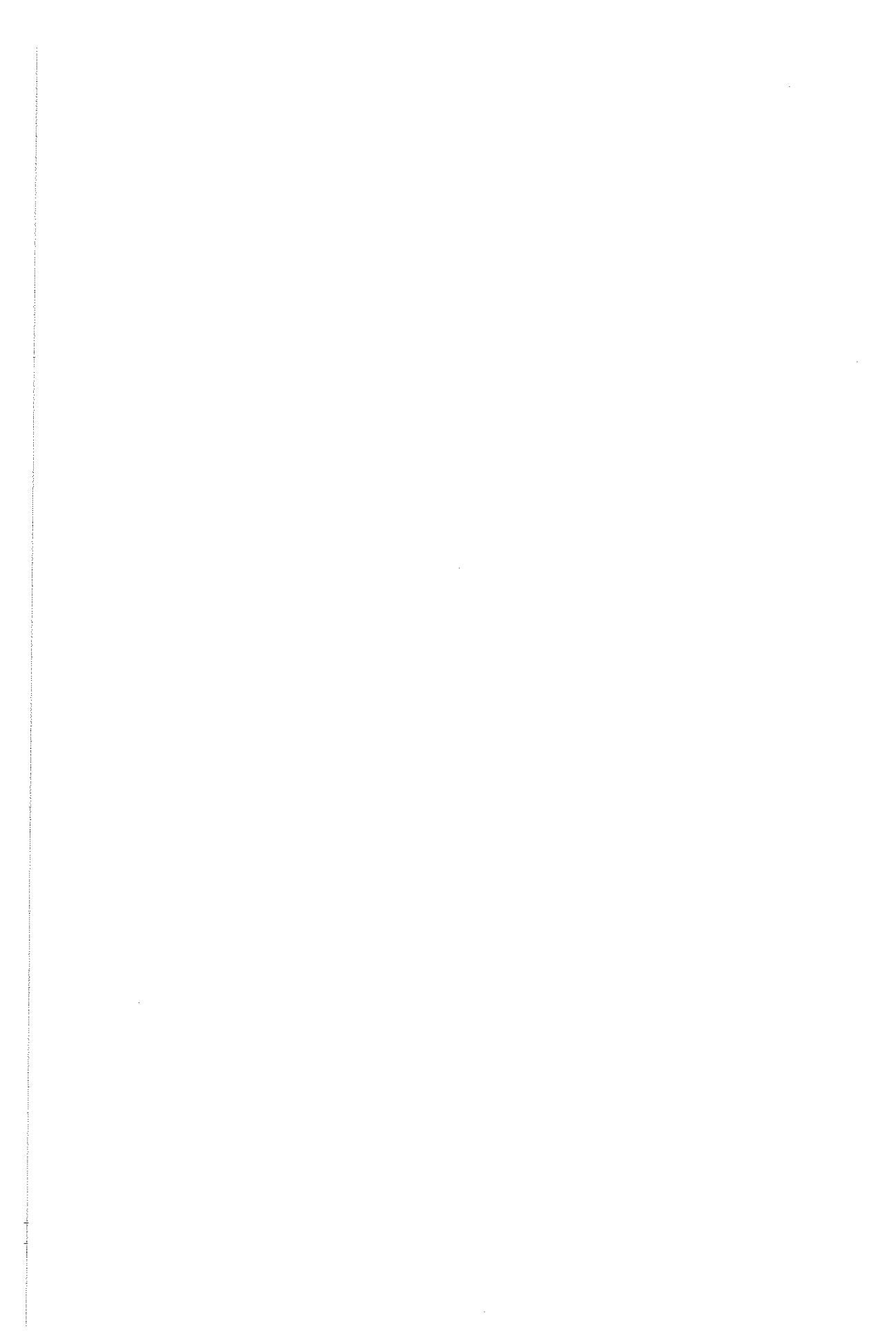
Acknowledgements

The Authors wish to express their heartfelt gratitude to Professor *Ove Pettersson*, Head of the Division of Structural Mechanics and Concrete Construction, Lund Institute of Technology, Lund, Sweden, who has provided the impetus to the investigation described in the present publication, and whose ever-active support has greatly contributed to the accomplishment of this task. Our thanks are furthermore due to Mr. *Ulf Hårdner*, Miss *Yvonne Fransson*, Miss *Kerstin Svensson*, and Miss *Lena Öberg*, for their valuable collaboration in editing the manuscript, and to Mr. *Ilya Cyon*, for the translation of the manuscript into English.

References

1. PETERSSON, O.: Structural Fire Engineering Research Today and Tomorrow. Acta Polytechnica Scandinavica. Civil Engineering and Building Construction. Series No. 33. Stockholm 1965.
2. KAWAGOE, K. & SEKINE, T.: Estimation of Fire Temperature-Time Curve in Rooms. Building Research Institute. Occasional Report. No. 11. Tokyo 1963.
3. ÖDEEN, K.: Theoretical Study of Fire Characteristics in Enclosed Spaces. Division of Building Construction, Royal Institute of Technology. Bulletin No. 10. Stockholm 1963.
4. BROWNE, F. L.: Theories of the Combustion of Wood and Its Control—A Survey of the Literature. Report No. 2136. Forest Products Laboratory, USDA 1958.
5. KAWAGOE, K.: Fire Behaviour in Rooms. Building Research Institute. Report No. 27. Tokyo 1958.
6. AHLQUIST, C. & THELANDERSSON, S.: Redovisning och bearbetning av fullskaleförsök med bränder utförda av Statens provningsanstalt. (Description and Evaluation of Full-Scale Fire Tests Made by the National Swedish Institute for Materials Testing.) Examensarbete vid institutionen för byggnadsstatik, Lunds Tekniska Högskola. (Thesis for Master of Engineering Degree. Division of Structural Mechanics and Concrete Construction, Lund Institute of Technology.) Lund 1968.
7. THOMAS, P. H. & HINKLEY, P. L. & THEOBALD, C. R. & SIMMS, D. L.: Investigations into the Flow of Hot Gases in Roof Venting. Fire Research Technical Paper No. 7. London 1963.
8. SCHLYTER, S. & ODEMARK, N.: Brandsäkerheten hos vissa bjälklagskonstruktioner jämte teoretisk bestämning av brandtemperaturer, uppkommande i byggnadskonstruktioner. (Fire Resistance of Some Floor Slab Structures and Theoretical Determination of Fire Temperatures Occurring in Building Structures.) Statens provningsanstalt (National Swedish Institute for Materials Testing.) Meddelande (Bulletin No.) 65. Stockholm 1935.
9. ÖDEEN, K.: Teoretisk bestämning av temperaturförloppet i några av brand påverkade konstruktioner. (Theoretical Determination of Temperature Development in a Number of Constructions Subjected to Fire.) Institutionen för konstruktionslära, Kungl. Tekniska Högskolan (Division of Building Construction, Royal Institute of Technology). Bulletin No. 9. 1963.
10. YOKOI, S.: Study on the Prevention of Firespread Caused by Hot Upward Current. Japanese Ministry of Construction, Building Research Institute. Report No. 34. Tokyo Nov. 1960.
11. BUTCHER, E. G., BEDFORD, G. K. & FARDELL, P. J.: Further experiments on the temperatures reached by structural steel in building fires. Fire Research Symposium No. 2, Paper 1. London 1968. H. M. Stationery Office.
12. HESELDEN, A. J. M.: Parameters determining the severity of fire. Fire Research Symposium No. 2, Paper 2. London 1968. H. M. Stationery Office.

13. YOKOI, S.: Japanese Ministry of Construction, Building Research Institute. Report No. 29. Tokyo 1959.
14. KAWAGOE, K.: Estimation of Fire Temperature-Time Curve in Rooms. Building Research Institute. Research Paper No. 29. Tokyo 1967.
15. THOMAS, P. H. & HINKLEY, P. L.: Design of Roof-Venting Systems for Single-Storey Buildings. Fire Research Technical Paper No. 10. London 1964.
16. BROWN, W. G. & WILSON, A. G. & SOLVASON, K. R.: Heat and Moisture Flow Through Openings by Convection. National Research Council of Canada, Division of Building Research. Research Paper No. 200. Ottawa 1963.
17. SJÖLIN, W.: Brand i bostadsrum antända genom värmestrålning från kärnvapen. (Fires in Residential Spaces Ignited by Heat Radiation from Nuclear Weapons.) Stockholm 1969.
18. ÖDEEN, K.: Experimentellt och teoretiskt studium av brandförlopp i byggnader. (Experimental and Theoretical Study of Processes of Fire Development in Buildings.) Statens institut för byggnadsforskning (National Swedish Institute of Building Research). Rapport (Report No.) 23. Stockholm 1968.
19. MAGNUSSON, S. E. & PETERSSON, O.: Brandteknisk dimensionering av isolerad stålkonstruktion i bärande eller avskiljande funktion. (Fire Engineering Design of Insulated Steel Structures which Perform Load-Bearing or Separating Functions.) Väg- och vattenbyggaren. Stockholm. 15(1969)4.
20. PETERSSON, O. & ÖDEEN, K.: Pågående och planerad byggnadsteknisk brandforskning i Sverige. (Structural Fire Engineering Research in Progress or in Process of Planning in Sweden.) Statens institut för byggnadsforskning (National Swedish Institute of Building Research). Rapport (Report No.) 34. Stockholm 1968.
21. ÖDEEN, K. & NORDSTRÖM, Å.: Brand- och rökspridning längs fasader och i ventilationskanaler. Delrapport 1. Instrumentering. (Spread of Fire and Smoke along External Walls and in Ventilation Ducts. Report. Part 1. Instrument Equipment.) Statens råd för byggnadsforskning (National Swedish Council for Building Research). Arbetshandling (Working Document No.) 12. Stockholm 1967.
22. FOX, L.: Numerical Solution of Ordinary and Partial Differential Equations. London (Pergamon Press) 1962.
23. GRANHOLM, H.: Träkonstruktioners brandstabilitet. (Fire stability of Timber Structures.) Chalmers Tekniska Högskolas Handlingar (Transactions of Chalmers University of Technology No.) 274. Göteborg 1963.
24. Svensk Byggnorm 1967 (SBN 67). (Swedish Building Regulations 1967 (SBR 67).) Statens Planverk (National Swedish Board of Urban Planning). Publikation (Publication No.) 1. 1967.
25. Aluminiumkonstruktioner. Försöksnorm och kommentarer. (Aluminium Structures, Draft Specification and Comments.) SVR:s Aluminiumnormkommitté. Stockholm 1966.

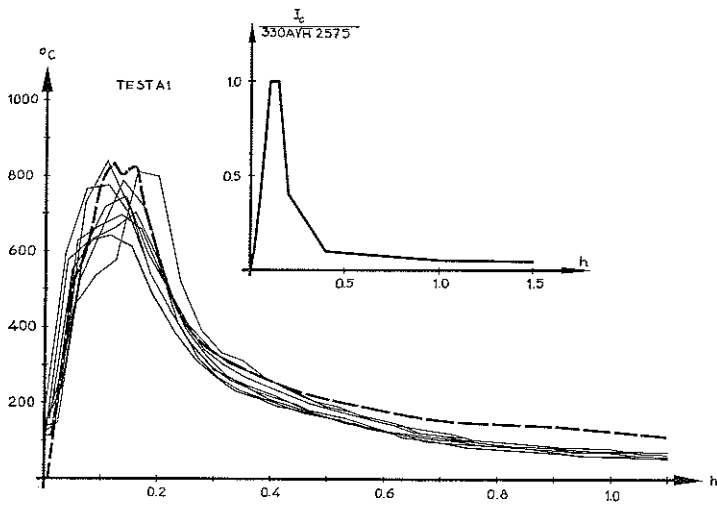


Appendix

APPENDIX 1

Time graphs of energy released per unit time and corresponding theoretically calculated time graphs of temperature of combustion gases.

Test series A. See chapter 5.



Test A1

Percentages of the total bounding surface area:

Concrete, 20 cm in thickness, 34.8 per cent.

Lightweight concrete, 12.5 cm in thickness, 42.2 per cent.

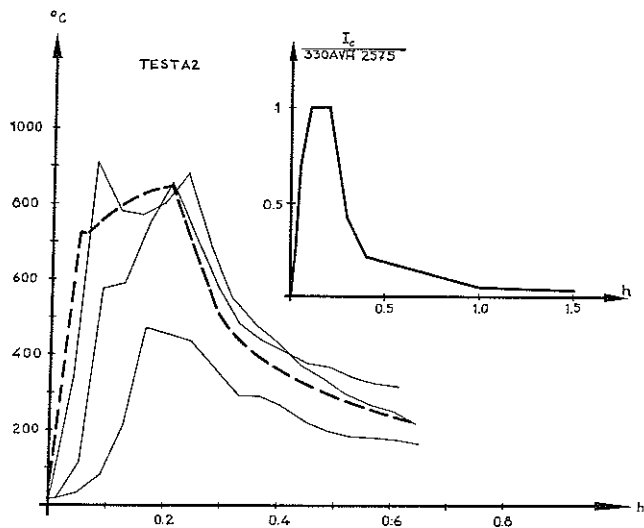
Concrete, 3 cm in thickness+lightweight concrete, 10 cm in thickness, 18.3 per cent.

Window area 4.7 per cent.

Opening factor $0.06 \text{ m}^{1/2}$ ($t > 0.1 \text{ h}$).

Duration of the fire 0.17 h.

Fire load $15.1 \text{ Mcal} \cdot \text{m}^{-2}$ of bounding surface area.



Test A2

Percentages of the total bounding surface area:

Concrete, 20 cm in thickness, 34.8 per cent.

Lightweight concrete, 12.5 cm in thickness, 42.2 per cent.

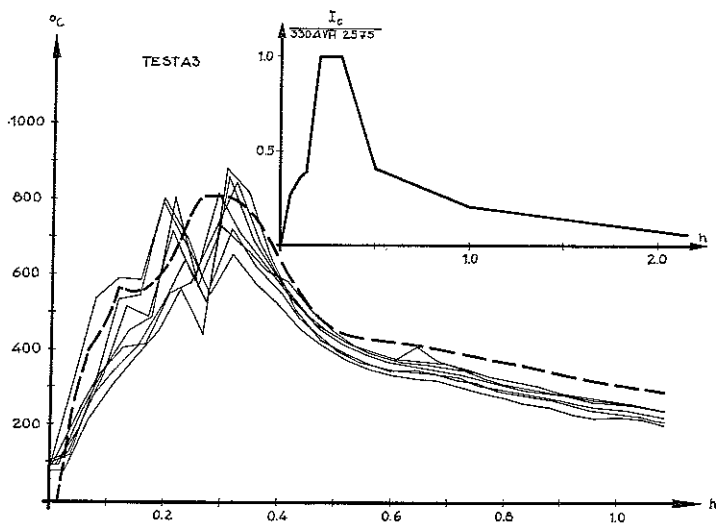
Concrete, 3 cm in thickness + lightweight concrete, 10 cm in thickness, 18.3 per cent.

Window area 4.7 per cent.

Opening factor $0.06 \text{ m}^{1/2}$ ($t > 0.1 \text{ h}$).

Duration of the fire 0.21 h.

Fire load $19 \text{ Mcal} \cdot \text{m}^{-2}$ of bounding surface area.



Test A3

Percentages of the total bounding surface area:

Concrete, 20 cm in thickness, 38.6 per cent.

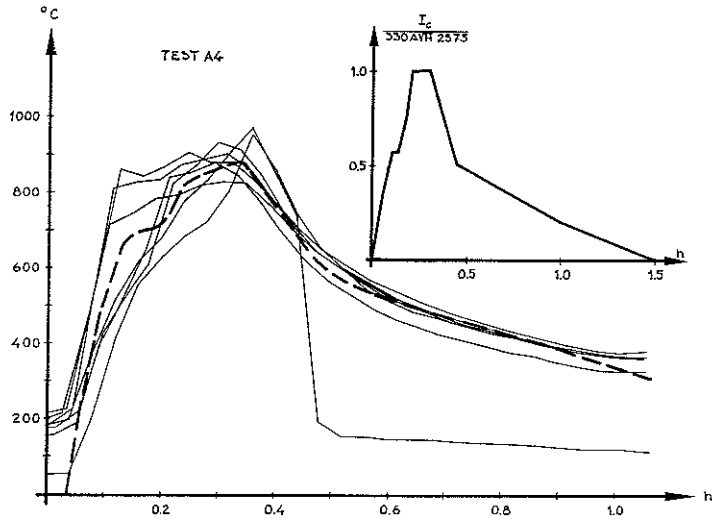
Lightweight concrete, 12.5 cm in thickness, 60.0 per cent.

Window area 1.4 per cent.

Opening factor $0.0356 \text{ m}^{1/2}$ ($t > 0.2 \text{ h}$).

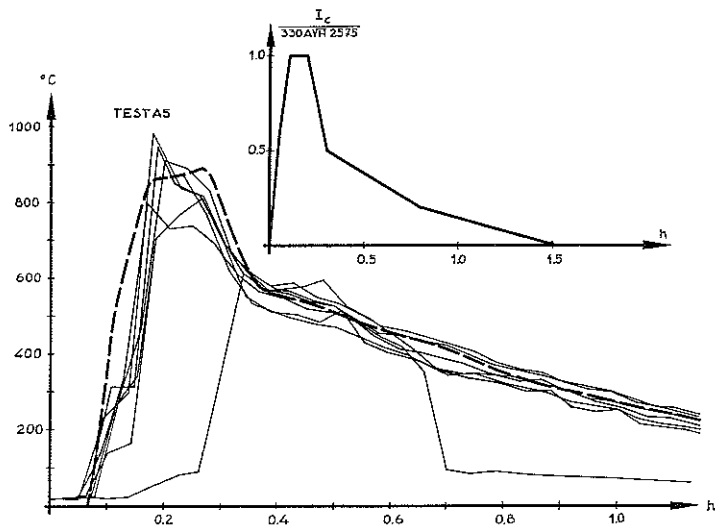
Duration of the fire 0.36 h.

Fire load $19.6 \text{ Mcal} \cdot \text{m}^{-2}$ of bounding surface area.



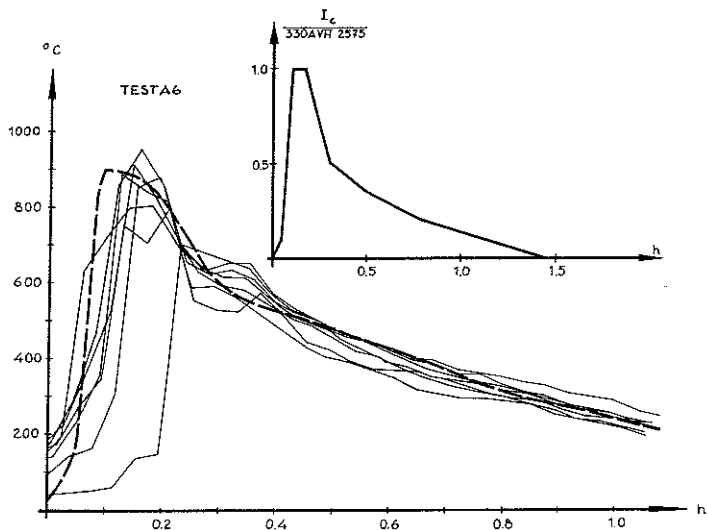
Test A4

Percentages of the total bounding surface area:
 Concrete, 20 cm in thickness, 38.3 per cent.
 Lightweight concrete, 12.5 cm in thickness, 59.4 per cent.
 Window area 2.3 per cent.
 Opening factor $0.0486 \text{ m}^{1/2}$ ($t > 0.2 \text{ h}$).
 Duration of the fire 0.325 h.
 Fire load $22.4 \text{ Mcal} \cdot \text{m}^{-2}$ of bounding surface area.



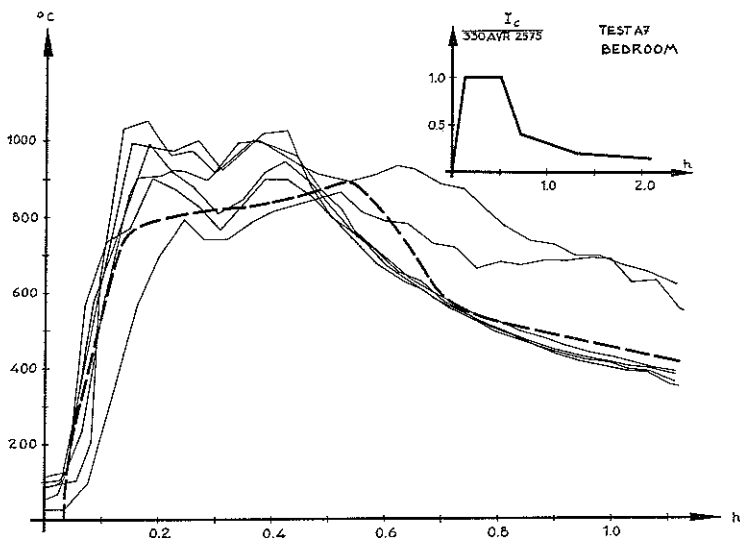
Test A5

Percentages of the total bounding surface area:
 Concrete, 20 cm in thickness, 38.3 per cent.
 Lightweight concrete, 12.5 cm in thickness, 59.4 per cent.
 Window area 2.3 per cent.
 Opening factor $0.0548 \text{ m}^{1/2}$.
 Duration of the fire 0.24 h.
 Fire load $20 \text{ Mcal} \cdot \text{m}^{-2}$ of bounding surface area.



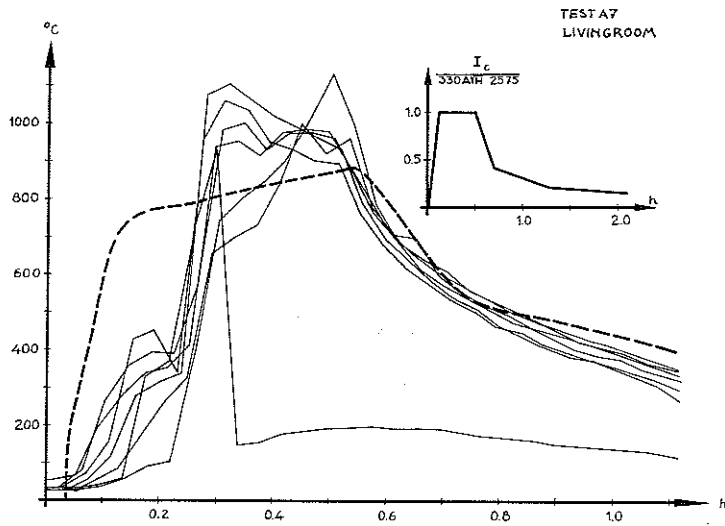
Test A6

Percentages of the total bounding surface area:
 Concrete, 20 cm in thickness, 37.8 per cent.
 Lightweight concrete, 12.5 cm in thickness, 58.6 per cent.
 Window area 3.6 per cent.
 Opening factor $0.068 \text{ m}^{1/2}$.
 Duration of the fire 0.23 h.
 Fire load $23 \text{ Mcal} \cdot \text{m}^{-2}$ of bounding surface area.



Test A7a

Living-room.
 Percentages of the total bounding surface area:
 Concrete, 20 cm in thickness, 40.8 per cent.
 Lightweight concrete, 12.5 cm in thickness, 47.3 per cent.
 Concrete, 3 cm in thickness+lightweight concrete 10 cm in thickness, 8.3 per cent.
 Window area 3.6 per cent.
 Opening factor $0.04 \text{ m}^{1/2}$.
 Duration of the fire 0.32 h.
 Fire load $32 \text{ Mcal} \cdot \text{m}^{-2}$ of bounding surface area.



Test A7b

Bedroom.

Percentages of the total bounding surface area:

Concrete, 20 cm in thickness, 40.8 per cent.

Lightweight concrete, 12.5 cm in thickness, 47.3 per cent.

Concrete, 3 cm in thickness + lightweight concrete 10 cm in thickness, 8.3 per cent.

Window area 3.6 per cent.

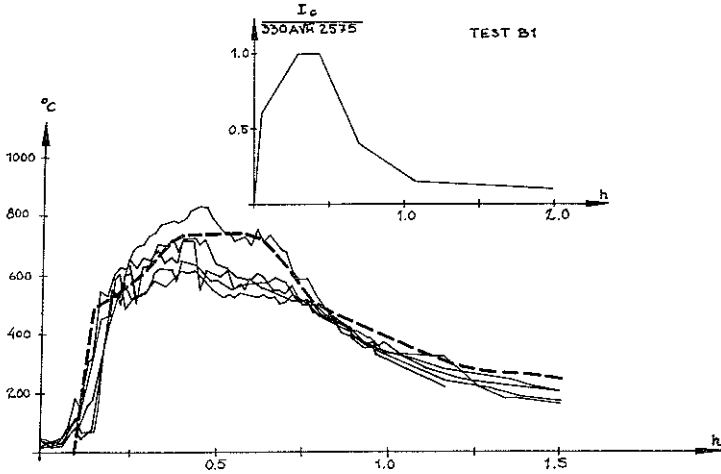
Opening factor $0.04 \text{ m}^{1/2}$.

Duration of the fire 0.32 h.

Fire load $32 \text{ Mcal} \cdot \text{m}^{-2}$ of bounding surface area.

APPENDIX 2

Time graphs of energy released per unit time and corresponding theoretically
calculated time graphs of temperature of combustion gases.
Test series B. See chapter 5.

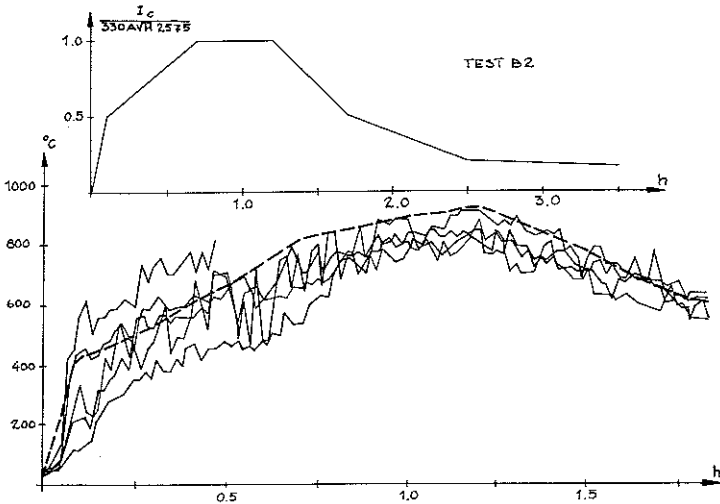


Test B1

Opening factor $0.0467 \text{ m}^{1/2}$.

Duration of the fire 0.48 h.

Fire load $33.3 \text{ Mcal} \cdot \text{m}^{-2}$ of bounding surface area.

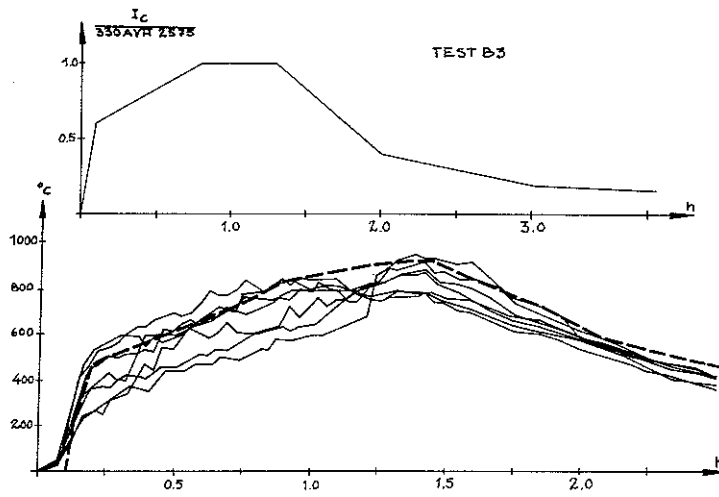


Test B2

Opening factor $0.0467 \text{ m}^{1/2}$.

Duration of the fire 1.07 h.

Fire load $75 \text{ Mcal} \cdot \text{m}^{-2}$ of bounding surface area.



Test B3

Opening factor $0.0467 \text{ m}^{1/2}$.

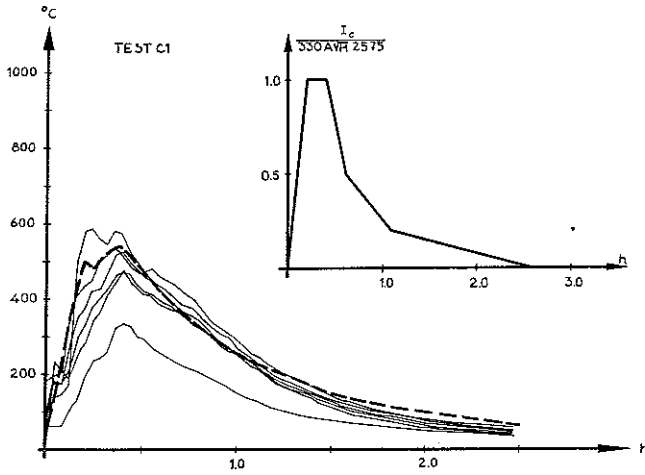
Duration of the fire 1.18 h.

Fire load $83.5 \text{ Mcal} \cdot \text{m}^{-2}$ of bounding surface area.

APPENDIX 3

Time graphs of energy released per unit time and corresponding theoretically calculated time graphs of temperature of combustion gases.

Test series C. See chapter 5.



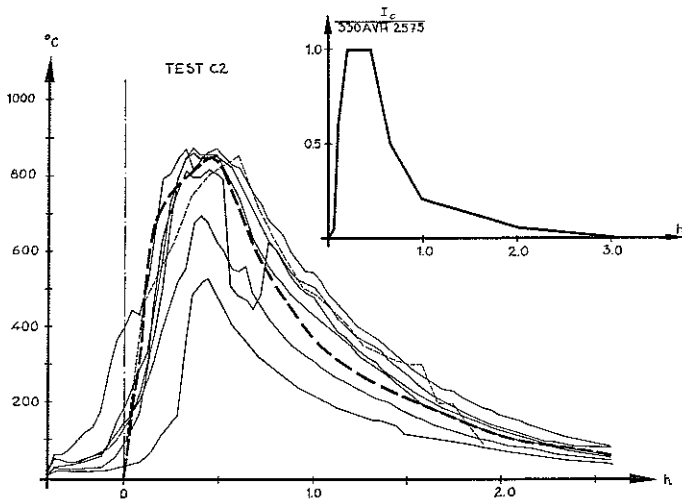
Test C1

Quantity of combustible material 270 kg.

Rate of air supply by fan 1.0 m³/s.

Opening factor 0.0234 m^{1/2}.

Hydraulic radius —.



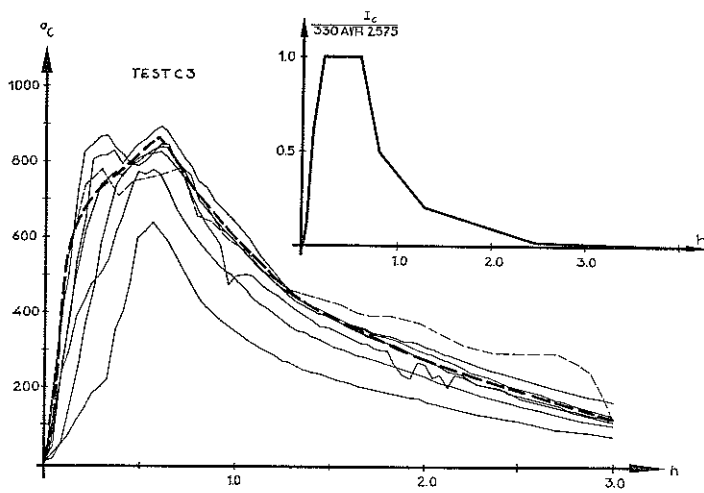
Test C2

Quantity of combustible material 675 kg.

Rate of air supply by fan 2.0 m³/s.

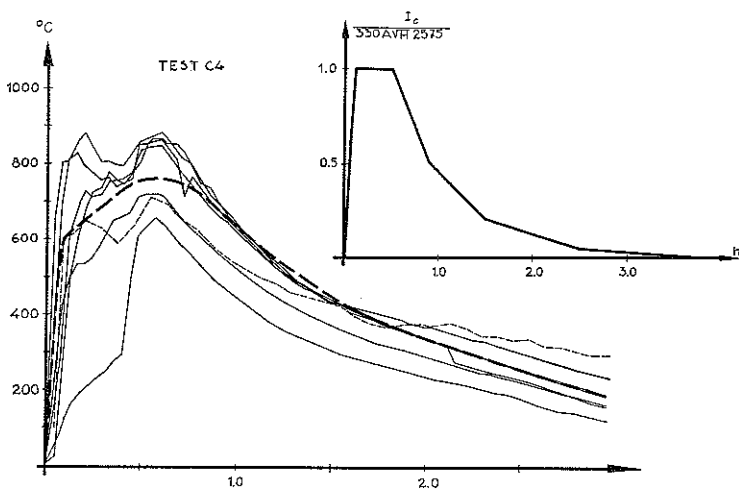
Opening factor 0.0601 m^{1/2}.

Hydraulic radius 1.0 cm.



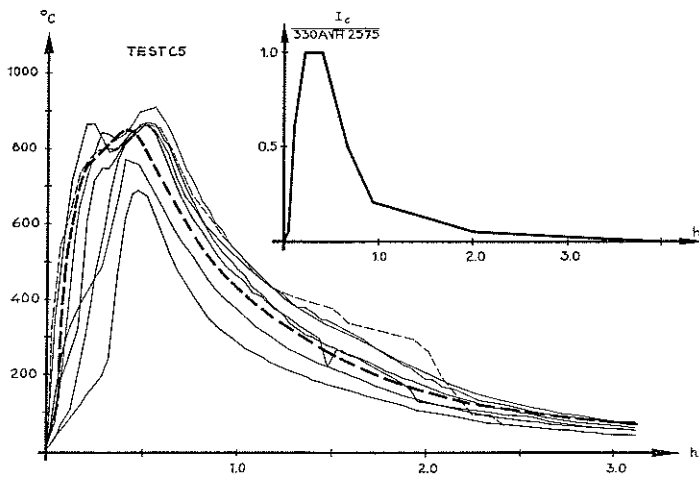
Test C3

Quantity of combustible material 675 kg.
 Rate of air supply by fan 1.0 m³/s.
 Opening factor 0.0434 m^{1/2}.
 Hydraulic radius 1.0 cm.



Test C4

Quantity of combustible material 675 kg.
 Rate of air supply by fan 0.7 m³/s.
 Opening factor 0.0351 m^{1/2}.
 Hydraulic radius 1.0 cm.



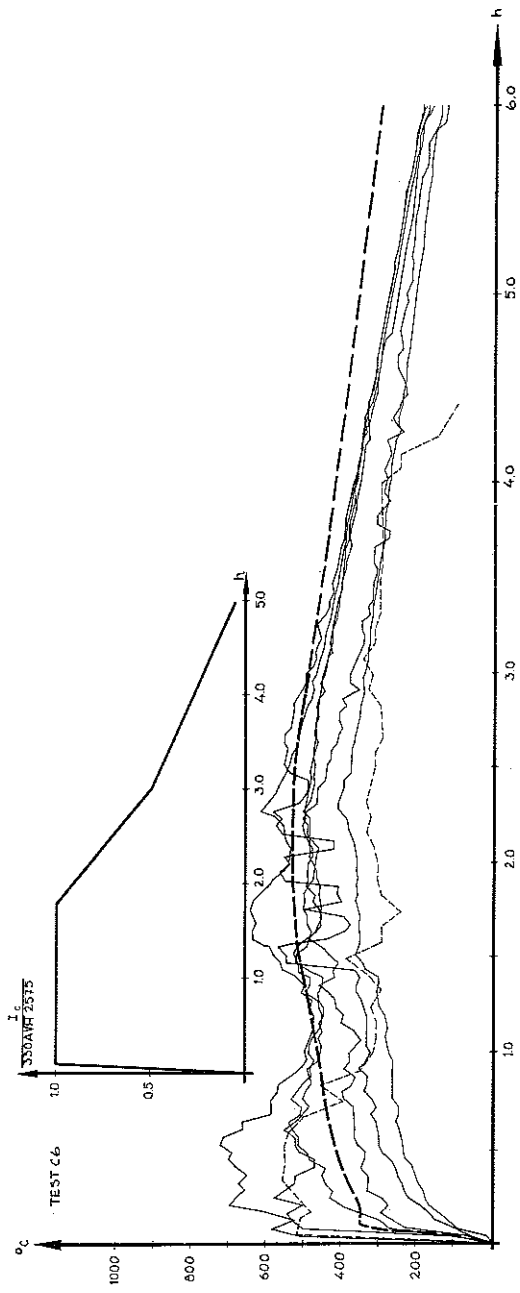
Test C5

Quantity of combustible material 675 kg.

Rate of air supply by fan 1.5 m³/s.

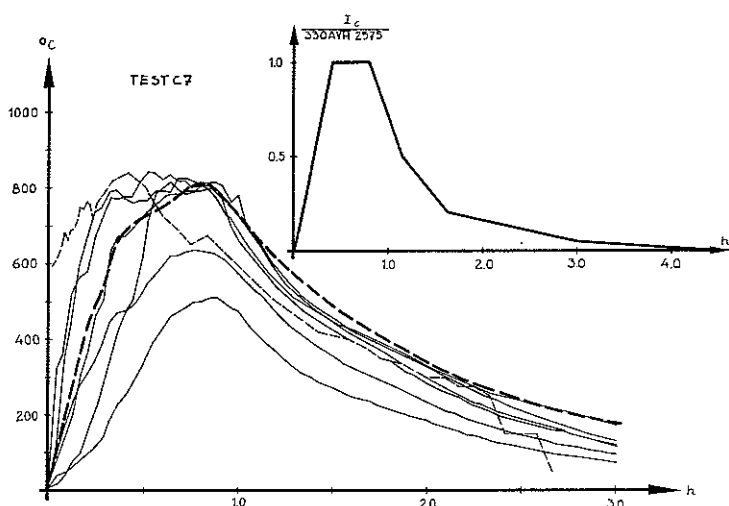
Opening factor 0.0551 m^{1/2}.

Hydraulic radius 1.0 cm.



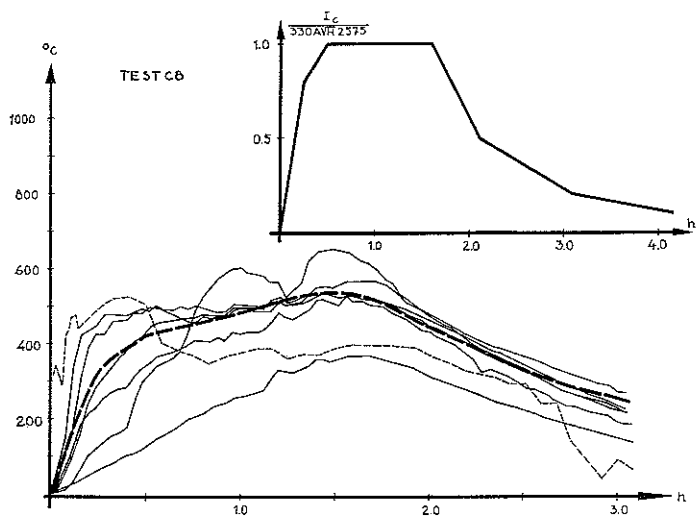
Test C6

Quantity of combustible material 675 kg.
Rate of air supply by fan $0.25 \text{ m}^3/\text{s}$.
Opening factor $0.01 \text{ m}^{1/2}$.
Hydraulic radius 1.0 cm.



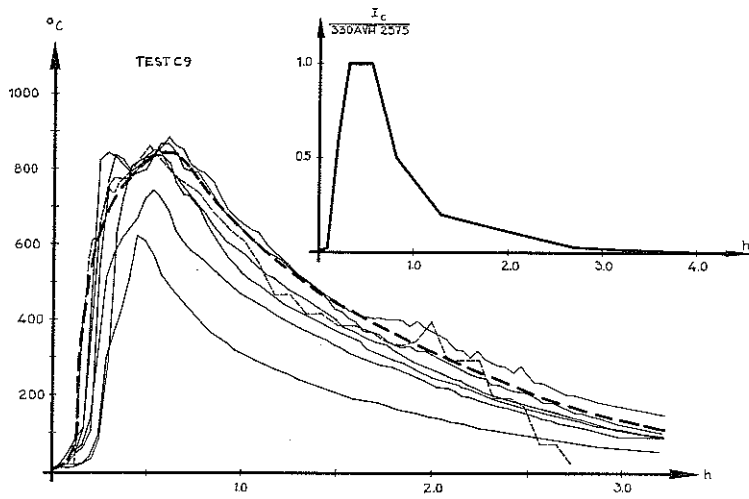
Test C7

Quantity of combustible material 675 kg.
 Rate of air supply by fan 1.0 m³/s.
 Opening factor 0.0367 m^{1/2}.
 Hydraulic radius 1.7 cm.



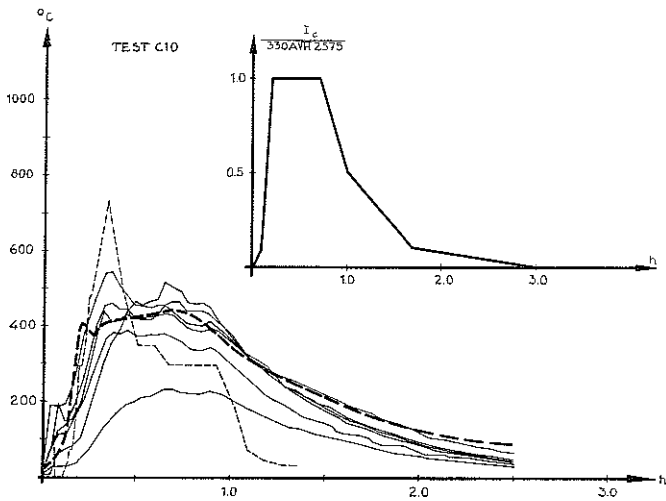
Test C8

Quantity of combustible material 675 kg.
 Rate of air supply by fan 0.7 m³/s.
 Opening factor 0.015 m^{1/2}.
 Hydraulic radius 1.7 cm.



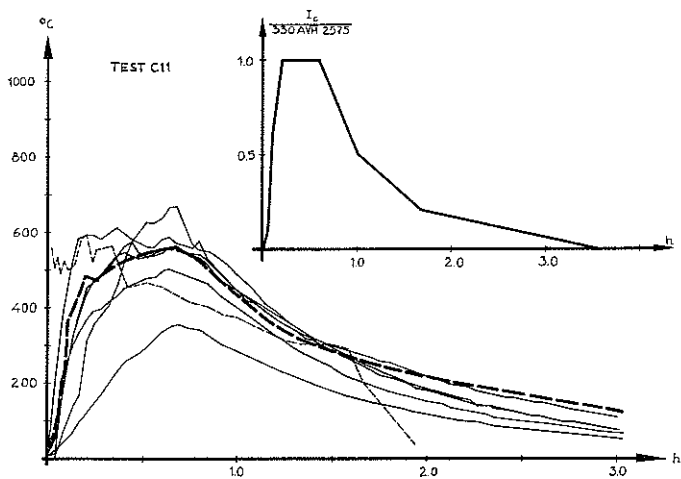
Test C9

Quantity of combustible material 675 kg.
 Rate of air supply by fan 1.0 m³/s.
 Opening factor 0.051 m^{1/2}.
 Hydraulic radius 0.6 cm.



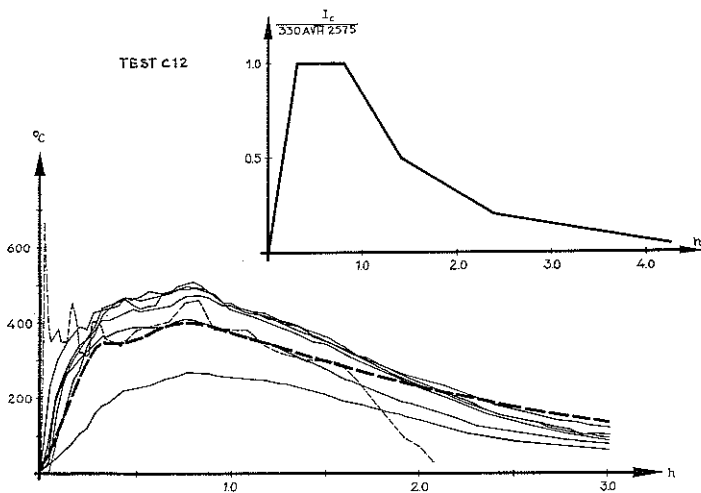
Test C10

Quantity of combustible material 270 kg.
 Rate of air supply by fan 0.7 m³/s.
 Opening factor 0.015 m^{1/2}.
 Hydraulic radius 1.0 cm.



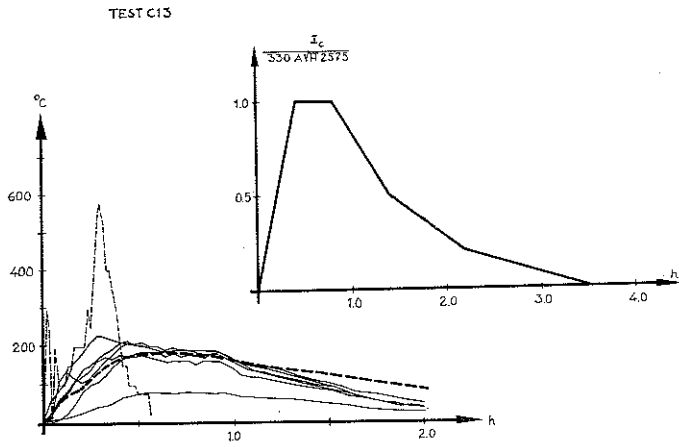
Test C11

Quantity of combustible material 405 kg.
 Rate of air supply by fan $0.7 \text{ m}^3/\text{s}$.
 Opening factor $0.02 \text{ m}^{1/2}$.
 Hydraulic radius 1.0 cm.



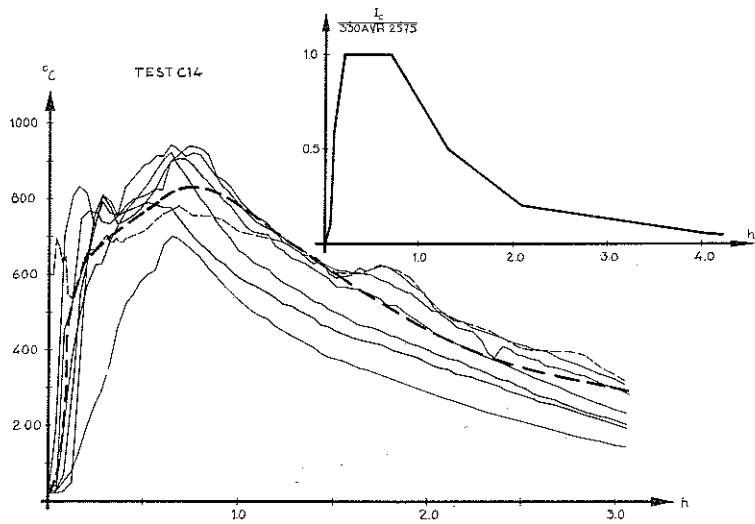
Test C12

Quantity of combustible material 405 kg.
 Rate of air supply by fan $0.7 \text{ m}^3/\text{s}$.
 Opening factor $0.012 \text{ m}^{1/2}$.
 Hydraulic radius 2.4 cm.



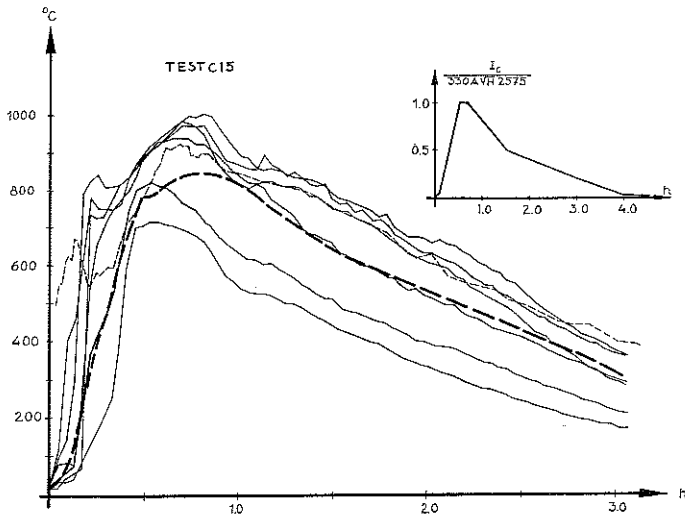
Test C13

Quantity of combustible material 135 kg.
 Rate of air supply by fan $0.7 \text{ m}^3/\text{s}$.
 Opening factor $0.005 \text{ m}^{1/2}$.
 Hydraulic radius 1.0 cm.



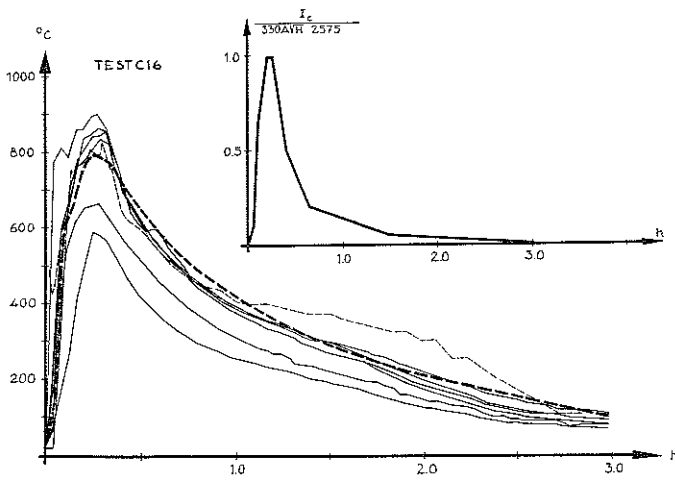
Test C14

Quantity of combustible material 945 kg.
 Rate of air supply by fan $1.0 \text{ m}^3/\text{s}$.
 Opening factor $0.0367 \text{ m}^{1/2}$.
 Hydraulic radius 1.6 cm.



Test C15

Quantity of combustible material 1350 kg.
 Rate of air supply by fan 2.0 m³/s.
 Opening factor 0.0601 m^{1/2}.
 Hydraulic radius 1.4 cm.



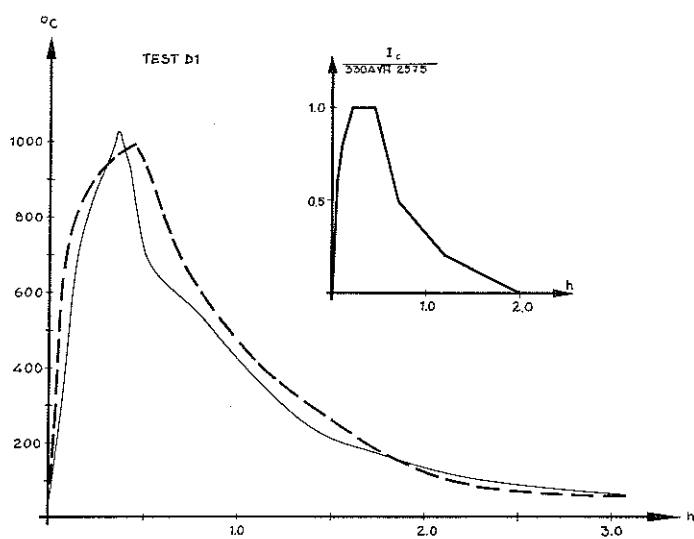
Test C16

Quantity of combustible material 405 kg.
 Rate of air supply by fan 0.7 m³/s.
 Opening factor 0.06 m^{1/2}.
 Hydraulic radius 0.4 cm.

APPENDIX 4

Time graphs of energy released per unit time and corresponding theoretically calculated time graphs of temperature of combustion gases.

Test series D. See chapter 5.



Test D1

Percentages of the total bounding surface area:

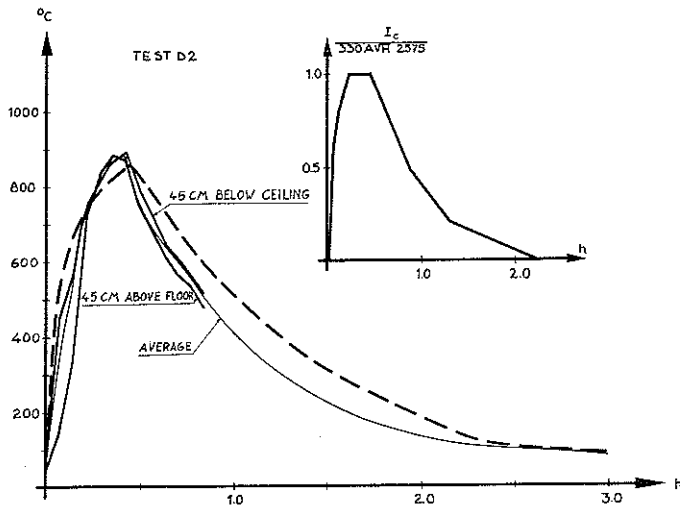
Lightweight concrete, 20 cm in thickness, 97.8 per cent.

Window area 2.2 per cent.

Opening factor $0.028 \text{ m}^{1/2}$.

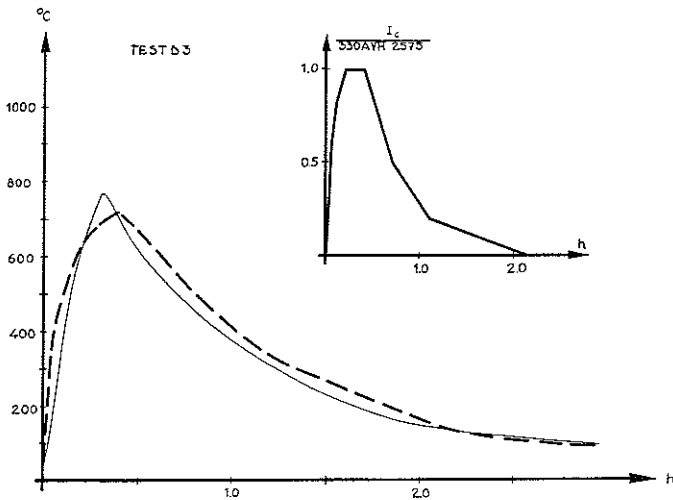
Duration of the fire 0.5 h.

Fire load $20.2 \text{ Mcal} \cdot \text{m}^{-2}$ of bounding surface area.



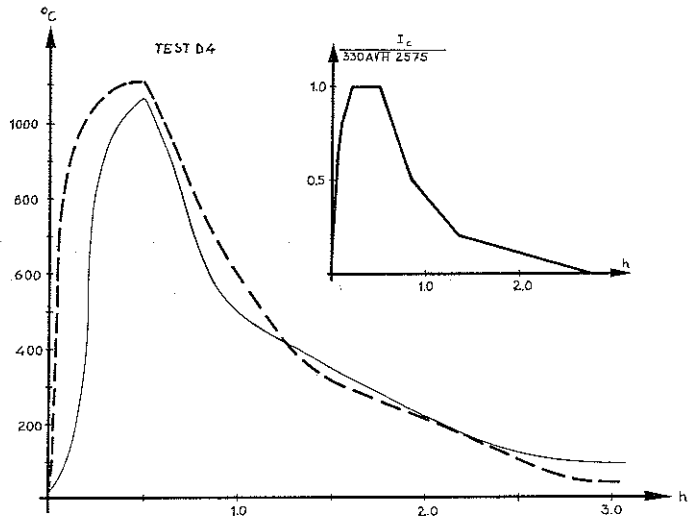
Test D2

Percentages of the total bounding surface area:
 Lightweight concrete, 20 cm in thickness, 98.7 per cent.
 Window area 1.3 per cent.
 Opening factor $0.0147 \text{ m}^{1/2}$.
 Duration of the fire 0.51 h.
 Fire load $11.2 \text{ Mcal} \cdot \text{m}^{-2}$ of bounding surface area.



Test D3

Percentages of the total bounding surface area:
 Lightweight concrete, 20 cm in thickness, 99.15 per cent.
 Window area 0.85 per cent.
 Opening factor $0.0092 \text{ m}^{1/2}$.
 Duration of the fire 0.47 h.
 Fire load $6.5 \text{ Mcal} \cdot \text{m}^{-2}$ of bounding surface area.



Test D4

Percentages of the total bounding surface area:

Lightweight concrete, 94.7 per cent.

Window area 5.3 per cent.

Opening factor $0.075 \text{ m}^{1/2}$.

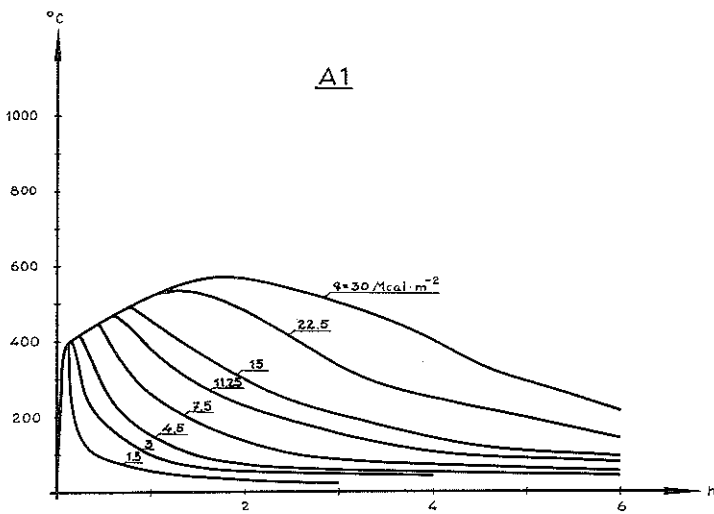
Duration of the fire 0.58 h.

Fire load $65 \text{ Mcal} \cdot \text{m}^{-2}$ of bounding surface area.

APPENDIX 5

Calculated time graphs of temperature of combustion gases for seven types of enclosed spaces differing in opening factor and in bounding structures.

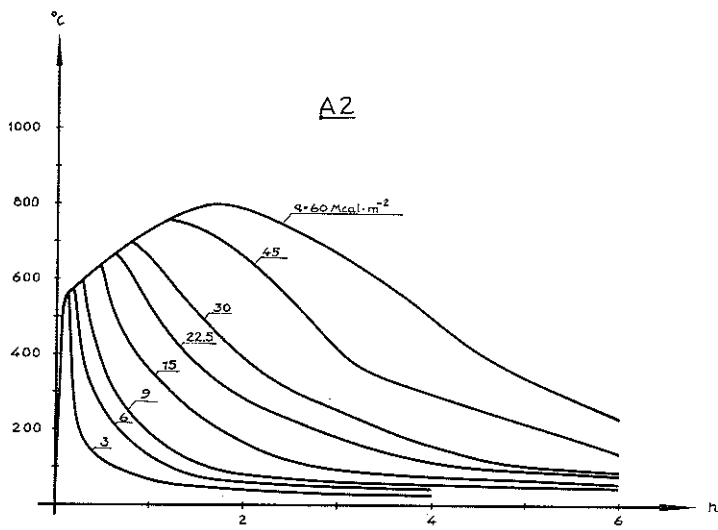
See chapter 7.



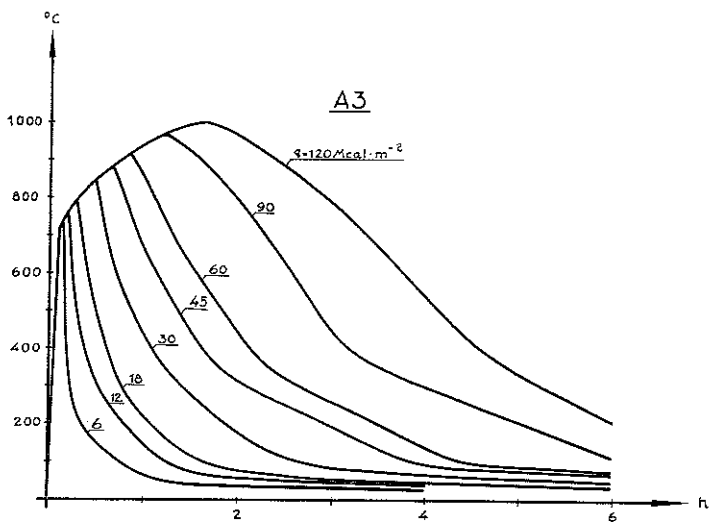
A1

Type A enclosed space.

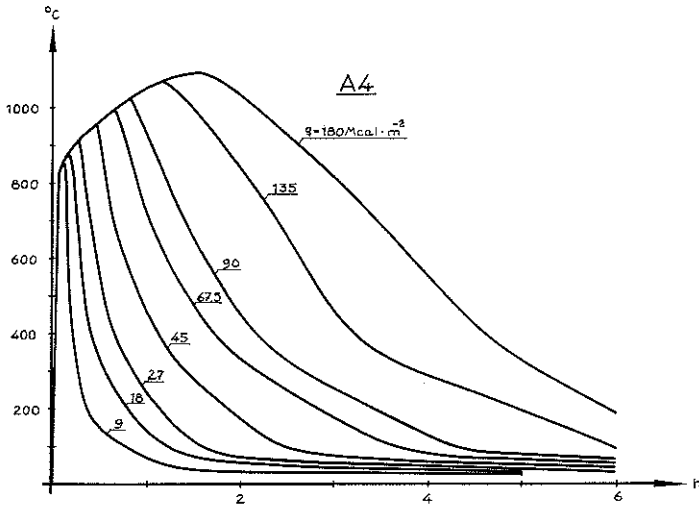
Opening factor $0.01 \text{ m}^2/\text{m}^3$.



A2
 Type A enclosed space.
 Opening factor $0.02 \text{ m}^{1/2}$.

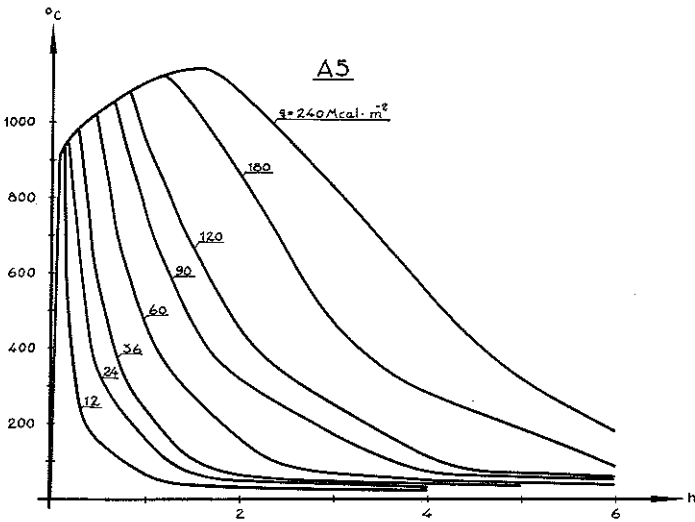


A3
 Type A enclosed space.
 Opening factor $0.04 \text{ m}^{1/2}$.



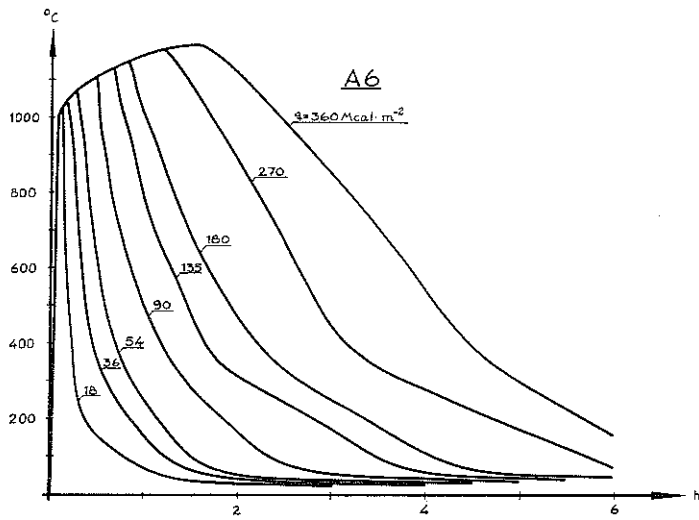
A4

Type A enclosed space.
Opening factor $0.06 \text{ m}^{1/2}$.

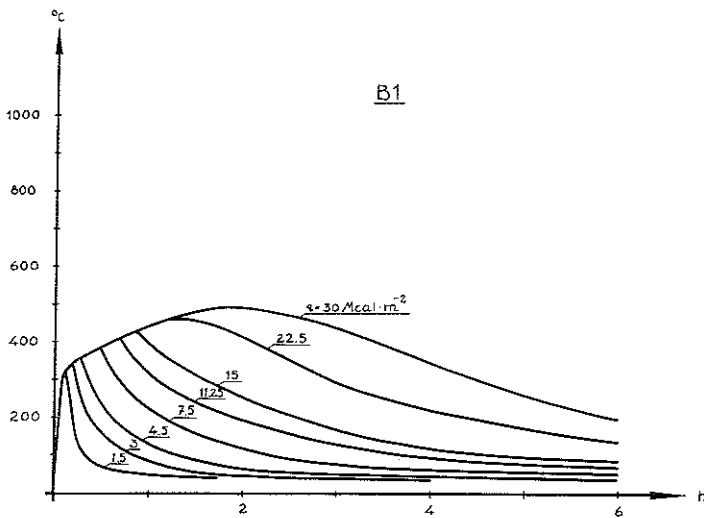


A5

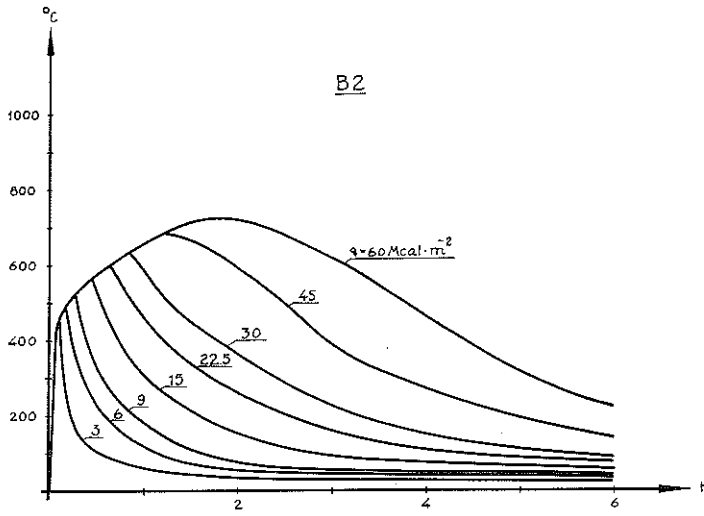
Type A enclosed space.
Opening factor $0.08 \text{ m}^{1/2}$.



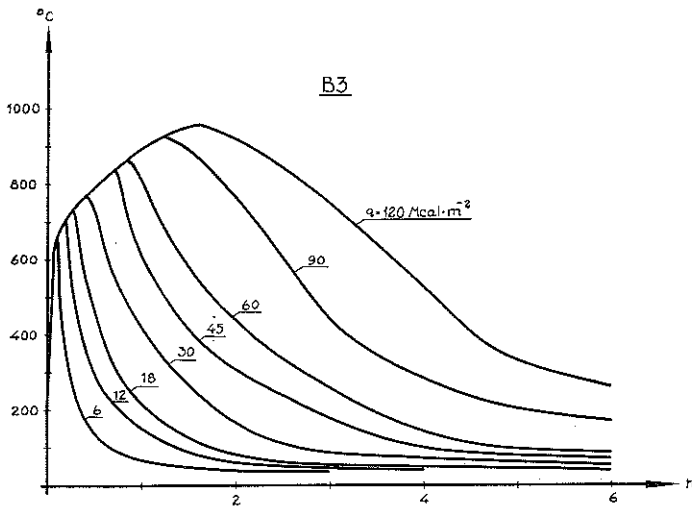
A6
 Type A enclosed space.
 Opening factor $0.12 \text{ m}^{1/2}$.



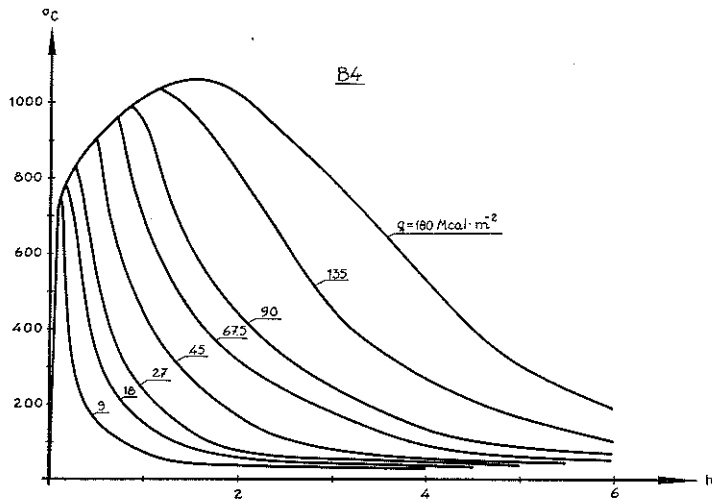
B1
 Type B enclosed space.
 Opening factor $0.01 \text{ m}^{1/2}$.



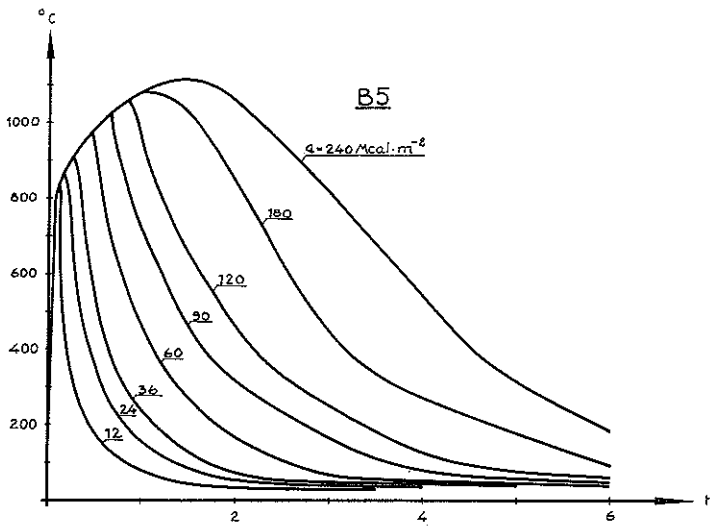
B2
 Type B enclosed space.
 Opening factor $0.02 \text{ m}^{1/2}$.



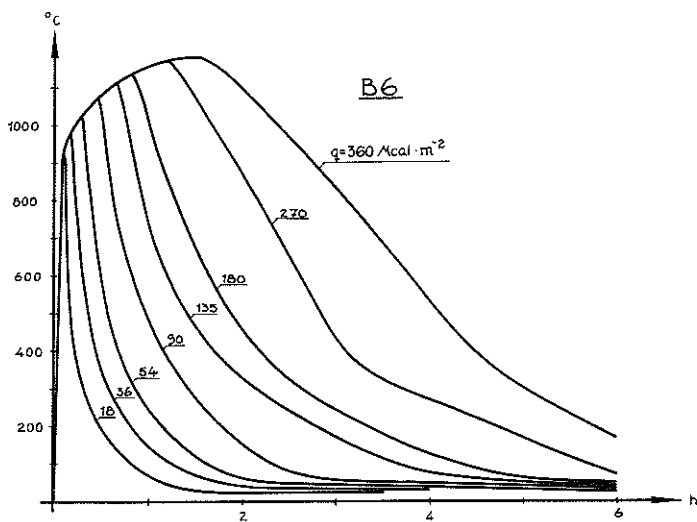
B3
 Type B enclosed space.
 Opening factor $0.04 \text{ m}^{1/2}$.



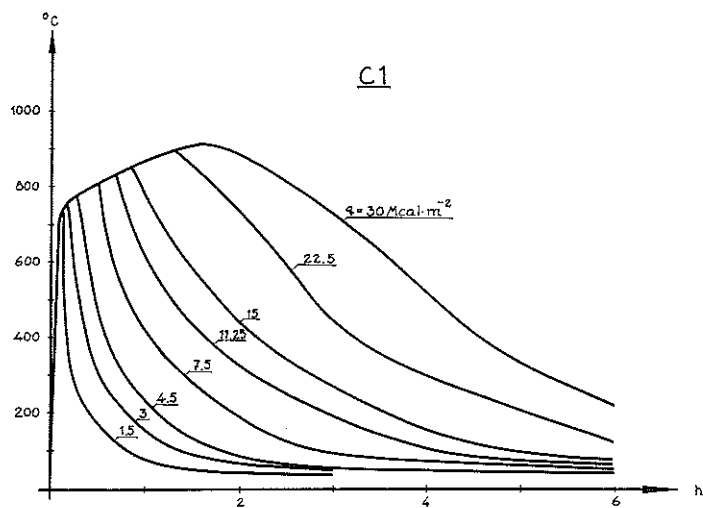
B4
 Type B enclosed space.
 Opening factor $0.06 \text{ m}^{1/2}$.



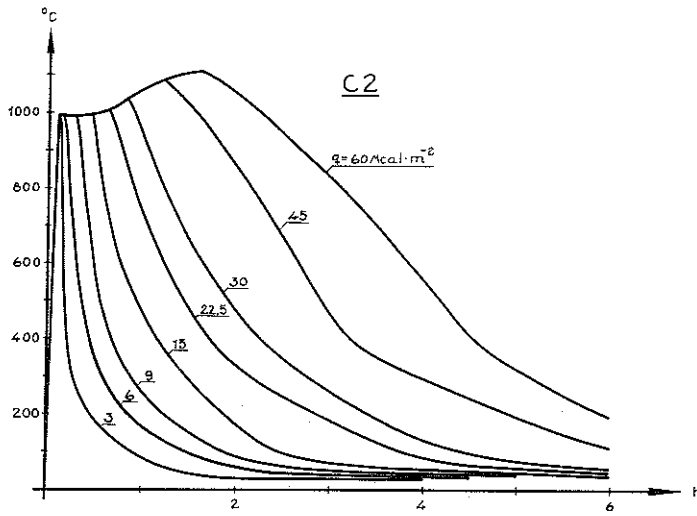
B5
 Type B enclosed space.
 Opening factor $0.08 \text{ m}^{1/2}$.



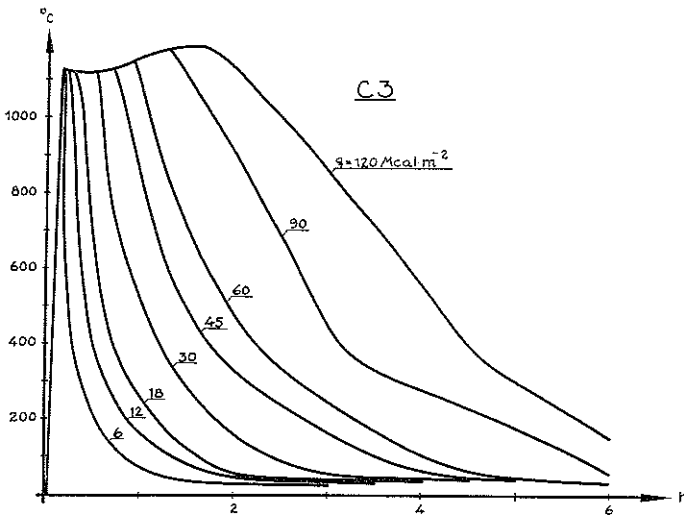
B6
 Type B enclosed space.
 Opening factor $0.12 \text{ m}^{1/2}$.



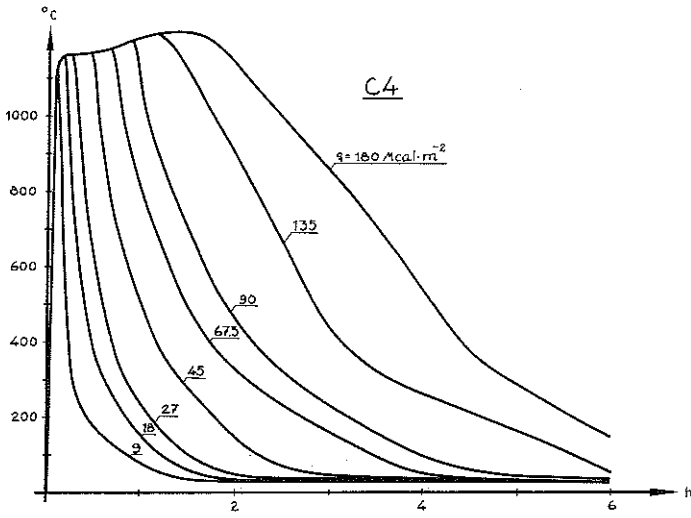
C1
 Type C enclosed space.
 Opening factor $0.01 \text{ m}^{1/2}$.



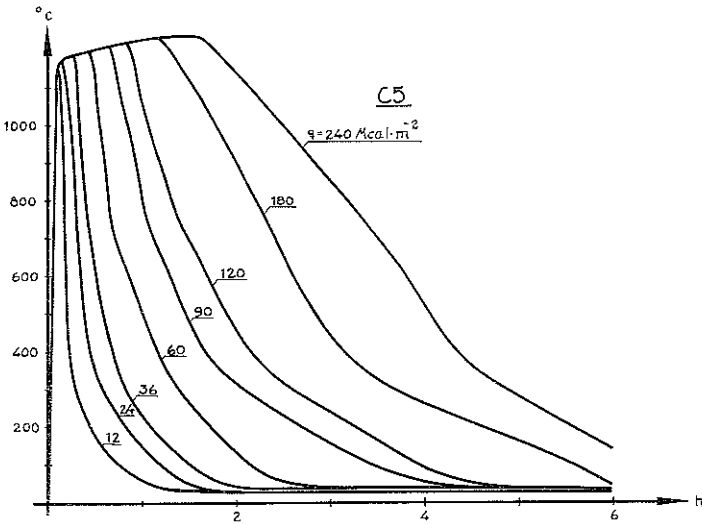
C2
 Type C enclosed space.
 Opening factor $0.02 \text{ m}^{1/2}$.



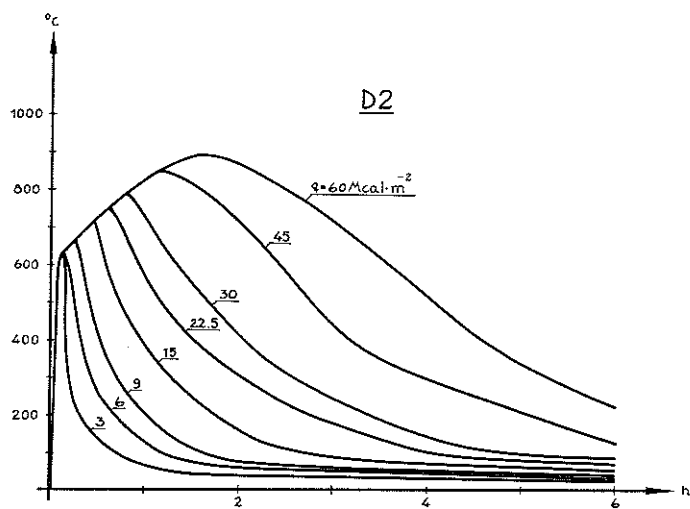
C3
 Type C enclosed space.
 Opening factor $0.04 \text{ m}^{1/2}$.



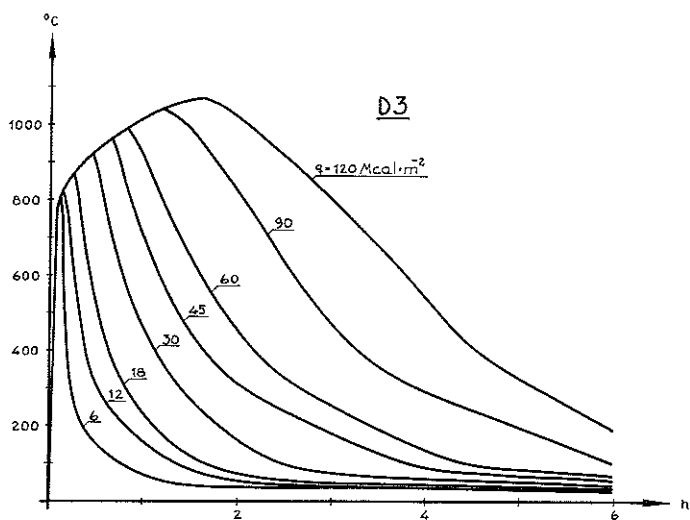
C4
 Type C enclosed space.
 Opening factor $0.06 \text{ m}^2/\text{m}^2$.



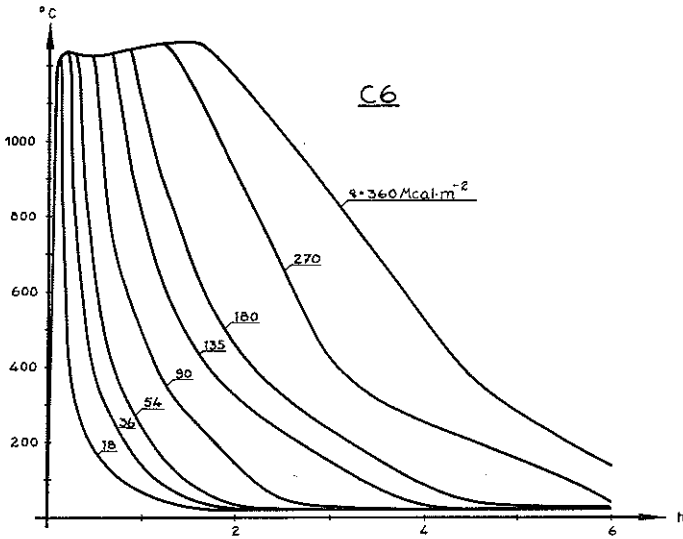
C5
 Type C enclosed space.
 Opening factor $0.08 \text{ m}^2/\text{m}^2$.



D2
 Type D enclosed space.
 Opening factor $0.02 \text{ m}^{1/2}$.

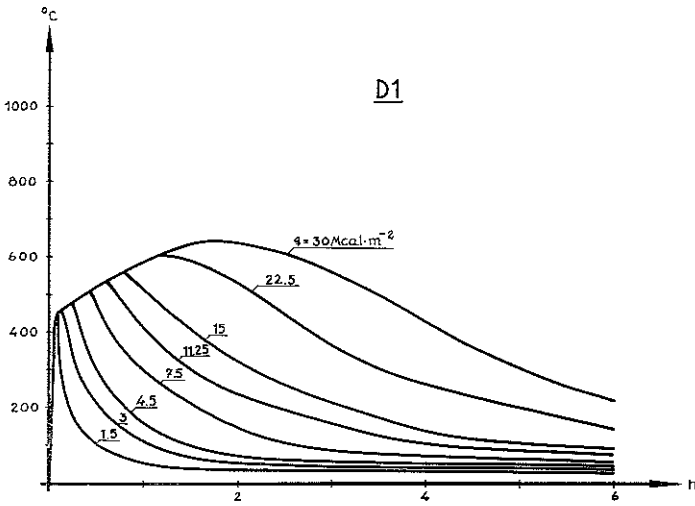


D3
 Type D enclosed space.
 Opening factor $0.04 \text{ m}^{1/2}$.



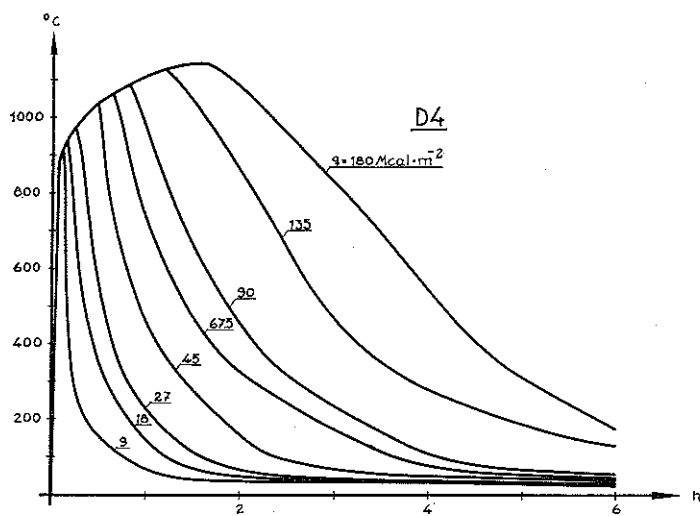
C6

Type C enclosed space.
Opening factor $0.12 \text{ m}^{1/2}$.

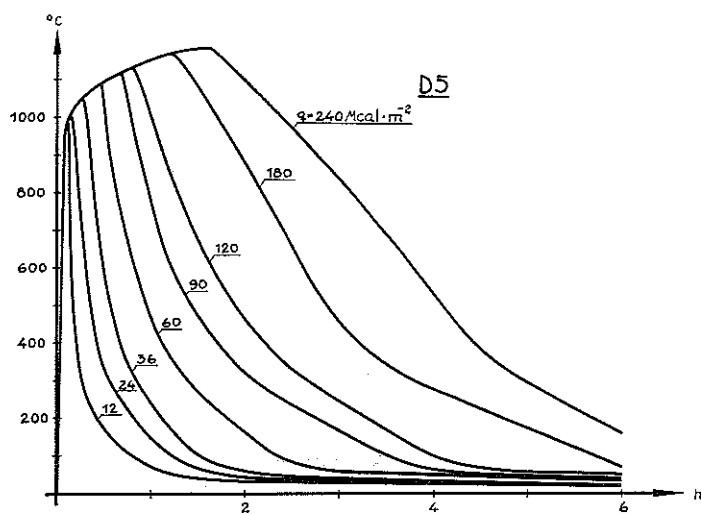


D1

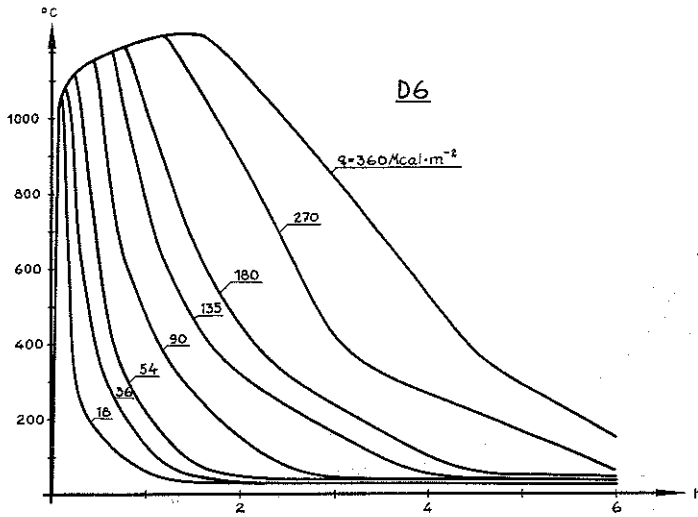
Type D enclosed space.
Opening factor $0.01 \text{ m}^{1/2}$.



D4
 Type D enclosed space.
 Opening factor $0.06 \text{ m}^{1/2}$.

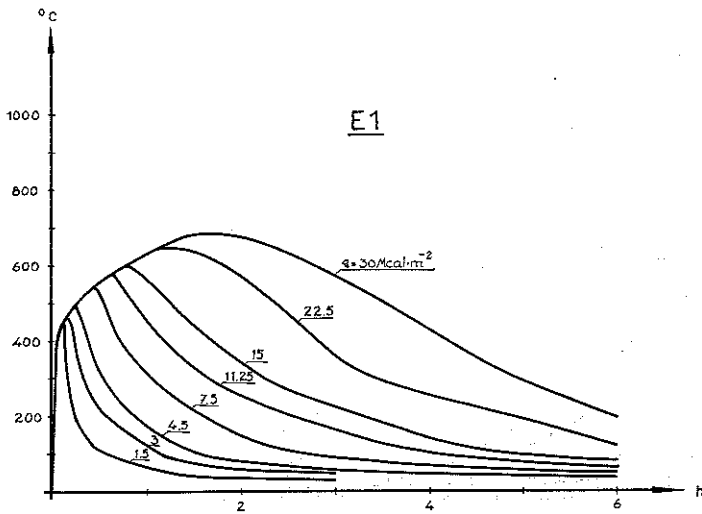


D5
 Type D enclosed space.
 Opening factor $0.08 \text{ m}^{1/2}$.



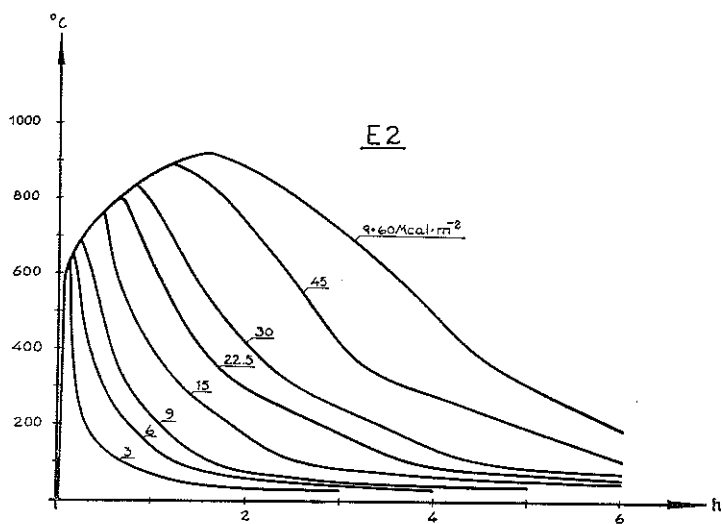
D6

Type D enclosed space.
Opening factor $0.12 \text{ m}^{1/2}$.

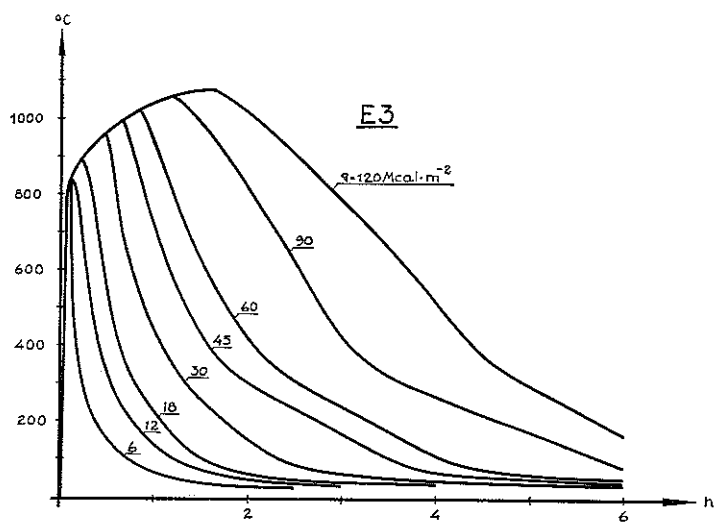


E1

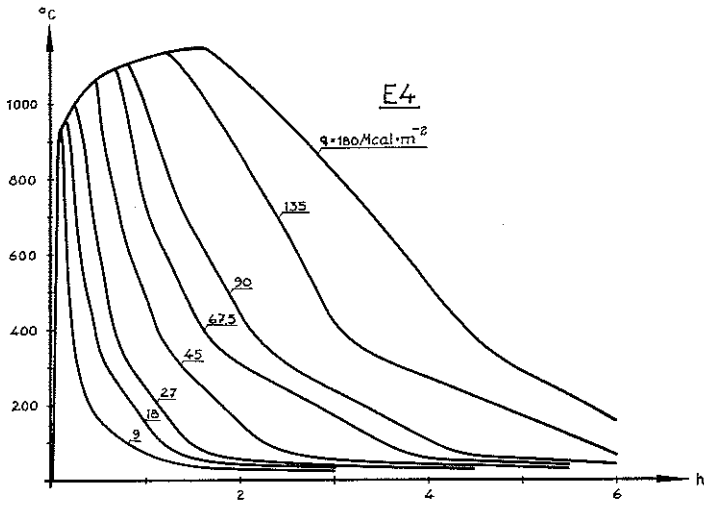
Type E enclosed space.
Opening factor $0.01 \text{ m}^{1/2}$.



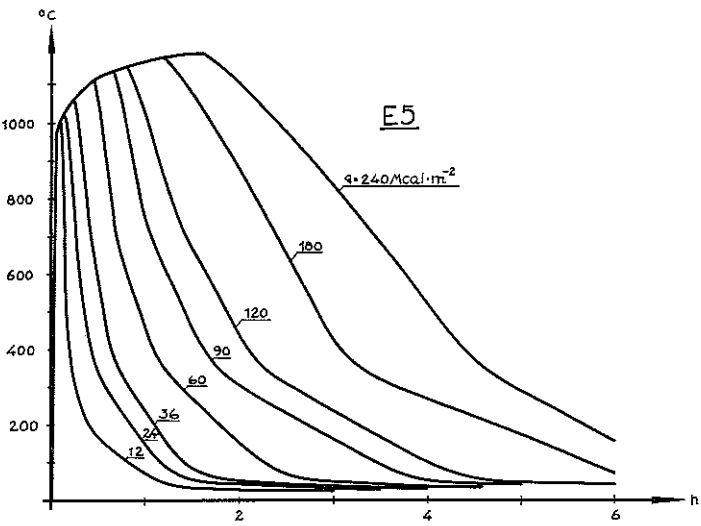
E2
 Type E enclosed space.
 Opening factor $0.02 \text{ m}^{1/2}$.



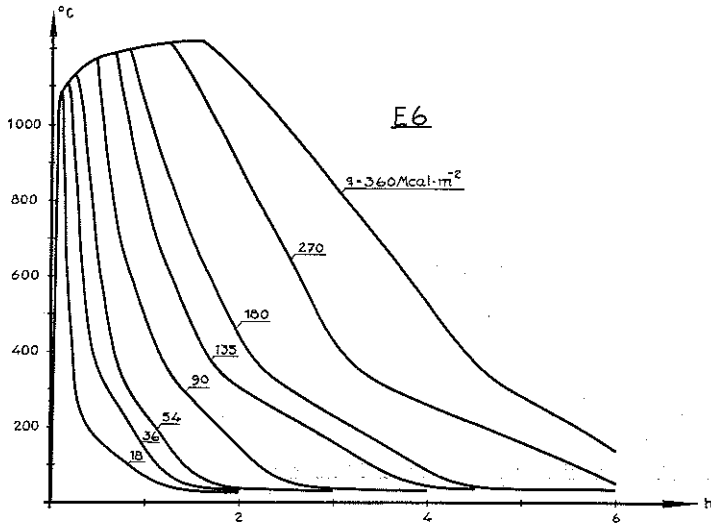
E3
 Type E enclosed space.
 Opening factor $0.04 \text{ m}^{1/2}$.



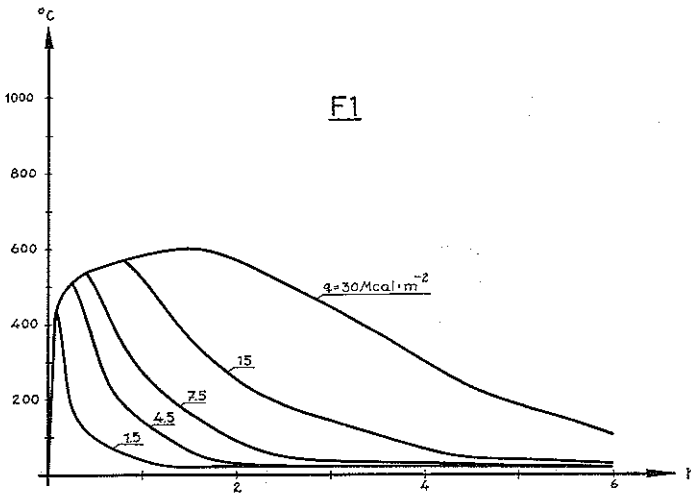
E4
 Type E enclosed space.
 Opening factor $0.06 \text{ m}^{1/2}$.



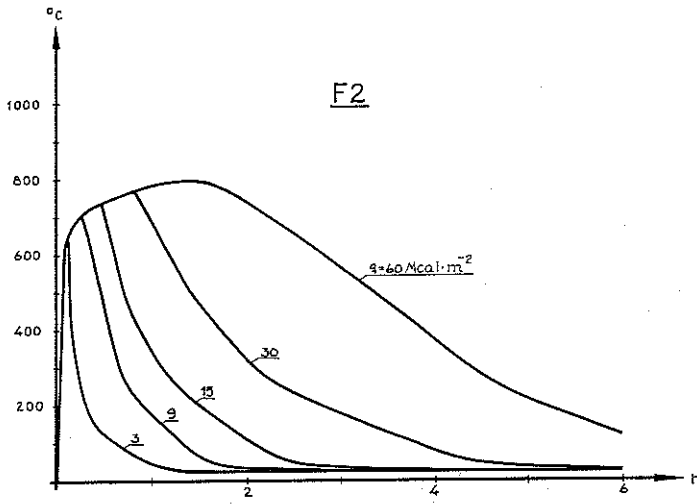
E5
 Type E enclosed space.
 Opening factor $0.08 \text{ m}^{1/2}$.



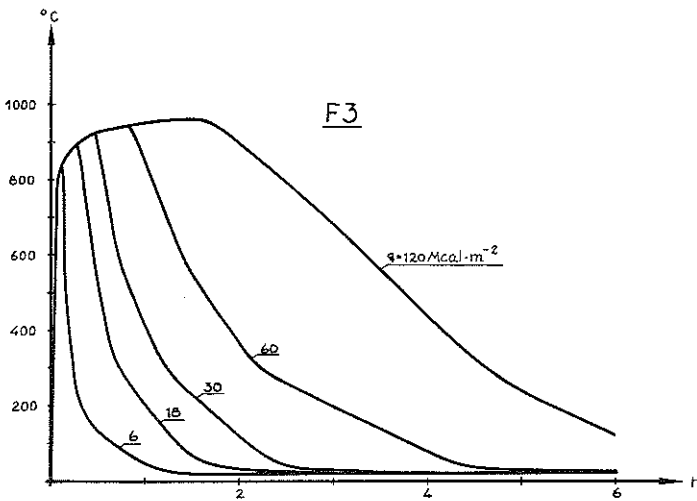
E6
 Type E enclosed space.
 Opening factor $0.12 \text{ m}^{1/2}$.



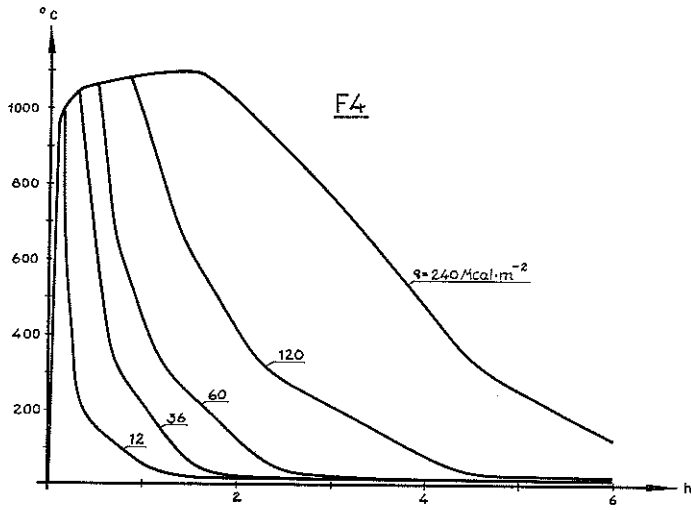
F1
 Type F enclosed space.
 Resultant emissivity 0.1.
 Opening factor $0.01 \text{ m}^{1/2}$.



F2
 Type F enclosed space.
 Resultant emissivity 0.1.
 Opening factor $0.02 \text{ m}^{1/2}$.

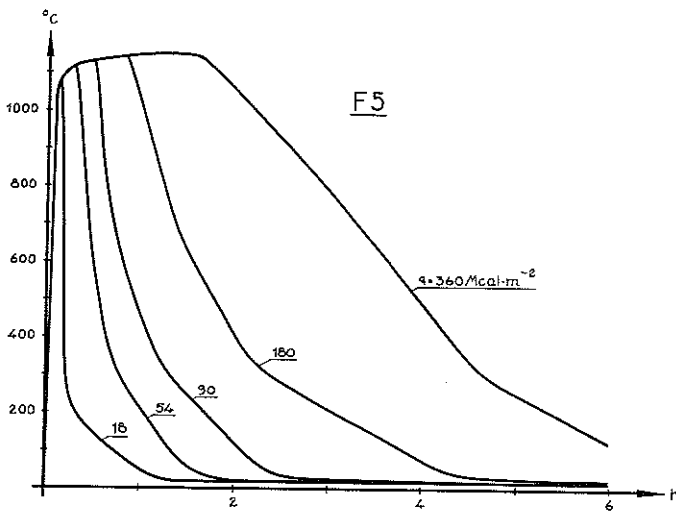


F3
 Type F enclosed space.
 Resultant emissivity 0.1.
 Opening factor $0.04 \text{ m}^{1/2}$.



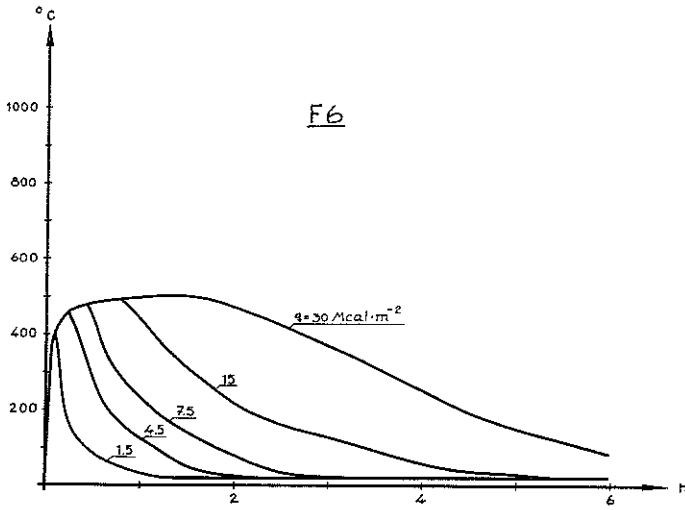
F4

Type F enclosed space.
Resultant emissivity 0.1.
Opening factor $0.08 \text{ m}^2/\text{m}^2$.



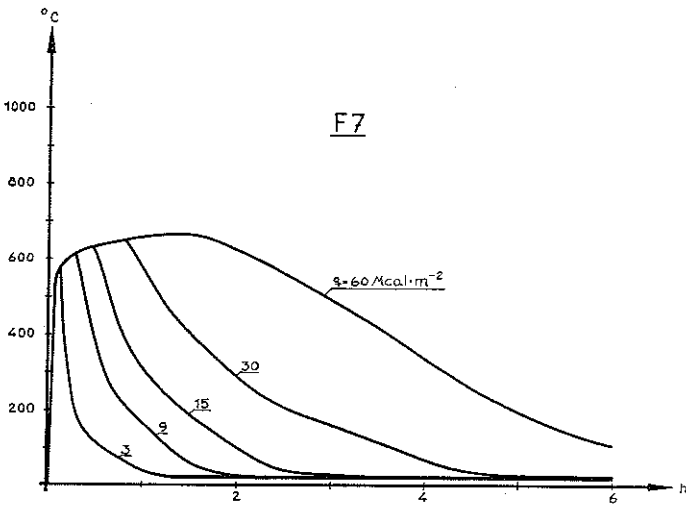
F5

Type F enclosed space.
Resultant emissivity 0.1.
Opening factor $0.12 \text{ m}^2/\text{m}^2$.



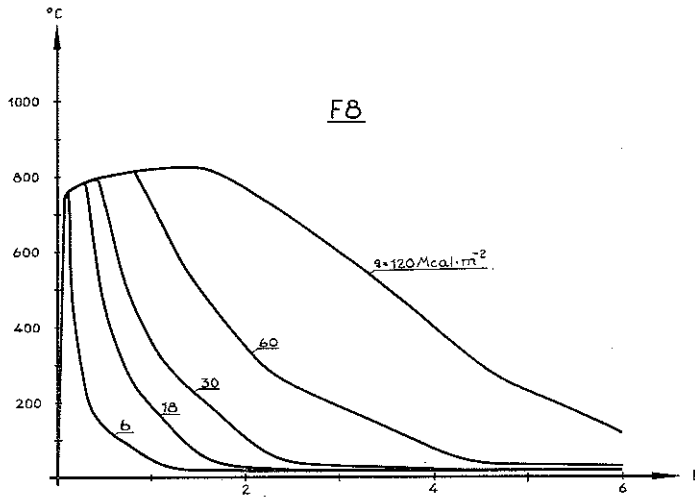
F6

Type F enclosed space.
 Resultant emissivity 0.35.
 Opening factor $0.01 \text{ m}^{1/2}$.

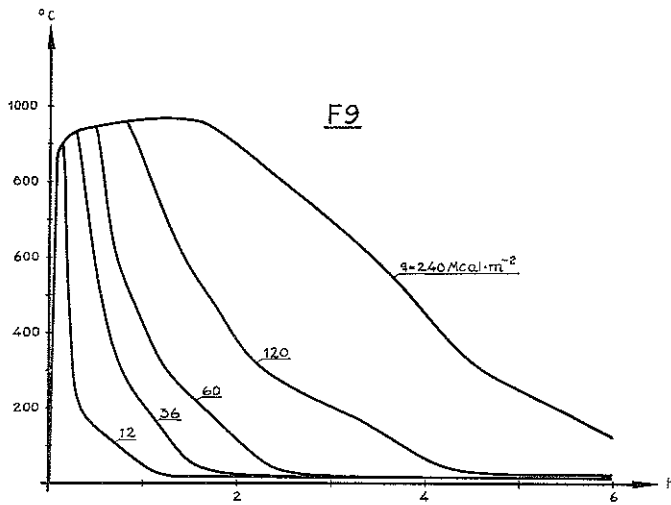


F7

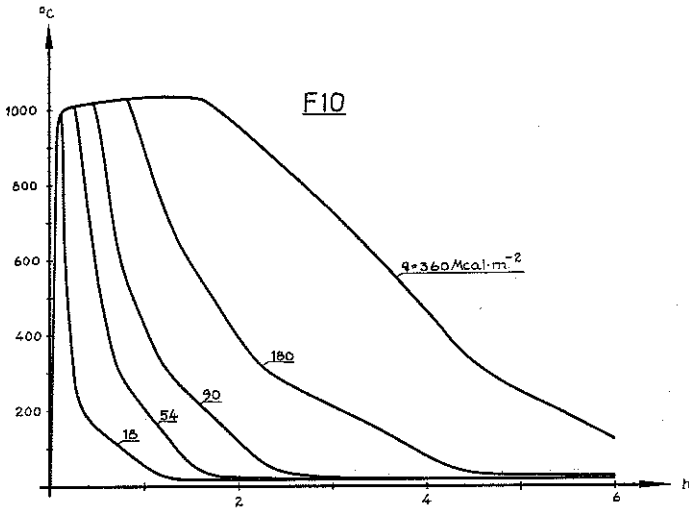
Type F enclosed space.
 Resultant emissivity 0.35.
 Opening factor $0.02 \text{ m}^{1/2}$.



F8
 Type F enclosed space.
 Resultant emissivity 0.35.
 Opening factor $0.04 \text{ m}^{1/2}$.

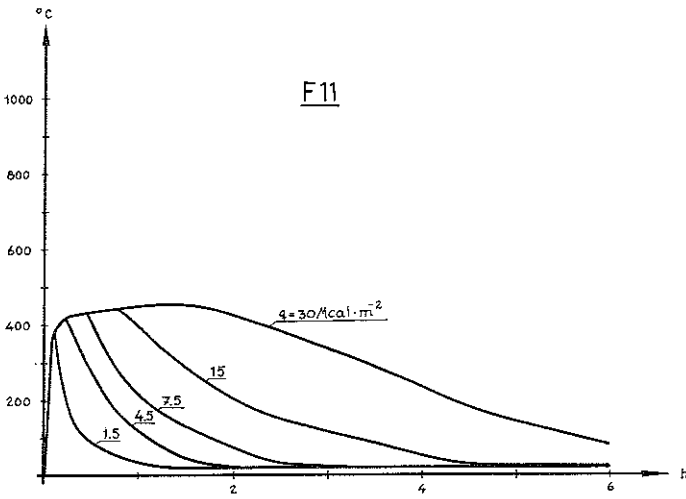


F9
 Type F enclosed space.
 Resultant emissivity 0.35.
 Opening factor $0.08 \text{ m}^{1/2}$.



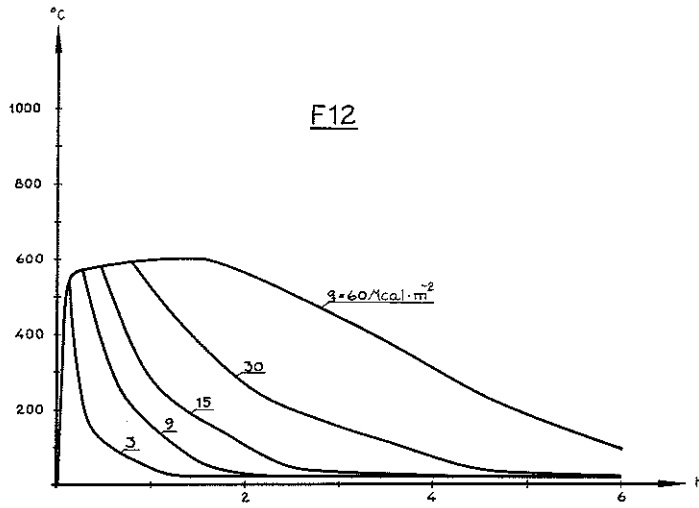
F10

Type F enclosed space.
 Resultant emissivity 0.35.
 Opening factor $0.12 \text{ m}^{1/2}$.

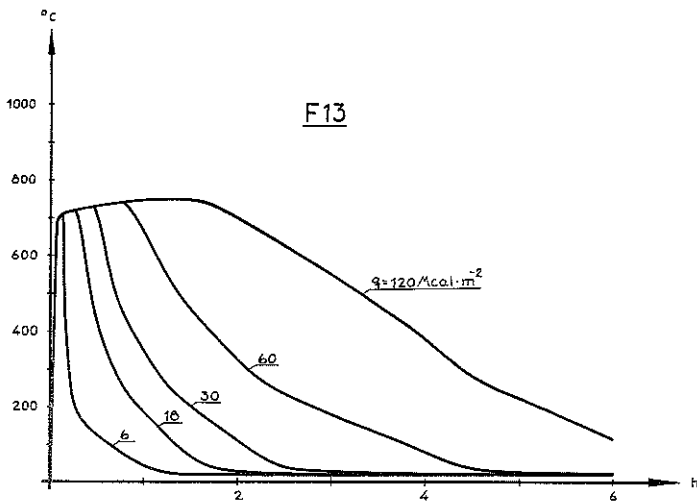


F11

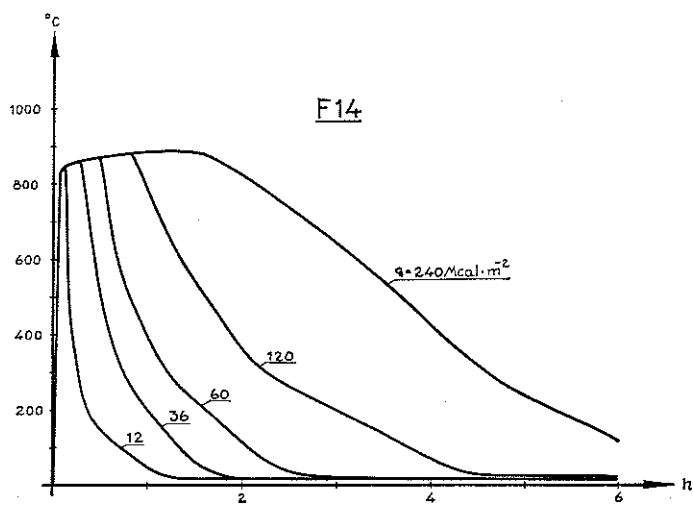
Type F enclosed space.
 Resultant emissivity 0.60.
 Opening factor $0.01 \text{ m}^{1/2}$.



F12
 Type F enclosed space.
 Resultant emissivity 0.60.
 Opening factor $0.02 \text{ m}^{1/2}$.

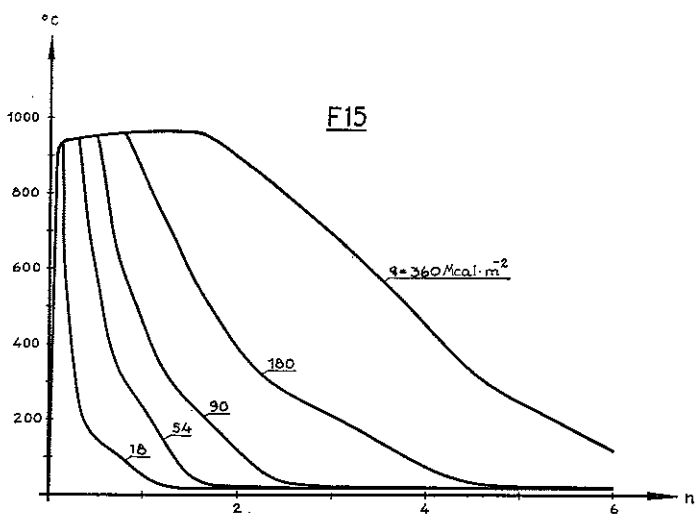


F13
 Type F enclosed space.
 Resultant emissivity 0.60.
 Opening factor $0.04 \text{ m}^{1/2}$.



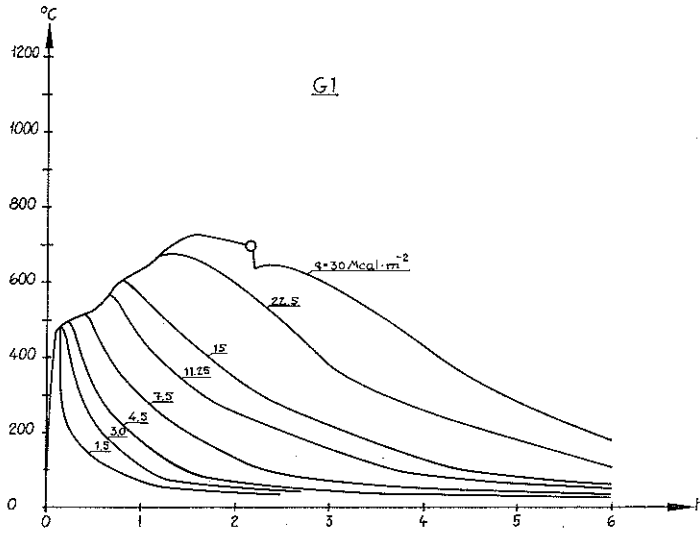
F14

Type F enclosed space.
 Resultant emissivity 0.60.
 Opening factor $0.08 \text{ m}^{1/2}$.



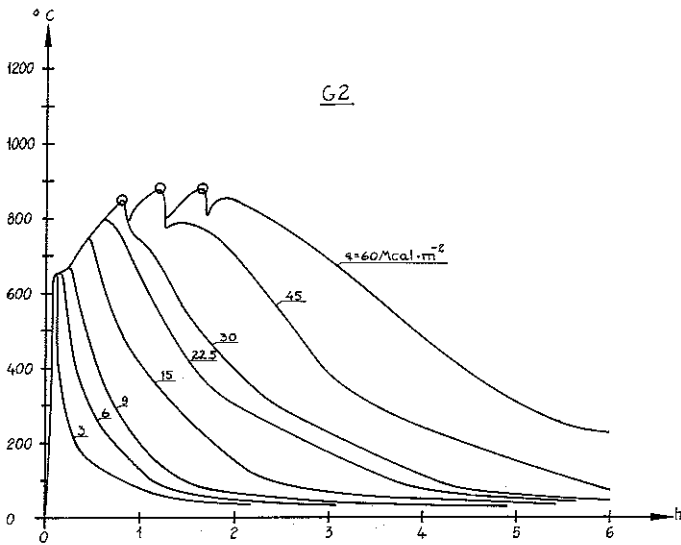
F15

Type F enclosed space.
 Resultant emissivity 0.60.
 Opening factor $0.12 \text{ m}^{1/2}$.



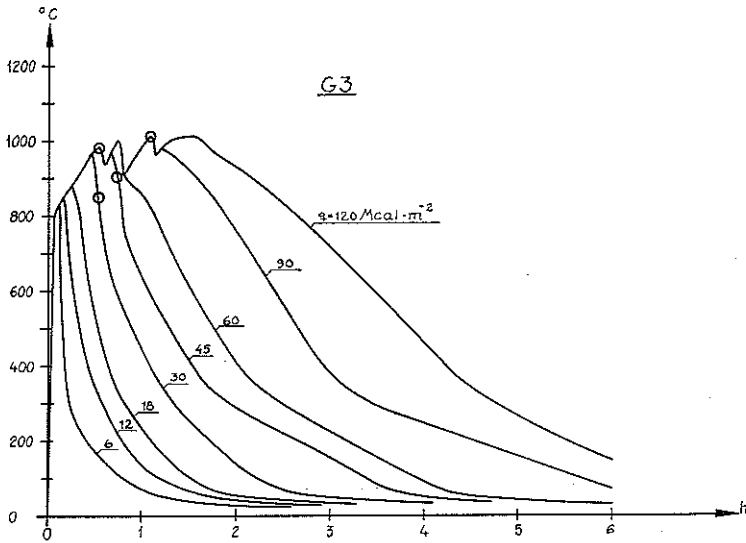
G1

Type G enclosed space.
 Opening factor $0.01 \text{ m}^{1/2}$.
 O=Plasterboard panel falls down.



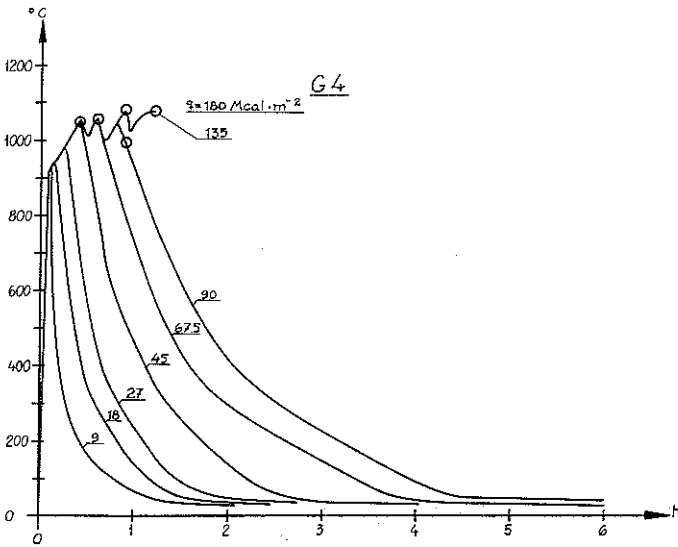
G2

Type G enclosed space.
 Opening factor $0.02 \text{ m}^{1/2}$.
 O=Plasterboard panel falls down.



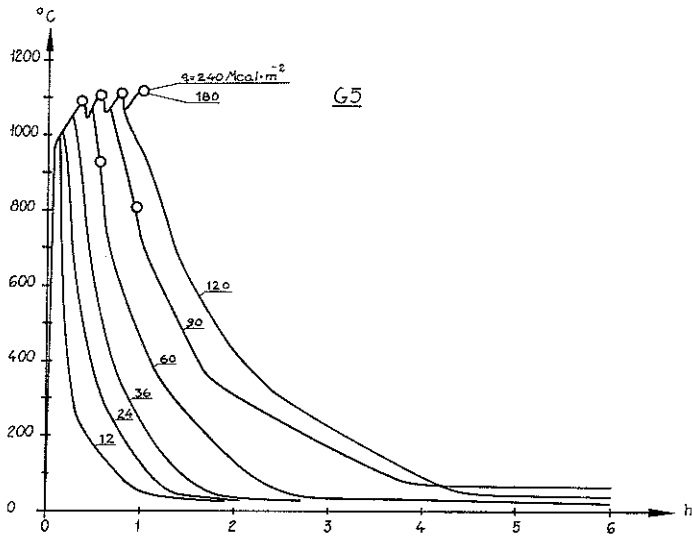
G3

Type G enclosed space.
 Opening factor $0.04 \text{ m}^{1/2}$.
 O=Plasterboard panel falls down.



G4

Type G enclosed space.
 Opening factor $0.06 \text{ m}^{1/2}$.
 O=Plasterboard panel falls down.

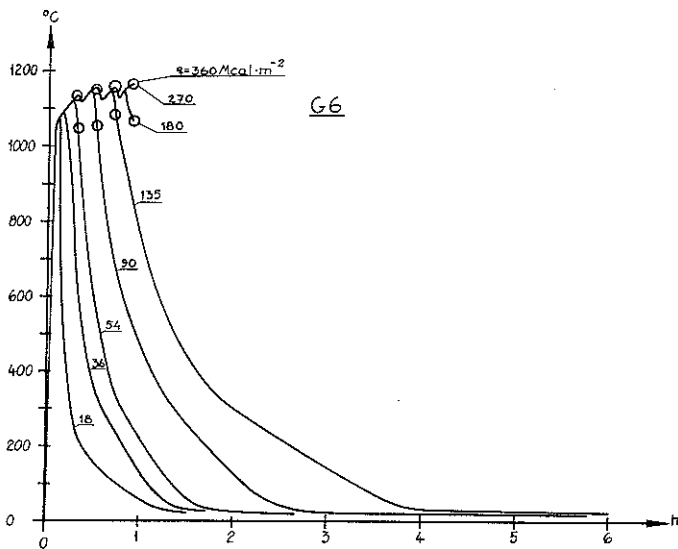


G5

Type G enclosed space.

Opening factor $0.08 \text{ m}^{1/2}$.

O=Plasterboard panel falls down.



G6

Type G enclosed space.

Opening factor $0.12 \text{ m}^{1/2}$.

O=Plasterboard panel falls down.

APPENDIX 6

Calculated time graphs of temperature of combustion gases represented in tabular form for seven types of enclosed spaces differing in opening factor and in bounding structures. See chapter 7.

A1

Time Graphs of Temperature of Combustion Gases. Type A Enclosed Space.

Opening Factor $A \cdot \sqrt{H}/A_t = 0.01 \text{ m}^{1/2}$

T	0.1	0.2	0.3	0.5	0.75	1.0	1.5	2.0			
q	1.5	3.0	4.5	7.5	11.25	15.0	22.5	30.0			
Time h	T	e	m	p	e	r	a	t	u	r	e
0.05	272	272	272	272	272	272	272	272			
0.10	395	395	395	395	328	328	328	328			
0.15	228	390	390	390	360	360	360	360			
0.20	196	368	401	401	406	406	406	406			
0.25	150	313	409	410	405	405	405	405			
0.30	98	257	385	421	415	415	415	415			
0.35	97	241	354	429	425	425	425	425			
0.40	94	218	320	437	434	434	434	434			
0.45	91	193	282	441	442	442	442	442			
0.50	88	167	269	412	449	449	449	449			
0.60	82	157	229	370	463	463	463	463			
0.65	79	150	215	355	460	470	470	470			
0.70	75	144	187	314	451	476	476	476			
0.80	69	131	178	302	426	488	488	488			
0.90	61	118	166	283	399	468	500	500			
1.00	54	104	154	263	367	456	511	511			
1.10	46	89	142	242	344	439	521	521			
1.20	45	74	129	218	331	421	531	531			
1.30	43	71	116	209	315	400	524	541			
1.40	42	68	102	199	299	376	524	550			
1.50	41	65	88	190	282	366	522	559			
1.60	40	63	85	180	263	353	515	567			
1.70	39	61	81	170	244	340	506	559			
1.80	38	59	79	160	237	326	496	562			
1.90	37	58	76	150	230	311	485	561			
2.00	36	56	74	139	223	296	473	560			
2.20	35	53	70	117	210	263	448	552			
2.40	34	51	66	103	197	249	422	542			
2.60	33	49	63	97	185	235	393	529			
2.80	32	47	61	92	172	221	361	514			
3.00	32	46	59	87	159	207	327	497			
3.20		44	56	83	146	194	301	480			
3.40		43	55	80	132	181	286	461			
3.60		42	53	77	118	168	273	441			
3.80		41	52	75	109	154	261	419			
4.00		40	50	72	104	140	249	396			
4.20		39	49	70	100	125	238	371			
4.40		39	48	68	96	119	227	345			
4.60		38	47	66	93	114	216	323			
4.80		37	46	65	90	110	205	307			
5.00		37	45	63	87	106	194	292			
5.20		36	44	62	85	103	184	277			
5.40		35	43	60	82	100	173	262			
5.60		35	42	59	80	97	162	247			
5.80		35	42	58	78	94	151	231			
6.00		34	41	57	77	92	140	216			

A2

Time Graphs of Temperature of Combustion Gases. Type A Enclosed Space.

Opening Factor $A \cdot \sqrt{H}/A_t = 0.02 \text{ m}^{1/2}$

T	0.1	0.2	0.3	0.5	0.75	1.0	1.5	2.0
q	3.0	6.0	9.0	15.0	22.5	30.0	45.0	60.0
Time h	T e m p e r a t u r e							
0.05	396	396	396	396	397	397	397	398
0.10	568	568	568	568	467	467	467	467
0.15	322	556	556	556	511	511	511	511
0.20	277	519	572	572	581	581	581	581
0.25	210	450	585	587	578	578	578	578
0.30	134	361	549	602	593	593	593	593
0.35	131	339	501	615	615	615	615	615
0.40	126	304	452	624	620	620	620	620
0.45	121	268	397	632	632	632	632	632
0.50	117	228	376	586	642	642	642	642
0.60	107	212	317	523	662	662	662	662
0.65	102	201	287	485	660	671	671	671
0.70	98	193	254	440	642	680	680	680
0.80	88	174	239	419	604	697	697	697
0.90	77	154	220	390	562	666	714	714
1.00	66	132	202	359	513	645	729	729
1.10	54	109	184	325	475	618	742	742
1.20	51	86	165	289	453	588	756	756
1.30	49	82	144	275	429	555	743	768
1.40	47	79	123	260	402	517	740	779
1.50	45	75	101	244	375	498	735	790
1.60	44	72	97	229	347	478	721	800
1.70	43	70	93	214	316	456	706	787
1.80	42	67	89	199	305	434	688	788
1.90	40	65	86	184	294	410	669	784
2.00	40	63	83	168	284	386	648	780
2.20	38	59	78	135	263	335	605	763
2.40	36	56	73	113	244	312	562	743
2.60	35	53	70	106	225	291	515	719
2.80	34	51	66	99	206	270	465	692
3.00	33	49	63	94	187	250	410	662
3.20	32	47	61	89	168	230	370	632
3.40	31	46	58	85	148	210	348	601
3.60	31	44	56	81	128	191	328	568
3.80	30	43	54	78	114	172	309	533
4.00	30	42	52	75	108	151	293	496
4.20		41	51	73	103	130	276	457
4.40		40	49	71	99	123	261	417
4.60		39	48	68	95	117	245	384
4.80		38	47	66	91	112	229	360
5.00		37	46	64	88	107	214	337
5.20		36	45	63	85	103	199	314
5.40		36	44	61	83	100	184	293
5.60		35	43	59	80	96	169	271
5.80		35	42	58	78	93	154	250
6.00		34	41	56	76	91	138	228

A3

Time Graphs of Temperature of Combustion Gases. Type A Enclosed Space.

Opening Factor $A \cdot \sqrt{H}/A_t = 0.04 \text{ m}^{1/2}$

T	0.1	0.2	0.3	0.5	0.75	1.0	1.5	2.0			
q	6.0	12.0	18.0	30.0	45.0	60.0	90.0	120.0			
Time h	T	e	m	p	e	r	a	t	u	r	e
0.05	504	504	504	504	504	504	504	504	504	504	504
0.10	745	745	745	745	621	621	621	621	621	621	621
0.15	422	747	747	747	681	681	681	681	681	681	681
0.20	360	696	767	767	777	777	777	777	777	777	777
0.25	268	587	784	784	776	776	776	776	776	776	776
0.30	164	472	734	799	793	793	793	793	793	793	793
0.35	162	437	665	814	808	808	808	808	808	808	808
0.40	155	389	593	828	822	822	822	822	822	822	822
0.45	148	337	513	841	836	836	836	836	836	836	836
0.50	142	281	481	779	848	848	848	848	848	848	848
0.60	128	259	397	682	874	874	874	874	874	874	874
0.65	120	246	352	626	882	882	882	882	882	882	882
0.70	114	232	307	565	839	894	894	894	894	894	894
0.80	100	204	285	527	785	912	912	912	912	912	912
0.90	86	178	260	483	720	862	928	928	928	928	928
1.00	71	149	235	437	645	827	942	942	942	942	942
1.10	54	118	208	388	589	787	955	955	955	955	955
1.20	51	85	183	337	555	740	967	967	967	967	967
1.30	49	82	156	316	518	688	942	977	977	977	977
1.40	46	77	128	296	480	632	931	987	987	987	987
1.50	45	74	98	276	441	602	919	996	996	996	996
1.60	43	70	94	255	400	571	895	1004	1004	1004	1004
1.70	41	68	89	235	358	540	870	981	981	981	981
1.80	40	65	85	214	343	507	843	973	973	973	973
1.90	39	62	82	194	328	474	813	963	963	963	963
2.00	38	60	79	174	313	440	781	953	953	953	953
2.20	36	56	73	131	288	369	718	923	923	923	923
2.40	35	52	69	104	263	339	655	890	890	890	890
2.60	33	50	64	96	238	311	587	853	853	853	853
2.80	32	47	61	90	214	286	516	813	813	813	813
3.00	31	45	57	84	190	261	442	769	769	769	769
3.20		43	55	80	166	236	388	727	727	727	727
3.40		42	52	76	141	211	362	682	682	682	682
3.60		40	50	72	115	187	338	635	635	635	635
3.80		39	48	69	99	163	316	587	587	587	587
4.00		38	47	66	94	137	296	537	537	537	537
4.20		37	45	64	89	110	277	485	485	485	485
4.40		36	44	61	85	104	258	431	431	431	431
4.60		35	42	59	81	99	240	388	388	388	388
4.80		34	41	57	78	94	221	360	360	360	360
5.00		33	40	55	75	90	204	332	332	332	332
5.20			39	53	73	87	186	305	305	305	305
5.40			38	52	70	83	168	280	280	280	280
5.60			37	50	68	81	150	255	255	255	255
5.80			37	49	66	78	131	229	229	229	229
6.00			36	48	64	75	111	203	203	203	203

A4

Time Graphs of Temperature of Combustion Gases. Type A Enclosed Space.

Opening Factor $A \cdot \sqrt{H}/A_t = 0.06 \text{ m}^{1/2}$

T	0.1	0.2	0.3	0.5	0.75	1.0	1.5	2.0
q	9.0	18.0	27.0	45.0	67.5	90.0	135.0	180.0
Time h	T e m p e r a t u r e							
0.05	575	575	575	575	575	575	575	575
0.10	858	858	858	858	704	704	704	704
0.15	493	861	861	861	784	784	784	784
0.20	404	802	879	879	882	882	882	882
0.25	296	679	898	898	889	889	889	890
0.30	175	538	838	914	908	908	908	908
0.35	174	490	761	928	923	923	923	923
0.40	166	430	669	942	936	936	937	937
0.45	159	369	572	954	949	949	949	949
0.50	151	303	532	877	961	961	961	961
0.60	136	277	433	762	982	982	982	982
0.65	128	262	402	694	992	992	992	992
0.70	120	247	326	620	939	1001	1001	1001
0.80	104	215	300	574	872	1018	1018	1018
0.90	89	185	272	520	795	954	1032	1032
1.00	71	152	243	466	705	909	1044	1044
1.10	51	116	213	409	637	858	1054	1054
1.20	48	80	184	343	593	803	1064	1064
1.30	45	76	155	327	550	742	1029	1072
1.40	43	72	123	303	505	675	1013	1080
1.50	41	68	89	281	460	640	996	1087
1.60	40	65	86	259	413	603	966	1093
1.70	38	62	81	236	364	567	935	1062
1.80	37	59	78	213	348	529	902	1049
1.90	36	56	74	191	332	491	866	1036
2.00	35	54	71	169	317	452	830	1022
2.20	33	50	66	121	289	371	756	984
2.40	32	47	61	93	263	340	683	943
2.60	31	44	57	85	236	310	605	900
2.80	30	42	54	79	210	283	524	854
3.00	29	40	51	74	185	257	440	805
3.20		39	48	70	159	230	381	756
3.40		37	46	67	131	204	355	705
3.60		36	44	63	103	178	331	652
3.80		35	42	60	86	152	308	597
4.00		34	41	57	81	123	288	541
4.20		33	40	55	77	95	269	483
4.40		32	38	53	73	90	249	423
4.60		31	37	51	70	85	230	377
4.80		31	36	49	67	81	211	348
5.00		30	35	47	64	77	193	319
5.20			35	46	62	74	174	292
5.40			34	44	59	71	155	265
5.60			33	43	57	69	135	238
5.80			32	42	55	66	114	210
6.00			32	41	54	64	94	185

A5

Time Graphs of Temperature of Combustion Gases. Type A Enclosed Space.

Opening Factor $A\sqrt{H}/A_t = 0.08 \text{ m}^{1/2}$

T	0.1	0.2	0.3	0.5	0.75	1.0	1.5	2.0
q	12.0	24.0	36.0	60.0	90.0	120.0	180.0	240.0
Time h	T e m p e r a t u r e							
0.05	622	622	622	622	622	622	622	622
0.10	935	935	935	935	766	766	766	767
0.15	432	937	937	937	853	853	853	853
0.20	532	869	955	955	959	959	959	959
0.25	314	734	973	973	965	965	965	965
0.30	181	575	903	987	981	981	981	982
0.35	180	521	818	1001	995	995	995	995
0.40	171	454	720	1013	1008	1008	1008	1008
0.45	163	386	611	1024	1020	1020	1020	1020
0.50	155	314	561	937	1031	1031	1031	1031
0.60	139	285	454	807	1050	1050	1050	1050
0.65	131	269	396	732	1058	1058	1058	1058
0.70	122	253	336	651	996	1066	1066	1066
0.80	106	219	306	598	920	1081	1081	1081
0.90	89	186	275	539	833	1005	1092	1092
1.00	70	151	245	479	735	953	1102	1102
1.10	47	113	214	417	659	897	1111	1111
1.20	44	73	183	352	612	836	1119	1119
1.30	42	70	151	328	564	769	1077	1126
1.40	40	66	117	304	516	695	1058	1132
1.50	39	62	81	281	466	657	1038	1138
1.60	37	59	78	257	415	618	1004	1143
1.70	36	56	74	234	363	577	969	1105
1.80	35	53	71	210	347	537	932	1090
1.90	34	51	68	187	331	496	893	1074
2.00	33	49	65	163	316	454	853	1058
2.20	31	46	59	112	287	368	774	1016
2.40	30	43	55	83	260	337	695	971
2.60	29	40	51	77	233	307	611	923
2.80	28	38	48	71	206	279	524	873
3.00	27	37	45	67	180	252	434	820
3.20		35	43	62	153	224	373	769
3.40		34	41	59	124	198	347	714
3.60		33	40	55	94	171	323	658
3.80		32	38	53	77	143	302	599
4.00		31	37	50	72	113	282	539
4.20			36	48	68	84	262	478
4.40			35	46	65	79	242	415
4.60			34	45	62	75	222	368
4.80			33	43	59	71	203	338
5.00			32	42	56	68	185	309
5.20				40	54	65	166	282
5.40				39	52	62	146	254
5.60				38	50	60	125	227
5.80				37	48	57	104	199
6.00				36	47	55	82	172

A6

Time Graphs of Temperature of Combustion Gases. Type A Enclosed Space.

Opening Factor $A \cdot \sqrt{H}/A_t = 0.12 \text{ m}^{1/2}$

T	0.1	0.2	0.3	0.5	0.75	1.0	1.5	2.0
q	18.0	35.0	54.0	90.0	135.0	180.0	270.0	360.0
Time h	T e m p e r a t u r e							
0.05	670	670	670	670	670	670	670	670
0.10	1027	1027	1027	1027	847	847	847	847
0.15	581	1033	1033	1033	933	933	933	933
0.20	465	951	1049	1049	1051	1051	1051	1051
0.25	333	799	1063	1063	1057	1057	1057	1057
0.30	186	620	981	1076	1071	1071	1071	1071
0.35	185	556	882	1088	1083	1083	1083	1083
0.40	176	480	774	1098	1094	1094	1094	1094
0.45	168	404	650	1107	1103	1103	1103	1103
0.50	159	324	593	1004	1112	1112	1112	1112
0.60	142	292	472	856	1127	1127	1127	1127
0.65	133	275	407	774	1133	1133	1133	1133
0.70	124	257	341	681	1060	1139	1139	1139
0.80	106	221	309	622	971	1150	1150	1150
0.90	88	186	276	556	873	1062	1159	1159
1.00	67	149	244	490	765	1001	1166	1166
1.10	41	107	211	422	680	937	1173	1173
1.20	39	63	178	351	628	868	1178	1178
1.30	37	60	145	327	575	794	1128	1183
1.40	36	56	108	301	523	713	1106	1188
1.50	34	53	69	277	469	672	1082	1192
1.60	33	50	67	253	414	629	1043	1195
1.70	32	47	63	228	358	585	1003	1151
1.80	31	45	60	203	343	542	962	1133
1.90	30	43	57	180	327	497	919	1114
2.00	29	42	54	155	311	452	874	1096
2.20		39	49	100	283	361	789	1048
2.40		37	46	70	255	330	704	998
2.60		35	43	64	227	300	613	946
2.80		33	40	59	200	272	519	891
3.00		32	38	54	173	245	423	834
3.20			37	51	144	216	361	780
3.40			35	48	113	190	336	721
3.60			34	46	83	162	313	660
3.80			33	43	64	132	293	598
4.00			32	42	59	102	273	534
4.20				40	55	69	253	469
4.40				39	52	65	233	403
4.60				37	50	61	213	355
4.80				36	48	58	194	325
5.00				35	46	55	175	297
5.20				34	44	52	155	269
5.40				33	42	50	134	241
5.60				33	41	48	112	213
5.80				32	40	46	91	186
6.00				31	38	45	67	158

B1

Time Graphs of Temperature of Combustion Gases. Type B Enclosed Space.

Opening Factor $A\sqrt{H}/A_t = 0.01 \text{ m}^{1/2}$

T	0.1	0.2	0.3	0.5	0.75	1.0	1.5	2.0			
q	1.5	3.0	4.5	7.5	11.25	15.0	22.5	30.0			
Time h	T	e	m	p	e	r	a	t	u	r	e
0.05	237	237	237	237	237	237	237	237	237	237	237
0.10	342	342	342	342	286	286	286	286	286	286	286
0.15	201	339	339	339	314	314	314	314	314	314	314
0.20	172	321	348	348	352	352	352	352	352	352	352
0.25	132	273	356	357	352	352	352	352	352	352	352
0.30	86	225	335	366	360	360	360	360	360	360	360
0.35	85	211	308	370	369	369	369	369	369	369	369
0.40	82	190	279	378	377	377	377	377	377	377	377
0.45	79	168	245	382	382	382	382	382	382	382	382
0.50	76	144	233	357	388	388	388	388	388	388	388
0.60	71	135	198	320	400	400	400	400	400	400	400
0.65	67	129	181	304	404	404	404	404	404	404	404
0.70	65	124	161	271	389	410	410	410	410	410	410
0.80	59	112	152	260	367	420	420	420	420	420	420
0.90	53	101	142	243	343	403	430	430	430	430	430
1.00	46	88	131	225	315	392	439	439	439	439	439
1.10	40	76	120	206	295	378	448	448	448	448	448
1.20	38	62	109	185	283	361	456	456	456	456	456
1.30	37	59	98	178	269	343	451	464	464	464	464
1.40	36	57	86	170	255	322	451	472	472	472	472
1.50	35	55	74	161	240	313	449	480	480	480	480
1.60	35	53	71	153	224	302	443	488	488	488	488
1.70	34	51	68	144	207	290	435	482	482	482	482
1.80	33	50	66	136	202	278	427	484	484	484	484
1.90	33	49	64	127	196	266	417	484	484	484	484
2.00	32	48	62	118	190	253	407	483	483	483	483
2.20		46	59	99	179	224	385	478	478	478	478
2.40		44	56	87	169	212	363	470	470	470	470
2.60		43	54	82	158	201	338	459	459	459	459
2.80		41	52	78	147	190	311	447	447	447	447
3.00		40	51	75	136	179	281	432	432	432	432
3.20		39	49	72	125	168	259	417	417	417	417
3.40		38	48	70	114	156	248	401	401	401	401
3.60		38	47	68	103	145	237	384	384	384	384
3.80		37	46	66	95	134	227	366	366	366	366
4.00		36	45	64	91	122	217	346	346	346	346
4.20		36	44	62	88	110	208	325	325	325	325
4.40		35	43	61	85	105	199	302	302	302	302
4.60		35	42	59	83	102	190	284	284	284	284
4.80		34	42	58	80	98	181	271	271	271	271
5.00		34	41	57	78	95	172	258	258	258	258
5.20		33	40	56	76	93	164	245	245	245	245
5.40		33	40	55	75	90	155	232	232	232	232
5.60		33	39	54	73	88	145	220	220	220	220
5.80		32	39	53	72	86	136	207	207	207	207
6.00		32	38	52	70	84	127	195	195	195	195

B2

Time Graphs of Temperature of Combustion Gases. Type B Enclosed Space.
Opening Factor $A \cdot \sqrt{H}/A_t = 0.02 \text{ m}^{1/2}$

T	0.1	0.2	0.3	0.5	0.75	1.0	1.5	2.0			
q	3.0	6.0	9.0	15.0	22.5	30.0	45.0	60.0			
Time											
h	T	e	m	p	e	r	a	t	u	r	e
0.05	353	353	354	354	354	354	354	355	356		
0.10	498	498	498	498	487	414	414	414	414		
0.15	288	487	487	487	451	451	451	451	451		
0.20	249	455	502	502	511	511	511	511	511		
0.25	189	392	513	516	506	506	506	506	506		
0.30	121	322	482	530	520	520	520	520	520		
0.35	118	303	443	540	538	538	538	538	538		
0.40	114	273	401	549	546	546	546	546	546		
0.45	109	240	353	554	559	559	559	559	559		
0.50	105	204	336	515	564	564	564	564	564		
0.60	96	190	283	463	583	583	583	583	583		
0.65	90	181	258	439	594	594	594	594	594		
0.70	87	173	226	390	567	600	600	600	600		
0.80	78	155	213	373	535	617	617	617	617		
0.90	69	137	197	347	499	590	633	633	633		
1.00	58	117	180	319	456	574	648	648	648		
1.10	48	97	164	289	424	552	663	663	663		
1.20	45	76	146	258	405	526	677	677	677		
1.30	44	73	128	245	383	496	668	691	691		
1.40	42	70	110	232	360	463	667	704	704		
1.50	41	67	91	218	336	447	664	716	716		
1.60	40	64	87	205	310	429	653	728	728		
1.70	39	62	83	192	284	410	640	717	717		
1.80	38	60	80	179	275	390	625	721	721		
1.90	37	58	77	166	265	370	608	719	719		
2.00	36	56	75	152	256	349	589	716	716		
2.20	35	53	70	123	238	303	552	702	702		
2.40	34	51	67	104	221	284	513	685	685		
2.60	33	49	64	97	205	265	471	663	663		
2.80	32	47	61	92	188	247	426	639	639		
3.00	31	46	58	87	172	229	377	612	612		
3.20		44	56	83	155	212	341	586	586		
3.40		43	55	80	138	195	321	557	557		
3.60		42	53	77	120	178	304	527	527		
3.80		41	51	74	108	161	288	495	495		
4.00		40	50	72	103	143	273	461	461		
4.20		39	49	70	99	124	259	426	426		
4.40		38	48	68	95	118	245	390	390		
4.60		38	47	66	92	113	231	360	360		
4.80		37	46	65	89	108	217	338	338		
5.00		37	45	63	86	105	204	318	318		
5.20		36	44	61	84	101	191	298	298		
5.40		35	43	60	81	98	178	279	279		
5.60		35	42	59	79	95	164	260	260		
5.80		34	42	57	77	93	150	240	240		
6.00		34	41	56	76	90	136	221	221		

B3

Time Graphs of Temperature of Combustion Gases. Type B Enclosed Space.

Opening Factor $A \cdot \sqrt{H}/A_c = 0.04 \text{ m}^{1/2}$

T	0.1	0.2	0.3	0.5	0.75	1.0	1.5	2.0			
q	6.0	12.0	18.0	30.0	45.0	60.0	90.0	120.0			
Time h	T	e	m	p	e	r	a	t	u	r	e
0.05	481	481	481	482	482	482	457	457			
0.10	675	675	675	675	557	557	558	558			
0.15	384	658	658	658	606	606	606	606			
0.20	331	615	676	676	693	693	693	693			
0.25	250	537	699	699	688	688	688	688			
0.30	155	431	657	716	709	709	709	709			
0.35	152	404	602	729	725	725	725	725			
0.40	145	361	542	755	742	742	742	742			
0.45	139	314	473	764	769	769	769	769			
0.50	132	263	446	711	778	778	778	778			
0.60	119	242	370	630	806	806	806	806			
0.65	112	229	324	581	822	822	822	822			
0.70	106	217	288	522	783	831	831	831			
0.80	94	192	268	492	733	855	855	855			
0.90	81	167	244	452	675	814	876	876			
1.00	67	140	220	410	607	783	893	893			
1.10	51	111	197	365	555	745	907	907			
1.20	48	81	173	318	523	701	919	919			
1.30	46	78	148	299	489	652	897	931			
1.40	44	74	122	280	454	599	889	942			
1.50	42	70	95	262	417	572	878	952			
1.60	41	67	91	243	380	543	856	962			
1.70	40	65	87	224	341	513	833	942			
1.80	39	62	83	205	327	483	807	934			
1.90	38	60	80	187	313	452	778	926			
2.00	37	58	77	168	300	420	748	917			
2.20	35	54	72	128	276	354	688	889			
2.40	34	51	68	103	253	326	629	858			
2.60	33	49	64	96	230	300	566	824			
2.80	32	47	61	90	207	277	499	785			
3.00	31	45	58	85	186	253	429	743			
3.20		43	55	81	163	230	378	703			
3.40		42	53	77	140	207	353	661			
3.60		41	51	74	116	185	331	616			
3.80		40	50	71	101	162	310	571			
4.00		39	48	69	96	138	291	523			
4.20		38	47	66	92	113	273	475			
4.40		37	45	64	88	107	255	424			
4.60		36	44	62	84	102	238	383			
4.80		36	43	60	81	98	220	356			
5.00		35	42	58	79	94	203	329			
5.20		34	41	57	76	91	187	304			
5.40		34	41	55	74	87	170	280			
5.60		33	40	54	72	85	153	255			
5.80		33	39	52	70	82	135	231			
6.00		32	38	51	68	80	117	206			

B4

Time Graphs of Temperature of Combustion Gases. Type B Enclosed Space

Opening Factor $A\sqrt{H}/A_t = 0.06 \text{ m}^{1/2}$

T	0.1	0.2	0.3	0.5	0.75	1.0	1.5	2.0
q	9.0	18.0	27.0	45.0	67.5	90.0	135.0	180.0
Time h	T e m p e r a t u r e							
0.05	528	528	528	528	528	528	528	528
0.10	761	761	761	761	632	632	632	632
0.15	440	766	766	766	703	703	703	703
0.20	378	720	790	790	806	806	806	806
0.25	281	615	818	818	805	805	805	805
0.30	170	496	770	838	829	829	829	829
0.35	167	460	702	859	850	850	850	850
0.40	159	408	627	877	869	869	869	869
0.45	152	352	541	895	887	887	887	887
0.50	145	291	506	830	905	905	905	905
0.60	130	266	414	726	935	935	935	935
0.65	122	252	377	663	949	949	949	949
0.70	115	237	315	595	902	962	962	962
0.80	100	208	290	551	840	979	979	979
0.90	85	179	263	500	765	920	995	995
1.00	69	147	235	449	680	878	1009	1009
1.10	49	114	207	395	612	830	1021	1021
1.20	47	79	180	339	573	776	1032	1032
1.30	44	75	152	317	532	717	999	1042
1.40	43	71	121	295	489	653	985	1051
1.50	41	68	90	274	446	620	969	1059
1.60	39	65	86	253	401	586	940	1067
1.70	38	62	82	231	355	551	910	1037
1.80	37	59	78	209	340	515	878	1025
1.90	36	57	75	189	324	478	844	1012
2.00	35	55	72	167	310	441	808	999
2.20	34	51	67	122	283	364	737	963
2.40	32	48	63	95	258	334	667	924
2.60	31	46	59	88	232	305	592	882
2.80	30	44	56	82	207	279	515	836
3.00	30	42	53	77	184	254	434	788
3.20		41	51	73	159	228	378	741
3.40		39	49	70	133	203	352	692
3.60		38	47	67	106	179	329	641
3.80		37	45	64	90	154	307	588
4.00		36	44	61	85	127	287	534
4.20		35	43	59	81	99	268	478
4.40		34	41	57	78	95	249	421
4.60		34	40	55	75	90	231	377
4.80		33	39	53	72	86	212	348
5.00		32	39	51	69	82	194	320
5.20			38	50	67	79	177	293
5.40			37	49	65	76	158	267
5.60			36	47	63	74	139	241
5.80			35	46	60	72	120	215
6.00			35	45	59	69	100	189

B5

Time Graphs of Temperature of Combustion Gases. Type B Enclosed Space.

Opening Factor $A\sqrt{H}/A_t = 0.08 \text{ m}^{1/2}$

T	0.1	0.2	0.3	0.5	0.75	1.0	1.5	2.0
q	12.0	24.0	36.0	60.0	90.0	120.0	180.0	240.0
Time	T e m p e r a t u r e							
h								
0.05	576	576	576	576	576	576	576	576
0.10	836	836	836	836	693	693	694	694
0.15	480	844	844	844	773	773	773	773
0.20	409	795	871	871	871	871	871	871
0.25	301	684	897	897	886	886	886	886
0.30	177	547	847	924	910	910	910	910
0.35	175	499	774	944	935	935	935	935
0.40	167	437	682	964	955	955	955	955
0.45	159	374	584	981	973	973	973	973
0.50	151	306	542	903	990	990	990	990
0.60	135	278	441	784	1018	1018	1018	1018
0.65	127	263	386	711	1027	1027	1027	1027
0.70	119	247	330	633	968	1036	1036	1036
0.80	103	214	300	582	896	1052	1052	1052
0.90	87	183	271	525	812	980	1066	1066
1.00	69	149	241	468	716	931	1077	1077
1.10	47	113	211	408	643	876	1087	1087
1.20	45	75	181	346	597	816	1097	1097
1.30	42	71	150	323	552	750	1056	1105
1.40	40	67	118	299	505	679	1038	1112
1.50	39	64	83	277	457	643	1019	1119
1.60	38	60	81	254	408	605	985	1124
1.70	36	57	77	231	359	566	951	1088
1.80	35	55	73	208	343	528	915	1073
1.90	34	53	70	186	327	488	877	1058
2.00	33	51	67	164	312	448	837	1042
2.20		48	62	115	284	365	760	1001
2.40		45	58	87	258	334	683	957
2.60		43	54	80	231	304	602	910
2.80		41	51	75	205	278	518	861
3.00		39	49	70	180	251	431	809
3.20		38	46	67	154	224	373	758
3.40		36	45	63	126	198	347	705
3.60		35	43	60	98	173	324	650
3.80		34	42	57	81	146	302	593
4.00		34	40	55	77	117	282	535
4.20			39	53	73	89	263	476
4.40			38	51	70	85	243	415
4.60			37	49	67	80	224	369
4.80			36	47	64	77	205	339
5.00			35	46	61	73	187	311
5.20			35	45	59	71	169	284
5.40			34	44	57	68	149	257
5.60			33	42	55	66	129	230
5.80			33	41	53	63	109	203
6.00			32	40	52	61	88	177

B6

Time Graphs of Temperature of Combustion Gases. Type B Enclosed Space.

Opening Factor $A \cdot \sqrt{H}/A_t = 0.12 \text{ m}^{1/2}$

T	0.1	0.2	0.3	0.5	0.75	1.0	1.5	2.0
q	18.0	35.0	54.0	90.0	135.0	180.0	270.0	360.0
Time h	T e m p e r a t u r e							
0.05	624	624	624	624	624	624	624	624
0.10	940	940	940	940	777	777	777	777
0.15	548	952	952	952	867	867	867	867
0.20	447	892	980	980	980	980	980	980
0.25	324	762	1006	1006	995	995	995	995
0.30	185	600	942	1029	1019	1019	1019	1019
0.35	183	541	855	1051	1040	1040	1040	1040
0.40	174	470	753	1068	1060	1060	1060	1060
0.45	166	397	636	1083	1076	1076	1076	1076
0.50	157	320	582	985	1089	1089	1089	1089
0.60	140	289	465	841	1106	1106	1106	1106
0.65	131	272	403	760	1113	1113	1113	1113
0.70	122	255	339	671	1043	1120	1120	1120
0.80	105	219	307	612	956	1133	1133	1133
0.90	87	185	275	548	859	1046	1143	1143
1.00	67	149	243	483	752	987	1152	1152
1.10	43	108	210	417	670	923	1159	1159
1.20	40	66	179	349	619	855	1165	1165
1.30	38	63	146	324	568	783	1116	1171
1.40	37	59	110	300	517	702	1093	1176
1.50	35	56	72	276	465	663	1070	1181
1.60	34	53	70	252	411	621	1031	1185
1.70	33	50	67	228	357	579	992	1141
1.80	32	48	63	204	341	536	951	1123
1.90	31	46	60	180	325	493	908	1105
2.00	31	44	57	156	310	450	864	1086
2.20		42	53	103	282	360	780	1039
2.40		39	49	74	254	329	696	989
2.60		37	46	68	227	300	608	938
2.80		36	44	63	200	273	517	884
3.00		35	42	59	174	245	423	827
3.20		33	40	55	146	217	362	773
3.40		32	38	52	116	191	338	715
3.60		31	37	50	86	164	314	656
3.80		31	36	48	69	135	294	594
4.00		30	35	46	64	105	274	532
4.20			34	44	61	74	254	469
4.40			33	42	57	71	234	404
4.60			32	41	55	67	215	357
4.80			32	40	52	63	196	327
5.00			31	39	50	60	178	299
5.20				38	49	58	158	272
5.40				37	47	55	138	244
5.60				36	45	53	116	216
5.80				35	44	51	96	189
6.00				34	43	49	73	162

C1

Time Graphs of Temperature of Combustion Gases. Type C Enclosed Space.

Opening Factor $A\sqrt{H}/A_t = 0.01 \text{ m}^{1/2}$

T	0.1	0.2	0.3	0.5	0.75	1.0	1.5	2.0
q	1.5	3.0	4.5	7.5	11.25	15.0	22.5	30.0
Time h	T e m p e r a t u r e							
0.05	502	502	502	502	502	502	502	502
0.10	778	778	778	778	630	630	630	630
0.15	430	769	769	769	696	696	696	696
0.20	347	704	773	773	777	777	777	777
0.25	255	584	779	779	776	776	776	776
0.30	156	459	719	784	782	782	782	782
0.35	154	417	645	790	788	788	788	788
0.40	148	368	569	797	795	795	795	795
0.45	142	319	488	803	801	801	801	801
0.50	137	267	455	738	808	808	808	808
0.60	125	249	379	640	821	821	821	821
0.65	119	237	339	586	825	825	825	825
0.70	113	225	297	530	782	828	828	828
0.80	101	201	278	498	727	836	836	836
0.90	88	177	255	460	668	790	845	845
1.00	75	151	232	419	604	758	856	856
1.10	60	123	209	376	557	724	869	869
1.20	57	93	186	331	527	685	880	880
1.30	54	90	161	313	496	643	861	890
1.40	52	85	135	294	463	596	853	899
1.50	49	81	108	275	429	572	844	907
1.60	47	77	103	257	392	546	825	914
1.70	46	73	98	238	355	519	804	897
1.80	44	70	93	219	341	491	781	890
1.90	42	68	89	199	327	462	756	883
2.00	41	65	85	181	313	431	730	875
2.20	39	60	78	140	288	368	676	851
2.40	37	56	73	113	264	339	622	823
2.60	35	52	68	104	241	312	565	791
2.80	34	50	64	96	217	288	503	757
3.00	32	47	60	89	195	264	437	720
3.20		45	57	84	172	240	388	684
3.40		43	54	79	148	216	361	645
3.60		41	51	75	123	193	338	605
3.80		40	49	71	107	169	317	564
4.00		38	47	68	100	145	297	520
4.20		37	45	65	94	119	279	475
4.40		36	44	62	89	111	261	427
4.60		35	42	59	84	105	243	387
4.80		34	41	57	81	99	225	360
5.00		33	40	55	77	94	208	333
5.20			39	53	74	90	191	307
5.40			38	51	71	86	173	283
5.60			37	50	69	82	156	259
5.80			36	48	66	79	137	234
6.00			35	47	64	76	118	209

C2

Time Graphs of Temperature of Combustion Gases. Type C Enclosed Space.

Opening Factor $A \cdot \sqrt{H}/A_c = 0.02 \text{ m}^{1/2}$

T	0.1	0.2	0.3	0.5	0.75	1.0	1.5	2.0			
q	3.0	6.0	9.0	15.0	22.5	30.0	45.0	60.0			
Time h	T	e	m	p	e	r	a	t	u	r	e
0.05	634	634	634	634	634	634	634	634	634		
0.10	992	992	992	992	805	805	805	805	805		
0.15	538	977	977	977	884	884	884	884	884		
0.20	425	889	979	979	986	986	986	986	986		
0.25	303	734	982	982	981	981	981	981	981		
0.30	175	563	901	987	985	985	985	985	985		
0.35	174	504	805	991	989	989	989	989	989		
0.40	167	439	701	997	995	995	995	995	995		
0.45	160	373	590	999	997	997	997	997	997		
0.50	153	304	542	906	999	999	999	999	999		
0.60	138	279	441	774	1003	1003	1003	1003	1003		
0.65	130	265	387	703	996	1010	1010	1010	1010		
0.70	122	250	331	627	946	1016	1016	1016	1016		
0.80	107	219	304	581	880	1032	1032	1032	1032		
0.90	91	188	276	529	803	967	1045	1045	1045		
1.00	73	155	248	474	715	922	1057	1057	1057		
1.10	53	120	218	417	648	872	1069	1069	1069		
1.20	50	82	189	356	605	817	1079	1079	1079		
1.30	47	78	159	333	562	756	1044	1088	1088		
1.40	45	73	126	309	517	689	1028	1095	1095		
1.50	42	69	93	286	470	654	1011	1102	1102		
1.60	41	66	88	263	422	616	980	1108	1108		
1.70	39	62	83	240	373	579	949	1076	1076		
1.80	37	59	78	217	356	540	915	1062	1062		
1.90	36	56	74	194	339	501	879	1048	1048		
2.00	35	53	71	172	322	462	841	1033	1033		
2.20	33	49	64	123	293	379	767	993	993		
2.40	31	45	59	93	266	345	693	951	951		
2.60	30	42	54	84	239	314	614	907	907		
2.80	29	40	50	77	212	286	532	860	860		
3.00	28	38	47	72	186	259	447	811	811		
3.20		36	44	67	160	232	386	762	762		
3.40		34	42	62	131	205	357	711	711		
3.60		33	40	58	102	179	332	658	658		
3.80		32	38	55	85	151	309	602	602		
4.00		31	37	52	79	122	288	546	546		
4.20			36	49	74	93	268	488	488		
4.40			34	47	70	87	249	428	428		
4.60			33	45	66	81	229	380	380		
4.80			32	43	62	77	209	349	349		
5.00			32	42	59	73	191	318	318		
5.20				40	56	69	172	290	290		
5.40				39	54	66	152	263	263		
5.60				38	51	63	132	236	236		
5.80				37	49	60	111	208	208		
6.00				36	48	57	90	182	182		

C3

Time Graphs of Temperature of Combustion Gases. Type C Enclosed Space.

Opening Factor $A\sqrt{H}/A_t = 0.04 \text{ m}^{1/2}$

T	0.1	0.2	0.3	0.5	0.75	1.0	1.5	2.0			
q	6.0	12.0	18.0	30.0	45.0	60.0	90.0	120.0			
Time h	T	e	m	p	e	r	a	t	u	r	e
0.05	726	726	726	726	726	726	726	726			
0.10	1126	1126	1126	1126	916	916	916	916			
0.15	618	1110	1110	1110	1002	1002	1002	1002			
0.20	478	1005	1111	1111	1122	1122	1122	1122			
0.25	334	829	1112	1112	1111	1111	1111	1111			
0.30	183	631	1013	1114	1113	1113	1113	1113			
0.35	182	559	902	1115	1115	1115	1115	1115			
0.40	174	480	784	1116	1118	1118	1118	1118			
0.45	166	401	651	1115	1117	1117	1117	1117			
0.50	158	320	593	1005	1115	1115	1115	1115			
0.60	141	290	469	852	1126	1126	1126	1126			
0.65	132	273	404	770	1131	1132	1132	1132			
0.70	123	256	338	679	1058	1137	1137	1137			
0.80	106	221	308	621	970	1148	1148	1148			
0.90	88	186	276	557	874	1061	1158	1158			
1.00	67	149	244	491	767	1002	1166	1166			
1.10	41	107	211	424	684	938	1172	1172			
1.20	39	63	178	353	631	870	1178	1178			
1.30	37	60	144	328	579	797	1128	1182			
1.40	35	55	107	302	526	717	1105	1184			
1.50	34	52	68	278	473	676	1081	1187			
1.60	32	48	66	254	418	631	1043	1189			
1.70	31	46	62	229	361	589	1003	1146			
1.80	30	43	58	204	345	545	962	1128			
1.90	29	41	54	180	328	500	919	1110			
2.00	28	39	51	155	312	456	875	1091			
2.20		36	46	100	283	363	790	1045			
2.40		34	42	69	255	331	703	996			
2.60		32	39	61	227	300	614	945			
2.80		30	37	55	199	272	521	890			
3.00		29	35	51	172	244	425	834			
3.20			33	47	143	216	362	780			
3.40			31	44	112	189	336	722			
3.60			30	41	81	161	312	661			
3.80			29	39	61	131	291	599			
4.00			28	37	56	100	271	535			
4.20				36	51	66	251	471			
4.40				34	48	62	231	404			
4.60				33	45	57	211	355			
4.80				32	43	53	193	324			
5.00				31	41	50	173	295			
5.20					39	47	153	267			
5.40					38	45	132	239			
5.60					36	43	110	210			
5.80					35	41	89	184			
6.00					34	39	64	155			

C4

Time Graphs of Temperature of Combustion Gases. Type C Enclosed Space.

Opening Factor $A\sqrt{H}/A_t = 0.06 \text{ m}^{1/2}$

T	0.1	0.2	0.3	0.5	0.75	1.0	1.5	2.0			
q	9.0	18.0	27.0	45.0	67.5	90.0	135.0	180.0			
Time h	T	e	m	p	e	r	a	t	u	r	e
0.05	766	766	766	766	766	766	766	766	766		
0.10	1183	1183	1183	1183	962	962	962	962	962		
0.15	650	1165	1165	1165	1052	1052	1052	1052	1052		
0.20	500	1053	1165	1165	1178	1178	1178	1178	1178		
0.25	346	867	1166	1166	1166	1166	1166	1166	1166		
0.30	185	659	1060	1168	1167	1167	1167	1167	1167		
0.35	185	581	941	1167	1167	1167	1167	1167	1167		
0.40	176	498	815	1166	1167	1167	1167	1167	1167		
0.45	168	411	674	1166	1166	1166	1166	1166	1166		
0.50	159	323	611	1048	1166	1166	1166	1166	1166		
0.60	142	292	477	884	1177	1177	1177	1177	1177		
0.65	132	275	408	795	1181	1181	1181	1181	1181		
0.70	123	257	336	696	1100	1186	1186	1186	1186		
0.80	105	220	307	634	1003	1194	1194	1194	1194		
0.90	85	183	273	564	898	1096	1201	1201	1201		
1.00	64	144	240	494	782	1031	1207	1207	1207		
1.10	35	101	206	422	693	961	1211	1211	1211		
1.20	33	53	173	348	637	887	1214	1214	1214		
1.30	32	49	137	323	582	809	1158	1216	1216		
1.40	30	45	98	297	526	723	1132	1218	1218		
1.50	29	42	56	273	469	681	1107	1220	1220		
1.60	28	40	54	248	412	635	1064	1222	1222		
1.70	27	38	50	222	353	589	1022	1174	1174		
1.80	26	36	47	197	338	543	978	1153	1153		
1.90	26	34	44	173	321	497	933	1134	1134		
2.00	25	33	42	147	306	450	885	1114	1114		
2.20			38	90	278	354	796	1064	1064		
2.40			35	55	250	323	707	1012	1012		
2.60			33	49	221	294	612	957	957		
2.80			31	44	194	266	514	900	900		
3.00			29	41	166	238	414	841	841		
3.20				38	136	209	351	784	784		
3.40				36	105	182	326	723	723		
3.60				34	71	153	304	660	660		
3.80				32	49	122	284	595	595		
4.00				31	44	91	264	529	529		
4.20					41	54	244	462	462		
4.40					39	49	224	394	394		
4.60					37	45	205	344	344		
4.80					35	42	186	314	314		
5.00					34	40	166	286	286		
5.20						38	146	258	258		
5.40						36	124	229	229		
5.60						35	102	201	201		
5.80						34	79	174	174		
6.00						33	51	144	144		

C5

Time Graphs of Temperature of Combustion Gases. Type C Enclosed Space.

Opening Factor $A\sqrt{H}/A_t = 0.08 \text{ m}^{1/2}$

T	0.1	0.2	0.3	0.5	0.75	1.0	1.5	2.0			
q	12.0	24.0	36.0	60.0	90.0	120.0	180.0	240.0			
Time h	T	e	m	p	e	r	a	t	u	r	e
0.05	788	788	788	788	788	788	788	788			
0.10	1215	1215	1215	1215	987	987	987	987			
0.15	668	1196	1196	1196	1079	1079	1079	1079			
0.20	512	1079	1196	1196	1210	1210	1210	1210			
0.25	352	889	1196	1196	1196	1196	1196	1196			
0.30	186	675	1086	1198	1197	1197	1197	1197			
0.35	186	593	963	1197	1197	1197	1197	1197			
0.40	177	504	832	1196	1196	1196	1196	1196			
0.45	168	416	687	1195	1197	1197	1197	1197			
0.50	160	325	621	1073	1197	1197	1197	1197			
0.60	142	293	481	901	1206	1206	1206	1206			
0.65	132	275	410	807	1209	1209	1209	1209			
0.70	122	257	337	705	1123	1213	1213	1213			
0.80	104	219	305	640	1021	1219	1219	1219			
0.90	84	181	273	569	910	1115	1225	1225			
1.00	61	141	239	496	790	1046	1229	1229			
1.10	32	97	205	422	697	973	1231	1231			
1.20	30	46	171	346	639	896	1233	1233			
1.30	29	42	135	320	582	814	1174	1235			
1.40	28	39	96	294	525	726	1147	1237			
1.50	27	37	50	269	467	682	1120	1238			
1.60	26	35	46	244	408	635	1076	1240			
1.70	25	33	43	219	348	588	1032	1189			
1.80	25	32	40	194	334	541	987	1169			
1.90	24	31	38	169	318	494	940	1149			
2.00	23	30	36	142	303	446	891	1128			
2.20			33	84	275	349	799	1076			
2.40			31	47	247	319	707	1022			
2.60			29	42	218	290	609	965			
2.80			28	38	191	262	509	907			
3.00			27	36	163	234	407	846			
3.20				33	132	206	344	787			
3.40				32	100	178	321	724			
3.60				30	66	149	300	659			
3.80				29	42	118	280	592			
4.00				28	38	86	260	525			
4.20					36	46	240	457			
4.40					34	42	220	388			
4.60					32	39	201	338			
4.80					31	37	182	308			
5.00					30	35	163	281			
5.20						33	142	253			
5.40						32	119	224			
5.60						31	98	196			
5.80						30	74	169			
6.00						29	44	138			

C6

Time Graphs of Temperature of Combustion Gases. Type C Enclosed Space.

Opening Factor $A\sqrt{H}/A_t = 0.12 \text{ m}^{1/2}$

T	0.1	0.2	0.3	0.5	0.75	1.0	1.5	2.0
q	18.0	35.0	54.0	90.0	135.0	180.0	270.0	360.0
Time h	T e m p e r a t u r e							
0.05	812	812	812	812	812	812	812	812
0.10	1250	1250	1250	1250	1014	1014	1014	1014
0.15	688	1230	1230	1230	1109	1109	1109	1109
0.20	525	1109	1230	1230	1245	1245	1245	1245
0.25	359	912	1230	1230	1230	1230	1230	1230
0.30	186	691	1115	1231	1230	1230	1230	1230
0.35	186	606	987	1230	1230	1230	1230	1230
0.40	177	513	851	1229	1229	1229	1229	1229
0.45	169	421	701	1229	1230	1230	1230	1230
0.50	160	326	632	1100	1231	1231	1231	1231
0.60	141	293	485	918	1237	1237	1237	1237
0.65	132	275	411	820	1239	1239	1239	1239
0.70	122	256	335	713	1148	1242	1242	1242
0.80	103	217	303	645	1039	1247	1247	1247
0.90	82	179	270	571	922	1136	1250	1250
1.00	58	138	236	496	796	1063	1253	1253
1.10	28	93	202	420	700	986	1254	1254
1.20	27	38	167	342	641	905	1256	1256
1.30	26	35	130	316	582	820	1192	1257
1.40	25	33	90	290	523	728	1164	1258
1.50		31	40	266	464	683	1136	1259
1.60		30	38	241	403	635	1089	1260
1.70		29	35	215	342	587	1043	1206
1.80		28	33	190	329	539	996	1185
1.90		27	32	164	313	491	947	1163
2.00		26	31	137	299	442	897	1142
2.20				78	271	343	802	1087
2.40				38	243	314	707	1031
2.60				35	215	286	607	972
2.80				32	188	258	504	912
3.00				30	159	230	400	849
3.20					128	202	337	789
3.40					96	174	315	724
3.60					60	145	295	658
3.80					34	113	276	590
4.00					32	80	256	521
4.20						37	237	452
4.40						34	216	381
4.60						32	198	332
4.80						31	179	303
5.00						29	159	275
5.20							137	247
5.40							115	219
5.60							93	191
5.80							68	163
6.00							36	132

D1

Time Graphs of Temperature of Combustion Gases. Type D Enclosed Space.

Opening Factor $A \cdot \sqrt{H}/A_t = 0.01 \text{ m}^{1/2}$

T	0.1	0.2	0.3	0.5	0.75	1.0	1.5	2.0			
q	1.5	3.0	4.5	7.5	11.25	15.0	22.5	30.0			
Time h	T	e	m	p	e	r	a	t	u	r	e
0.05	315	315	315	315	315	315	315	315			
0.10	453	453	453	453	376	376	376	376			
0.15	261	445	445	445	411	411	411	411			
0.20	224	416	457	457	456	456	456	456			
0.25	171	361	466	466	460	460	460	460			
0.30	110	291	438	480	472	472	472	472			
0.35	108	274	401	490	484	484	484	484			
0.40	104	247	363	496	494	494	494	494			
0.45	100	217	319	501	502	502	502	502			
0.50	97	186	303	466	509	509	509	509			
0.60	89	174	257	418	525	525	525	525			
0.65	85	116	232	385	532	532	532	532			
0.70	82	159	207	353	509	539	539	539			
0.80	74	144	196	338	481	553	553	553			
0.90	66	128	182	316	449	529	566	566			
1.00	57	111	168	292	412	514	579	579			
1.10	47	94	154	266	384	495	591	591			
1.20	45	76	139	239	368	473	603	603			
1.30	44	73	123	228	350	448	594	614			
1.40	42	69	107	216	330	420	594	624			
1.50	41	67	90	205	309	406	591	634			
1.60	40	64	86	194	288	391	581	644			
1.70	39	62	83	182	265	375	571	634			
1.80	38	60	80	170	257	358	558	636			
1.90	37	58	77	159	248	341	544	635			
2.00	36	56	75	146	240	323	529	633			
2.20	35	53	70	121	225	284	498	623			
2.40	34	51	67	104	210	267	467	610			
2.60	33	49	64	97	195	250	432	593			
2.80	32	47	61	92	181	234	393	574			
3.00	31	46	58	87	166	219	352	552			
3.20		44	56	83	151	204	321	531			
3.40		43	54	80	135	189	304	507			
3.60		42	53	77	119	173	289	482			
3.80		41	51	74	109	158	275	456			
4.00		40	50	72	103	142	261	428			
4.20		39	49	70	99	125	249	398			
4.40		38	48	68	95	119	236	367			
4.60		38	47	66	92	114	223	342			
4.80		37	46	65	89	109	211	323			
5.00		37	45	63	86	105	199	305			
5.20		36	44	61	84	102	187	287			
5.40		35	43	60	82	99	175	270			
5.60		35	42	59	80	96	163	253			
5.80		34	42	58	78	93	151	236			
6.00		34	41	56	76	91	138	218			

D2

Time Graphs of Temperature of Combustion Gases. Type D Enclosed Space.

Opening Factor $A \cdot \sqrt{H}/A_t = 0.02 \text{ m}^{1/2}$

T	0.1	0.2	0.3	0.5	0.75	1.0	1.5	2.0			
q	3.0	6.0	9.0	15.0	22.5	30.0	45.0	60.0			
Time h	T	e	m	p	e	r	a	t	u	r	e
0.05	444	444	444	444	444	445	445	446			
0.10	631	631	631	631	520	520	520	520			
0.15	358	616	616	616	566	566	566	566			
0.20	307	574	635	635	645	645	646	646			
0.25	232	499	649	649	641	641	641	641			
0.30	145	400	609	664	658	658	658	658			
0.35	142	375	557	681	672	672	672	672			
0.40	137	335	502	697	686	686	686	686			
0.45	131	292	438	704	702	702	702	702			
0.50	125	247	414	654	717	717	717	717			
0.60	113	228	346	581	740	740	740	740			
0.65	108	217	309	533	752	752	752	752			
0.70	103	206	272	485	719	763	763	763			
0.80	91	184	255	459	675	783	783	783			
0.90	79	161	234	424	623	746	801	801			
1.00	67	137	212	387	564	720	818	818			
1.10	53	111	191	348	519	688	834	834			
1.20	50	84	170	306	492	650	847	847			
1.30	48	81	147	289	463	609	831	860			
1.40	46	77	124	272	432	564	826	871			
1.50	44	73	99	255	400	541	818	882			
1.60	43	70	95	238	367	515	800	892			
1.70	41	67	90	221	332	489	780	877			
1.80	40	65	86	203	319	463	758	873			
1.90	39	62	83	187	306	435	733	867			
2.00	38	60	80	169	294	407	707	860			
2.20	36	57	75	133	272	348	655	838			
2.40	35	54	70	109	250	322	603	812			
2.60	34	51	67	101	228	298	548	782			
2.80	33	49	63	95	207	275	488	748			
3.00	32	47	60	89	187	253	424	711			
3.20		45	58	85	166	231	377	676			
3.40		44	55	81	145	210	353	638			
3.60		42	53	77	122	189	331	599			
3.80		41	52	74	108	167	311	558			
4.00		40	50	72	102	145	293	515			
4.20		39	49	69	97	122	276	470			
4.40		38	47	67	93	115	259	424			
4.60		37	46	65	89	109	242	386			
4.80		37	45	63	86	105	225	360			
5.00		36	44	61	83	100	209	335			
5.20		35	43	59	80	97	193	310			
5.40		35	42	58	78	93	177	287			
5.60		34	41	56	76	90	161	264			
5.80		34	40	55	74	87	145	241			
6.00		33	40	54	72	85	127	217			

D3

Time Graphs of Temperature of Combustion Gases. Type D Enclosed Space.

Opening Factor $A \cdot \sqrt{H} / A_t = 0.04 \text{ m}^{1/2}$

T	0.1	0.2	0.3	0.5	0.75	1.0	1.5	2.0
q	6.0	12.0	18.0	30.0	45.0	60.0	90.0	120.0
Time h	T e m p e r a t u r e							
0.05	547	547	547	547	547	547	547	547
0.10	797	797	797	797	660	660	660	660
0.15	456	802	802	802	734	734	734	734
0.20	387	752	825	825	826	826	826	826
0.25	286	638	851	851	837	837	837	837
0.30	172	510	799	870	862	862	862	862
0.35	169	470	729	889	881	881	881	881
0.40	161	416	643	906	898	898	898	898
0.45	154	358	552	921	915	915	915	915
0.50	147	295	515	851	930	930	930	930
0.60	132	270	420	740	955	955	955	955
0.65	124	255	370	674	966	966	966	966
0.70	117	241	319	603	914	974	974	974
0.80	102	210	293	559	849	990	990	990
0.90	87	181	266	507	774	930	1006	1006
1.00	70	150	238	455	688	887	1019	1019
1.10	51	116	210	400	622	839	1031	1031
1.20	48	80	182	343	580	785	1042	1042
1.30	45	77	154	321	539	725	1009	1051
1.40	43	72	123	298	495	661	994	1060
1.50	42	69	91	277	452	627	978	1068
1.60	40	65	87	255	406	592	949	1075
1.70	39	62	83	234	360	557	918	1045
1.80	37	60	79	211	344	521	886	1032
1.90	36	57	75	190	328	484	851	1020
2.00	35	55	72	169	313	446	815	1006
2.20	34	51	67	123	286	368	743	969
2.40	32	48	62	95	260	337	672	929
2.60	31	46	58	87	234	308	597	887
2.80	30	43	55	81	209	281	519	841
3.00	29	42	52	76	185	255	437	793
3.20		40	50	72	159	229	380	745
3.40		39	48	69	133	204	354	696
3.60		37	46	65	105	179	330	644
3.80		36	44	62	89	153	308	591
4.00		35	43	60	84	126	288	537
4.20		34	42	57	80	98	269	481
4.40		34	40	55	76	93	250	423
4.60		33	39	53	73	88	231	378
4.80		32	38	51	70	84	212	348
5.00		32	37	50	68	81	194	320
5.20			37	48	65	77	176	293
5.40			36	47	63	75	157	267
5.60			35	46	61	72	138	240
5.80			34	44	59	70	118	214
6.00			34	43	57	68	98	188

D4

Time Graphs of Temperature of Combustion Gases. Type D Enclosed Space.

Opening Factor $A\sqrt{H}/A_t = 0.06 \text{ m}^{1/2}$

T	0.1	0.2	0.3	0.5	0.75	1.0	1.5	2.0			
q	9.0	18.0	27.0	45.0	67.5	90.0	135.0	180.0			
Time h	T	e	m	p	e	r	a	t	u	r	e
0.05	613	613	613	613	613	613	614	614			
0.10	903	903	903	903	746	746	746	746			
0.15	525	911	911	911	831	831	831	831			
0.20	429	853	936	936	937	937	937	937			
0.25	312	727	959	959	949	949	949	949			
0.30	181	573	898	980	971	971	971	971			
0.35	179	519	816	1000	990	990	990	990			
0.40	170	453	720	1016	1009	1009	1009	1009			
0.45	162	384	610	1030	1024	1024	1024	1024			
0.50	154	313	560	941	1036	1036	1036	1036			
0.60	138	284	452	808	1053	1053	1053	1053			
0.65	129	268	394	732	1062	1062	1062	1062			
0.70	121	251	334	649	991	1070	1070	1070			
0.80	104	218	304	596	915	1083	1083	1083			
0.90	88	185	274	536	828	1006	1095	1095			
1.00	69	150	244	476	729	953	1106	1106			
1.10	46	112	213	414	655	896	1115	1115			
1.20	44	73	183	350	609	834	1123	1123			
1.30	42	69	151	326	561	766	1080	1130			
1.40	40	65	117	301	513	692	1060	1136			
1.50	38	61	81	278	463	654	1040	1142			
1.60	37	58	78	255	413	614	1004	1147			
1.70	35	55	74	232	361	574	968	1108			
1.80	34	53	70	208	345	534	930	1092			
1.90	33	50	67	185	328	493	891	1076			
2.00	32	49	64	162	313	451	850	1059			
2.20		45	58	111	285	366	770	1016			
2.40		43	54	82	258	334	691	970			
2.60		40	51	76	231	304	607	921			
2.80		38	48	70	204	277	520	870			
3.00		37	45	66	178	250	430	817			
3.20		35	43	62	151	222	370	765			
3.40		34	41	58	123	196	345	711			
3.60		33	40	55	94	170	321	654			
3.80		32	39	52	76	142	299	595			
4.00		32	37	50	72	112	279	536			
4.20			36	48	68	83	260	475			
4.40			35	46	65	79	240	412			
4.60			34	45	61	75	221	365			
4.80			34	43	59	71	202	335			
5.00			33	42	56	68	183	307			
5.20				41	54	65	164	279			
5.40				40	52	62	145	252			
5.60				39	50	60	124	225			
5.80				38	49	57	103	198			
6.00				37	47	55	82	171			

05

Time Graphs of Temperature of Combustion Gases. Type D Enclosed Space.

Opening Factor $A \cdot \sqrt{H}/A_t = 0.08 \text{ m}^{1/2}$

T	0.1	0.2	0.3	0.5	0.75	1.0	1.5	2.0			
q	12.0	24.0	36.0	60.0	90.0	120.0	180.0	240.0			
Time h	T	e	m	p	e	r	a	t	u	r	e
0.05	642	642	642	642	642	642	642	642			
0.10	975	975	975	975	803	803	803	803			
0.15	560	983	983	983	888	888	888	888			
0.20	454	916	1008	1008	1005	1005	1005	1005			
0.25	327	778	1030	1030	1020	1020	1020	1020			
0.30	185	607	959	1049	1041	1041	1041	1041			
0.35	183	546	866	1067	1058	1058	1058	1058			
0.40	174	473	761	1081	1075	1075	1075	1075			
0.45	166	399	640	1092	1087	1087	1087	1087			
0.50	158	321	584	990	1095	1095	1095	1095			
0.60	140	289	466	843	1109	1109	1109	1109			
0.65	132	273	403	762	1116	1116	1116	1116			
0.70	123	255	339	672	1045	1122	1122	1122			
0.80	105	220	307	614	958	1134	1134	1134			
0.90	87	185	275	550	862	1048	1144	1144			
1.00	67	149	243	485	755	989	1153	1153			
1.10	43	108	211	419	672	925	1160	1160			
1.20	40	66	179	350	621	857	1166	1166			
1.30	38	63	146	325	570	785	1117	1172			
1.40	37	59	110	300	519	705	1095	1176			
1.50	35	55	72	277	466	665	1071	1180			
1.60	34	52	70	253	413	623	1032	1184			
1.70	33	50	66	228	358	581	993	1140			
1.80	32	47	63	204	342	538	952	1122			
1.90	31	45	59	181	326	495	910	1104			
2.00	30	44	56	156	310	451	866	1086			
2.20		41	52	102	282	361	782	1039			
2.40		38	48	73	255	330	698	990			
2.60		36	45	67	227	300	609	938			
2.80		35	42	62	200	273	518	884			
3.00		34	40	57	174	245	423	828			
3.20			39	54	146	217	362	774			
3.40			37	51	115	191	337	716			
3.60			36	48	85	164	314	657			
3.80			35	46	67	135	293	595			
4.00			34	44	63	104	273	533			
4.20				42	59	73	254	469			
4.40				41	56	69	234	404			
4.60				39	53	65	214	357			
4.80				38	51	61	196	327			
5.00				37	49	58	177	298			
5.20				36	47	56	157	271			
5.40				35	45	53	137	243			
5.60				34	44	51	115	215			
5.80				34	42	49	83	188			
6.00				33	41	48	71	161			

D6

Time Graphs of Temperature of Combustion Gases. Type D Enclosed Space.

Opening Factor $A \cdot \sqrt{H}/A_t = 0.12 \text{ m}^{1/2}$

T	0.1	0.2	0.3	0.5	0.75	1.0	1.5	2.0
q	18.0	35.0	54.0	90.0	135.0	180.0	270.0	360.0
Time h	T e m p e r a t u r e							
0.05	697	697	697	697	697	697	697	697
0.10	1056	1056	1056	1056	874	874	874	874
0.15	605	1070	1070	1070	965	965	965	965
0.20	483	991	1094	1094	1093	1093	1093	1093
0.25	343	834	1113	1113	1104	1104	1104	1104
0.30	189	646	1027	1128	1121	1121	1121	1121
0.35	187	575	921	1142	1135	1135	1135	1135
0.40	178	494	805	1151	1148	1148	1148	1148
0.45	169	412	671	1156	1154	1154	1154	1154
0.50	160	327	611	1043	1159	1159	1159	1159
0.60	142	294	478	881	1171	1171	1171	1171
0.65	133	276	410	792	1176	1176	1176	1176
0.70	123	258	340	694	1095	1181	1181	1181
0.80	105	221	308	631	998	1190	1190	1190
0.90	86	184	274	561	892	1091	1197	1197
1.00	65	146	241	492	776	1025	1203	1203
1.10	37	103	207	420	687	955	1208	1208
1.20	35	56	174	347	632	881	1212	1212
1.30	34	52	139	323	577	803	1155	1215
1.40	32	49	101	297	522	717	1130	1218
1.50	31	46	60	273	466	675	1104	1221
1.60	30	44	58	248	410	630	1061	1223
1.70	29	42	54	223	352	585	1018	1174
1.80	29	40	51	198	337	540	974	1154
1.90	28	39	49	174	321	494	929	1134
2.00	27	37	47	148	306	448	881	1114
2.20		35	43	93	278	354	793	1063
2.40		33	40	60	250	324	703	1010
2.60		32	38	54	222	295	609	955
2.80		30	36	50	195	267	513	897
3.00		29	34	47	168	239	413	838
3.20				44	138	210	352	781
3.40				42	107	184	328	721
3.60				40	75	156	306	658
3.80				38	54	125	286	593
4.00				37	50	94	266	528
4.20				35	47	60	246	462
4.40				34	45	55	226	394
4.60				33	43	52	207	346
4.80				32	41	49	188	316
5.00				32	40	47	169	288
5.20					38	45	149	261
5.40					37	43	127	233
5.60					36	41	106	205
5.80					35	40	84	177
6.00					34	39	58	149

E1

Time Graphs of Temperature of Combustion Gases. Type E Enclosed Space.

Opening Factor $A\sqrt{H}/A_t = 0.01 \text{ m}^{1/2}$

T	0.1	0.2	0.3	0.5	0.75	1.0	1.5	2.0
q	1.5	3.0	4.5	7.5	11.25	15.0	22.5	30.0
Time h	T e m p e r a t u r e							
0.05	312	312	312	312	312	312	312	312
0.10	472	472	472	472	392	392	392	392
0.15	280	465	465	465	428	428	428	428
0.20	242	443	482	482	486	486	486	486
0.25	189	384	494	494	488	488	488	488
0.30	130	321	467	506	502	502	502	502
0.35	127	302	435	517	516	516	516	516
0.40	122	275	397	528	529	529	529	529
0.45	117	242	363	538	534	534	534	534
0.50	112	210	330	516	547	547	547	547
0.60	103	197	288	466	572	572	572	572
0.65	99	188	262	435	580	580	580	580
0.70	95	180	236	400	562	588	588	588
0.80	86	163	220	377	534	604	604	604
0.90	77	146	204	351	499	584	620	620
1.00	68	128	188	323	458	567	632	632
1.10	56	108	172	293	425	543	643	643
1.20	52	89	156	263	402	519	656	656
1.30	49	84	139	249	380	491	647	665
1.40	46	80	121	236	358	459	644	675
1.50	44	76	102	223	334	440	640	686
1.60	42	73	97	210	308	421	628	694
1.70	40	70	92	197	283	403	616	686
1.80	39	68	88	184	273	383	600	684
1.90	38	64	85	171	263	363	583	681
2.00	37	61	82	158	254	342	566	676
2.20	35	56	76	130	237	298	528	662
2.40	34	52	72	110	220	277	491	644
2.60	32	49	66	102	204	259	450	622
2.80	31	47	61	95	188	242	406	599
3.00	30	45	58	90	172	225	359	572
3.20		43	55	85	155	208	322	546
3.40		41	52	80	138	192	303	518
3.60		40	50	75	120	175	287	489
3.80		39	48	71	108	158	272	460
4.00		38	47	68	102	140	258	427
4.20		37	45	65	96	121	244	394
4.40		36	44	63	92	114	230	359
4.60		35	43	60	87	108	217	330
4.80		34	42	58	82	103	204	309
5.00		33	40	56	79	98	191	290
5.20			40	55	76	94	178	272
5.40			39	53	73	89	165	254
5.60			38	52	71	85	152	236
5.80			37	50	68	82	138	217
6.00			36	49	66	79	124	199

E2

Time Graphs of Temperature of Combustion Gases. Type E Enclosed Space.

Opening Factor $A \cdot \sqrt{E}/A_t = 0.02 \text{ m}^{1/2}$.

T	0.1	0.2	0.3	0.5	0.75	1.0	1.5	2.0			
g	3.0	6.0	9.0	15.0	22.5	30.0	45.0	60.0			
Time h	T	e	m	p	e	r	a	t	u	r	e
0.05	441	441	441	441	442	442	442	443			
0.10	637	637	637	637	536	536	536	536			
0.15	378	642	642	642	598	598	598	598			
0.20	328	609	665	665	671	671	671	671			
0.25	249	524	683	683	674	674	674	674			
0.30	163	433	643	700	693	693	693	693			
0.35	161	405	607	721	712	712	712	712			
0.40	153	364	553	738	731	731	731	731			
0.45	146	320	489	756	748	748	748	748			
0.50	139	273	456	712	763	763	763	763			
0.60	126	250	381	635	792	792	792	792			
0.65	119	237	341	588	804	804	804	804			
0.70	113	224	299	536	775	815	815	815			
0.80	101	200	274	497	730	835	835	835			
0.90	88	175	250	455	674	802	853	853			
1.00	74	149	226	413	608	771	869	869			
1.10	60	122	203	368	555	734	881	881			
1.20	56	93	180	321	520	692	891	891			
1.30	54	88	156	300	486	644	874	901			
1.40	50	83	131	281	451	591	864	910			
1.50	46	78	104	263	415	563	853	919			
1.60	44	75	99	244	378	534	832	926			
1.70	42	71	93	226	339	504	809	909			
1.80	40	68	89	208	323	475	783	901			
1.90	38	66	85	190	308	444	754	892			
2.00	37	63	81	172	295	413	725	882			
2.20	35	58	75	133	272	348	666	855			
2.40	33	52	70	107	250	319	608	824			
2.60	32	49	65	98	228	293	547	789			
2.80	31	46	60	91	206	270	482	751			
3.00	30	43	56	85	184	248	413	711			
3.20		42	53	80	163	225	363	671			
3.40		40	50	76	140	203	337	630			
3.60		38	48	70	116	181	315	588			
3.80		37	46	67	100	159	296	543			
4.00		36	44	63	94	135	278	497			
4.20		35	43	60	88	111	260	449			
4.40		34	41	58	84	103	243	400			
4.60		33	40	55	79	97	226	360			
4.80		32	39	53	75	92	210	333			
5.00		32	38	51	71	88	194	308			
5.20			37	50	68	83	177	284			
5.40			36	48	66	79	161	261			
5.60			35	47	63	75	144	238			
5.80			34	45	61	72	126	215			
6.00			34	44	59	70	108	192			

E3

Time Graphs of Temperature of Combustion Gases. Type E Enclosed Space.

Opening Factor $A \cdot \sqrt{H}/A_t = 0.04 \text{ m}^{1/2}$

T	0.1	0.2	0.3	0.5	0.75	1.0	1.5	2.0
q	6.0	12.0	18.0	30.0	45.0	60.0	90.0	120.0
Time h	T e m p e r a t u r e							
0.05	547	547	547	547	547	547	547	547
0.10	844	844	844	844	689	689	689	689
0.15	478	831	831	831	759	759	759	759
0.20	406	783	857	857	865	865	865	865
0.25	305	681	878	878	869	869	867	869
0.30	186	555	839	906	895	895	895	895
0.35	183	506	770	928	919	919	919	919
0.40	173	445	689	947	939	939	939	939
0.45	165	382	595	963	956	956	956	956
0.50	156	315	550	897	971	971	971	971
0.60	140	282	449	782	997	997	997	997
0.65	131	266	392	713	1006	1006	1006	1006
0.70	123	251	336	638	955	1013	1013	1013
0.80	107	218	303	582	885	1027	1027	1027
0.90	91	186	273	525	804	965	1038	1038
1.00	74	154	244	467	711	917	1047	1047
1.10	55	119	213	408	637	864	1056	1056
1.20	51	82	184	347	592	806	1063	1063
1.30	48	77	155	321	547	741	1030	1070
1.40	45	73	123	298	500	671	1011	1076
1.50	43	69	90	276	453	633	992	1081
1.60	40	65	85	253	405	595	961	1086
1.70	38	61	80	231	356	558	929	1055
1.80	36	58	76	209	338	519	894	1041
1.90	34	56	72	187	322	480	857	1026
2.00	33	54	69	165	307	441	818	1010
2.20		48	63	117	280	360	741	971
2.40		44	59	89	254	327	667	929
2.60		41	53	81	229	298	588	883
2.80		39	49	75	203	272	506	835
3.00		37	46	70	179	247	421	784
3.20		35	43	65	153	221	362	734
3.40		34	41	59	125	195	335	682
3.60		33	39	55	97	170	312	629
3.80		32	38	52	80	144	292	574
4.00		31	37	50	75	115	273	517
4.20			35	47	70	87	254	460
4.40			34	45	68	81	235	400
4.60			33	43	61	76	217	354
4.80			32	42	57	72	199	325
5.00			32	40	54	67	181	298
5.20				39	52	63	162	272
5.40				38	50	60	143	246
5.60				37	48	57	123	220
5.80				36	46	55	103	195
6.00				35	45	52	83	169

E4

Time Graphs of Temperature of Combustion Gases. Type E Enclosed Space.

Opening Factor $A \cdot \sqrt{H}/A_t = 0.06 \text{ m}^{1/2}$

T	0.1	0.2	0.3	0.5	0.75	1.0	1.5	2.0
q	9.0	13.0	27.0	45.0	67.5	90.0	135.0	180.0
Time h	T e m p e r a t u r e							
0.05	615	615	615	615	615	615	615	615
0.10	929	929	929	929	766	766	766	766
0.15	532	937	937	937	854	854	854	854
0.20	445	882	958	958	959	959	959	960
0.25	323	759	987	987	976	976	976	976
0.30	192	608	935	1013	1002	1002	1002	1002
0.35	189	546	853	1032	1024	1024	1024	1024
0.40	179	478	757	1050	1042	1042	1042	1042
0.45	170	406	645	1063	1058	1058	1058	1058
0.50	161	329	590	980	1070	1070	1070	1070
0.60	144	292	470	843	1085	1085	1085	1085
0.65	135	274	409	764	1091	1091	1091	1091
0.70	126	257	344	676	1030	1097	1097	1097
0.80	108	222	308	611	947	1107	1107	1107
0.90	91	188	276	548	854	1031	1115	1115
1.00	72	153	245	483	749	976	1122	1122
1.10	49	114	213	417	665	913	1129	1129
1.20	45	73	181	349	613	847	1134	1134
1.30	43	69	149	323	564	775	1092	1139
1.40	40	64	114	298	512	697	1070	1143
1.50	39	60	77	275	461	655	1047	1147
1.60	36	56	74	251	408	613	1011	1151
1.70	34	53	70	228	355	572	973	1113
1.80	33	50	66	204	338	529	934	1095
1.90	31	48	62	181	321	487	893	1078
2.00	30	46	59	157	306	444	850	1060
2.20		41	54	105	279	357	766	1015
2.40		38	49	76	252	324	684	967
2.60		36	45	69	225	295	598	917
2.80		34	41	63	199	269	508	864
3.00		32	39	58	173	242	415	809
3.20			37	53	145	215	354	755
3.40			36	49	116	189	329	698
3.60			34	46	86	162	307	640
3.80			33	43	68	134	287	581
4.00			32	41	62	104	268	519
4.20				40	58	73	248	458
4.40				38	53	68	229	394
4.60				37	50	63	210	347
4.80				36	47	59	192	317
5.00				34	45	54	173	290
5.20					43	51	154	264
5.40					41	49	133	237
5.60					40	46	112	209
5.80					38	45	92	183
6.00					37	43	69	156

E5

Time Graphs of Temperature of Combustion Gases. Type E Enclosed Space.

Opening Factor $A \cdot \sqrt{H}/A_t = 0.08 \text{ m}^{1/2}$

T	0.1	0.2	0.3	0.5	0.75	1.0	1.5	2.0			
q	12.0	24.0	36.0	60.0	90.0	120.0	180.0	240.0			
Time h	T	e	m	p	e	r	a	t	u	r	e
0.05	663	663	663	663	663	663	663	663	663		
0.10	999	999	999	999	831	831	831	831	831		
0.15	577	1005	1005	1005	913	913	913	913	913		
0.20	468	942	1026	1026	1027	1027	1027	1027	1027		
0.25	335	805	1055	1055	1043	1043	1043	1043	1043		
0.30	194	638	988	1076	1067	1067	1067	1067	1067		
0.35	191	568	897	1093	1086	1086	1086	1086	1086		
0.40	181	494	792	1107	1101	1101	1101	1101	1101		
0.45	172	417	669	1118	1113	1113	1113	1113	1113		
0.50	163	334	608	1023	1122	1122	1122	1122	1122		
0.60	145	295	480	872	1133	1133	1133	1133	1133		
0.65	135	277	414	788	1138	1138	1138	1138	1138		
0.70	126	259	345	693	1068	1143	1143	1143	1143		
0.80	108	223	309	624	979	1151	1151	1151	1151		
0.90	90	187	276	557	879	1069	1158	1158	1158		
1.00	69	150	244	489	767	1005	1164	1164	1164		
1.10	44	109	210	419	677	938	1169	1169	1169		
1.20	41	65	179	348	623	867	1173	1173	1173		
1.30	39	61	145	322	571	792	1125	1177	1177		
1.40	37	56	108	297	517	708	1102	1180	1180		
1.50	36	53	70	273	463	664	1076	1183	1183		
1.60	33	49	66	249	408	621	1037	1186	1186		
1.70	31	47	62	224	352	577	996	1143	1143		
1.80	30	45	58	200	335	532	954	1124	1124		
1.90	29	43	54	176	319	489	911	1105	1105		
2.00	28	41	52	152	304	444	866	1086	1086		
2.20		37	47	98	277	353	778	1038	1038		
2.40		34	43	67	250	321	692	987	987		
2.60		32	39	60	222	293	601	934	934		
2.80		31	37	54	195	266	507	879	879		
3.00		30	35	50	169	238	411	821	821		
3.20				46	140	210	349	765	765		
3.40				42	109	184	324	706	706		
3.60				40	79	157	303	645	645		
3.80				38	58	127	283	582	582		
4.00				36	54	97	264	519	519		
4.20				45	49	64	244	455	455		
4.40				34	46	58	225	389	389		
4.60				33	43	55	206	341	341		
4.80				32	41	50	187	312	312		
5.00				31	39	47	168	285	285		
5.20					37	44	148	258	258		
5.40					36	42	128	231	231		
5.60					35	40	106	203	203		
5.80					34	39	85	177	177		
6.00					33	37	60	148	148		

E6

Time Graphs of Temperature of Combustion Gases. Type E Enclosed Space.

Opening Factor $A\sqrt{H}/A_t = 0.12 \text{ m}^{1/2}$

T	0.1	0.2	0.3	0.5	0.75	1.0	1.5	2.0
q	18.0	35.0	54.0	90.0	135.0	180.0	270.0	360.0
Time h	T e m p e r a t u r e							
0.05	709	709	709	709	709	709	709	709
0.10	1086	1086	1086	1086	899	899	899	899
0.15	610	1087	1087	1087	985	985	985	985
0.20	494	1013	1108	1108	1106	1106	1106	1106
0.25	348	860	1130	1130	1122	1122	1122	1122
0.30	194	670	1049	1148	1141	1141	1141	1141
0.35	192	594	944	1161	1155	1155	1155	1155
0.40	183	509	827	1169	1166	1166	1166	1166
0.45	173	424	692	1175	1172	1172	1172	1172
0.50	164	336	627	1069	1178	1178	1178	1178
0.60	145	297	488	903	1187	1187	1187	1187
0.65	135	278	417	811	1190	1190	1190	1190
0.70	126	260	343	709	1111	1194	1194	1194
0.80	106	222	307	637	1013	1200	1200	1200
0.90	87	184	274	565	904	1105	1205	1205
1.00	66	145	241	494	784	1037	1209	1209
1.10	38	102	207	420	688	966	1212	1212
1.20	36	55	174	345	632	890	1215	1215
1.30	34	50	138	319	576	810	1160	1218
1.40	32	46	100	294	520	718	1134	1220
1.50	31	43	58	270	463	673	1107	1222
1.60	29	41	54	245	405	627	1064	1224
1.70	28	39	50	220	347	582	1021	1175
1.80	27	37	47	195	331	536	976	1155
1.90	26	36	44	171	315	489	930	1134
2.00	25	34	42	145	301	443	881	1113
2.20			39	89	274	348	789	1062
2.40			35	54	246	317	698	1007
2.60			33	48	218	289	602	951
2.80			31	44	191	262	504	893
3.00			30	40	164	234	404	833
3.20				37	134	206	341	775
3.40				35	103	179	318	713
3.60				33	70	151	298	649
3.80				32	47	120	279	583
4.00				31	44	89	259	518
4.20					40	52	240	451
4.40					37	47	220	384
4.60					35	43	201	335
4.80					34	40	182	306
5.00					33	38	163	279
5.20						36	142	252
5.40						35	121	224
5.60						33	99	197
5.80						32	77	169
6.00						31	48	140

F1

Time Graphs of Temperature of Combustion Gases. Type F Enclosed Space. $\epsilon_{res} = 0.10$
 Opening Factor $A \cdot \sqrt{H}/A_t = 0.01 \text{ m}^{1/2}$

T	0.1	0.3	0.5	1.0	2.0
q	1.5	4.5	7.5	15.0	30.0
Time h	T e m p e r a t u r e				
0.05	252	252	252	252	252
0.10	418	418	418	350	350
0.15	297	456	456	413	413
0.20	261	489	489	480	480
0.25	208	506	506	498	498
0.30	148	483	518	513	513
0.35	129	452	528	524	524
0.40	114	409	537	535	535
0.45	103	359	540	540	540
0.50	94	329	516	544	544
0.60	81	270	442	553	553
0.65	75	239	404	557	557
0.70	70	207	367	560	560
0.80	59	180	332	566	566
0.90	49	159	299	538	572
1.00	38	140	268	510	577
1.10	28	122	236	480	581
1.20		105	202	449	585
1.30		88	185	414	589
1.40		70	170	377	592
1.50		50	157	355	595
1.60		42	144	334	598
1.70		37	131	314	585
1.80		33	118	293	576
1.90		31	105	273	568
2.00		29	92	251	560
2.20			65	207	538
2.40			44	186	515
2.60			37	170	490
2.80			33	155	463
3.00			31	140	436
3.20				125	409
3.40				110	382
3.60				96	354
3.80				80	325
4.00				64	294
4.20				47	264
4.40				40	231
4.60				37	205
4.80				35	189
5.00				33	174
5.20					159
5.40					144
5.60					129
5.80					113
6.00					98

F2

Time Graphs of Temperature of Combustion Gases. Type F Enclosed Space. $\epsilon_{res} = 0.10$
 Opening Factor $A \cdot \sqrt{H}/A_t = 0.02 \text{ m}^{1/2}$

T	0.1	0.3	0.5	1.0	2.0
q	3.0	9.0	15.0	30.0	60.0
Time h	T e m p e r a t u r e				
0.05	382	382	382	382	382
0.10	612	612	612	508	508
0.15	413	645	645	585	585
0.20	354	684	684	676	676
0.25	273	699	699	691	691
0.30	184	666	711	706	706
0.35	161	610	722	716	716
0.40	143	547	732	725	725
0.45	130	474	734	733	733
0.50	120	433	689	741	741
0.60	104	351	597	750	750
0.65	97	308	545	755	755
0.70	90	264	489	759	759
0.80	77	230	439	765	765
0.90	63	203	395	722	771
1.00	48	180	351	679	776
1.10	32	156	306	638	780
1.20		133	260	592	783
1.30		108	237	544	786
1.40		84	218	492	788
1.50		57	200	462	790
1.60		47	184	435	792
1.70		41	167	407	772
1.80		38	149	379	759
1.90		35	132	350	748
2.00		33	113	321	736
2.20			77	260	706
2.40			48	235	673
2.60			41	214	639
2.80			37	195	603
3.00			34	176	565
3.20				157	529
3.40				137	492
3.60				116	454
3.80				96	414
4.00				74	373
4.20				50	331
4.40				43	287
4.60				39	253
4.80				37	232
5.00				35	212
5.20				33	193
5.40				32	174
5.60				31	155
5.80				30	135
6.00				29	114

F3

Time Graphs of Temperature of Combustion Gases, Type F Enclosed Space. $\epsilon_{res} = 0.10$
 Opening Factor $A \cdot \sqrt{H}/A_t = 0.04 \text{ m}^{1/2}$

T	0.1	0.3	0.5	1.0	2.0
q	6.0	18.0	30.0	60.0	120.0
Time h	T e m p e r a t u r e				
0.05	522	522	522	522	522
0.10	815	815	815	673	674
0.15	525	841	841	763	763
0.20	437	870	870	874	874
0.25	327	892	892	884	884
0.30	206	841	901	896	897
0.35	181	767	909	905	905
0.40	163	679	916	913	913
0.45	150	574	921	919	919
0.50	139	521	855	924	924
0.60	121	414	731	936	936
0.65	112	359	661	939	939
0.70	105	302	585	941	941
0.80	89	264	525	944	944
0.90	72	234	469	877	948
1.00	54	205	413	824	951
1.10	33	178	356	771	953
1.20		149	296	713	955
1.30		119	272	651	957
1.40		88	250	583	959
1.50		54	229	548	960
1.60		44	208	514	962
1.70		39	188	479	931
1.80		36	168	443	917
1.90		34	147	407	903
2.00		32	124	370	888
2.20			79	294	851
2.40			44	268	811
2.60			37	244	765
2.80			34	221	720
3.00			32	198	672
3.20				176	627
3.40				152	581
3.60				128	533
3.80				102	483
4.00				76	432
4.20				46	379
4.40				38	325
4.60				35	284
4.80				33	261
5.00				32	238
5.20					214
5.40					192
5.60					169
5.80					146
6.00					120

F4

Time Graphs of Temperature of Combustion Gases. Type F Enclosed Space. $\epsilon_{res} = 0.10$
 Opening Factor $A \cdot \sqrt{H}/A_c = 0.08 \text{ m}^{1/2}$

T	0.1	0.3	0.5	1.0	2.0
q	12.0	36.0	60.0	120.0	240.0
Time h	T e m p e r a t u r e				
0.05	628	628	628	628	628
0.10	971	971	971	823	822
0.15	620	1012	1012	918	917
0.20	493	1032	1032	1025	1025
0.25	355	1043	1043	1037	1037
0.30	208	972	1052	1047	1047
0.35	188	878	1058	1055	1055
0.40	172	771	1062	1060	1060
0.45	160	647	1066	1065	1065
0.50	150	582	973	1068	1068
0.60	131	452	822	1072	1072
0.65	122	386	740	1075	1075
0.70	113	319	648	1077	1077
0.80	96	282	581	1079	1079
0.90	77	250	516	995	1081
1.00	55	218	451	936	1083
1.10	30	187	384	873	1084
1.20		156	315	805	1086
1.30		122	290	731	1087
1.40		86	267	650	1088
1.50		44	244	608	1089
1.60		36	221	569	1090
1.70		32	198	527	1048
1.80		30	176	486	1032
1.90			153	444	1014
2.00			128	401	996
2.20			75	314	952
2.40			36	287	905
2.60			31	262	857
2.80				236	806
3.00				211	750
3.20				186	697
3.40				161	642
3.60				133	584
3.80				105	527
4.00				76	468
4.20				37	407
4.40				32	346
4.60				30	301
4.80					276
5.00					251
5.20					226
5.40					201
5.60					176
5.80					150
6.00					122

F5

Time Graphs of Temperature of Combustion Gases. Type F Enclosed Space. $\epsilon_{res} = 0.10$
 Opening Factor $A \cdot \sqrt{H}/A_t = 0.12 \text{ m}^{1/2}$

T	0.1	0.3	0.5	1.0	2.0
q	18.0	54.0	90.0	180.0	360.0
Time h	T e m p e r a t u r e				
0.05	677	677	677	677	677
0.10	1060	1060	1060	880	880
0.15	657	1086	1086	981	981
0.20	514	1106	1106	1097	1097
0.25	364	1114	1114	1110	1110
0.30	205	1030	1121	1117	1117
0.35	189	924	1125	1123	1123
0.40	175	808	1128	1127	1127
0.45	164	673	1130	1129	1129
0.50	154	604	1021	1131	1131
0.60	135	465	859	1134	1134
0.65	125	395	771	1136	1136
0.70	115	324	672	1138	1138
0.80	98	288	603	1140	1140
0.90	78	255	534	1046	1142
1.00	55	222	465	981	1143
1.10	27	190	393	913	1144
1.20		157	321	840	1145
1.30		122	296	761	1146
1.40		84	272	675	1146
1.50		38	249	631	1147
1.60		31	225	588	1148
1.70			202	545	1100
1.80			179	501	1083
1.90			154	457	1064
2.00			128	412	1044
2.20			73	320	996
2.40			31	293	946
2.60				267	894
2.80				241	840
3.00				214	781
3.20				190	726
3.40				163	667
3.60				135	607
3.80				105	545
4.00				74	483
4.20				33	419
4.40					354
4.60					307
4.80					282
5.00					256
5.20					230
5.40					204
5.60					179
5.80					151
6.00					122

F6

Time Graphs of Temperature of Combustion Gases. Type F Enclosed Space. $\epsilon_{res} = 0.35$
 Opening Factor $A \cdot \sqrt{H}/A_t = 0.01 \text{ m}^{1/2}$

T	0.1	0.3	0.5	1.0	2.0
q	1.5	4.5	7.5	15.0	30.0
Time h	T e m p e r a t u r e				
0.05	241	241	241	241	241
0.10	387	387	387	327	327
0.15	283	419	419	382	382
0.20	243	447	447	440	440
0.25	193	455	455	451	451
0.30	135	430	461	458	458
0.35	116	401	466	464	464
0.40	102	361	470	469	469
0.45	93	316	471	471	471
0.50	85	289	451	473	473
0.60	73	238	380	478	478
0.65	68	211	348	480	480
0.70	63	183	316	481	481
0.80	54	160	288	485	485
0.90	44	142	263	459	488
1.00	34	126	236	434	490
1.10		110	208	410	493
1.20		94	179	383	495
1.30		78	164	355	497
1.40		61	152	324	498
1.50		43	140	307	500
1.60		35	129	290	501
1.70		31	117	274	490
1.80			106	257	483
1.90			94	239	476
2.00			82	221	470
2.20			57	183	452
2.40			37	166	434
2.60			31	152	414
2.80				139	393
3.00				126	372
3.20				112	351
3.40				99	329
3.60				85	306
3.80				71	282
4.00				56	257
4.20				39	231
4.40				34	203
4.60				31	181
4.80					167
5.00					154
5.20					141
5.40					127
5.60					114
5.80					100
6.00					86

E7

Time Graphs of Temperature of Combustion Gases, Type F Enclosed Space, $\epsilon_{res} = 0.35$
 Opening Factor $A \cdot \sqrt{H}/A_t = 0.02 \text{ m}^{1/2}$

T	0.1	0.3	0.5	1.0	2.0
q	3.0	9.0	15.0	30.0	60.0
Time h	T e m p e r a t u r e				
0.05	364	364	364	364	364
0.10	560	560	560	472	472
0.15	394	588	588	537	537
0.20	332	614	614	611	611
0.25	257	615	615	614	614
0.30	172	584	620	618	618
0.35	147	531	625	624	624
0.40	131	476	630	629	629
0.45	119	415	630	632	632
0.50	110	380	590	634	634
0.60	97	312	513	639	639
0.65	90	275	470	641	641
0.70	84	236	423	643	643
0.80	72	207	385	647	647
0.90	58	185	350	606	650
1.00	44	165	313	573	652
1.10	29	143	275	540	654
1.20		121	234	504	656
1.30		99	214	466	658
1.40		76	199	425	659
1.50		49	184	403	661
1.60		40	169	381	662
1.70		35	153	359	643
1.80		32	137	336	634
1.90		30	121	312	625
2.00			104	287	616
2.20			69	234	593
2.40			41	213	568
2.60			35	196	542
2.80			32	179	514
3.00				162	485
3.20				144	457
3.40				126	428
3.60				107	397
3.80				88	365
4.00				67	331
4.20				44	295
4.40				37	258
4.60				34	229
4.80				32	211
5.00				30	194
5.20					177
5.40					160
5.60					142
5.80					123
6.00					104

F8

Time Graphs of Temperature of Combustion Gases. Type F Enclosed Space. $\epsilon_{res} = 0.35$
 Opening Factor $A \cdot \sqrt{H}/A_c = 0.04 \text{ m}^{1/2}$

T	0.1	0.3	0.5	1.0	2.0
q	6.0	18.0	30.0	60.0	120.0
Time h	T e m p e r a t u r e				
0.05	473	473	473	473	473
0.10	751	751	751	628	628
0.15	501	763	763	698	698
0.20	407	770	770	784	784
0.25	305	779	779	778	778
0.30	191	734	783	780	780
0.35	168	670	790	788	788
0.40	152	588	796	795	795
0.45	141	507	793	797	797
0.50	132	465	737	799	799
0.60	115	376	634	803	803
0.65	107	329	578	805	805
0.70	100	278	516	806	806
0.80	85	246	471	809	809
0.90	69	219	426	740	811
1.00	50	194	379	717	812
1.10	30	168	328	674	813
1.20		141	276	627	815
1.30		112	254	577	816
1.40		83	235	522	816
1.50		48	215	494	817
1.60		39	197	466	818
1.70		34	178	437	793
1.80		32	159	406	784
1.90		30	139	376	773
2.00			117	344	757
2.20			73	276	727
2.40			39	252	696
2.60			34	231	663
2.80			31	210	627
3.00				189	590
3.20				168	555
3.40				146	518
3.60				122	479
3.80				98	438
4.00				73	394
4.20				42	349
4.40				35	301
4.60				32	266
4.80				31	245
5.00					224
5.20					203
5.40					182
5.60					161
5.80					138
6.00					114

F9

Time Graphs of Temperature of Combustion Gases. Type F Enclosed Space. $\epsilon_{res} = 0.35$
 Opening Factor $A \cdot \sqrt{H}/A_t = 0.08 \text{ m}^{1/2}$

T	0.1	0.3	0.5	1.0	2.0
q	12.0	36.0	60.0	120.0	240.0
Time h	T e m p e r a t u r e				
0.05	593	593	593	593	593
0.10	892	892	892	776	776
0.15	593	921	921	848	848
0.20	464	923	923	923	923
0.25	338	931	931	926	926
0.30	197	867	934	933	933
0.35	178	790	937	936	936
0.40	165	698	940	939	939
0.45	155	593	943	942	942
0.50	145	539	860	944	944
0.60	128	428	738	947	947
0.65	119	368	668	948	948
0.70	110	306	590	949	949
0.80	94	272	539	954	954
0.90	75	242	484	884	951
1.00	53	212	426	836	954
1.10	28	183	365	785	957
1.20		152	301	727	954
1.30		118	279	665	964
1.40		84	258	597	955
1.50		41	236	564	957
1.60		33	214	530	959
1.70		30	193	494	924
1.80			171	458	914
1.90			148	420	900
2.00			124	382	886
2.20			72	302	851
2.40			33	277	814
2.60				253	773
2.80				229	729
3.00				205	683
3.20				181	640
3.40				157	594
3.60				130	546
3.80				102	496
4.00				73	444
4.20				35	389
4.40				30	332
4.60					291
4.80					268
5.00					244
5.20					219
5.40					196
5.60					172
5.80					146
6.00					119

F10

Time Graphs of Temperature of Combustion Gases. Type F Enclosed Space. $\epsilon_{res} = 0.35$
 Opening Factor $A\sqrt{H}/A_t = 0.12 \text{ m}^{1/2}$

T	0.1	0.3	0.5	1.0	2.0
q	18.0	54.0	90.0	180.0	360.0
Time h	T e m p e r a t u r e				
0.05	640	640	640	640	640
0.10	985	985	985	852	852
0.15	631	1000	1000	921	921
0.20	489	1003	1003	1006	1006
0.25	350	1010	1010	1005	1005
0.30	197	934	1013	1012	1012
0.35	182	847	1016	1015	1015
0.40	170	746	1018	1017	1017
0.45	160	628	1020	1019	1019
0.50	150	569	934	1021	1021
0.60	132	447	800	1022	1022
0.65	123	382	721	1023	1023
0.70	114	315	633	1024	1024
0.80	96	281	572	1025	1025
0.90	77	250	509	946	1027
1.00	53	218	445	893	1030
1.10	26	187	379	837	1028
1.20		155	311	776	1029
1.30		120	288	706	1031
1.40		83	266	631	1030
1.50		36	243	595	1030
1.60		30	220	558	1031
1.70			198	519	992
1.80			175	480	979
1.90			151	439	964
2.00			125	397	948
2.20			71	311	909
2.40			30	286	868
2.60				261	824
2.80				236	777
3.00				211	726
3.20				186	678
3.40				160	628
3.60				132	575
3.80				103	520
4.00				73	464
4.20				31	404
4.40					344
4.60					300
4.80					276
5.00					251
5.20					225
5.40					200
5.60					175
5.80					149
6.00					120

F11

Time Graphs of Temperature of Combustion Gases. Type F Enclosed Space. $\epsilon_{res} = 0.60$
 Opening Factor $A \cdot \sqrt{H}/A_t = 0.01 \text{ m}^{1/2}$

T	0.1	0.3	0.5	1.0	2.0
q	1.5	4.5	7.5	15.0	30.0
Time h	T e m p e r a t u r e				
0.05	231	231	231	231	231
0.10	364	364	364	311	311
0.15	269	405	405	359	359
0.20	229	413	413	410	410
0.25	180	419	419	416	416
0.30	125	408	425	419	419
0.35	105	362	425	423	423
0.40	93	317	425	426	426
0.45	85	288	427	428	428
0.50	78	263	402	429	429
0.60	68	217	351	432	432
0.65	63	193	323	433	433
0.70	59	167	292	434	434
0.80	49	146	265	437	437
0.90	40	130	242	413	439
1.00	31	115	217	390	440
1.10		101	192	369	442
1.20		87	165	345	443
1.30		71	151	320	445
1.40		55	140	292	446
1.50		37	129	278	447
1.60		30	118	264	448
1.70			108	249	438
1.80			97	234	431
1.90			86	218	426
2.00			75	201	420
2.20			50	167	405
2.40			32	152	389
2.60				140	372
2.80				127	353
3.00				115	334
3.20				103	316
3.40				91	297
3.60				78	277
3.80				65	256
4.00				50	233
4.20				34	209
4.40					185
4.60					165
4.80					152
5.00					140
5.20					128
5.40					116
5.60					104
5.80					91
6.00					78

F12

Time Graphs of Temperature of Combustion Gases. Type F Enclosed Space. $\epsilon_{res} = 0.60$
 Opening Factor $A\sqrt{H}/A_t = 0.02 \text{ m}^{1/2}$

T	0.1	0.3	0.5	1.0	2.0
q	3.0	9.0	15.0	30.0	60.0
Time h	T e m p e r a t u r e				
0.05	348	348	348	348	349
0.10	525	525	525	447	447
0.15	374	547	547	502	502
0.20	310	562	562	564	564
0.25	240	560	560	561	561
0.30	159	531	564	562	562
0.35	136	481	568	567	567
0.40	121	433	571	571	571
0.45	111	378	570	573	573
0.50	104	348	534	574	574
0.60	91	287	464	577	577
0.65	85	254	426	579	579
0.70	80	218	385	580	580
0.80	68	193	353	582	582
0.90	55	173	322	542	584
1.00	41	154	289	515	586
1.10	27	134	254	486	587
1.20		113	217	455	588
1.30		92	200	421	590
1.40		70	186	385	591
1.50		44	172	368	592
1.60		35	158	349	593
1.70		31	143	329	576
1.80			128	308	567
1.90			112	287	560
2.00			97	265	552
2.20			63	217	532
2.40			37	199	511
2.60			31	184	488
2.80				168	464
3.00				152	439
3.20				135	415
3.40				118	390
3.60				100	363
3.80				82	335
4.00				62	304
4.20				39	273
4.40				33	239
4.60				30	212
4.80					197
5.00					182
5.20					166
5.40					149
5.60					132
5.80					115
6.00					97

F13

Time Graphs of Temperature of Combustion Gases. Type F Enclosed Space. $\epsilon_{res} = 0.60$
 Opening Factor $A \cdot \sqrt{H}/A_t = 0.04 \text{ m}^{1/2}$

T	0.1	0.3	0.5	1.0	2.0
q	6.0	18.0	30.0	60.0	120.0
Time h	T e m p e r a t u r e				
0.05	450	450	450	450	450
0.10	708	708	708	597	597
0.15	470	703	703	650	650
0.20	381	709	709	720	720
0.25	288	710	710	711	711
0.30	180	669	714	711	711
0.35	158	613	717	716	716
0.40	144	537	719	718	718
0.45	134	467	722	723	723
0.50	125	431	668	728	728
0.60	110	352	578	729	729
0.65	104	308	529	731	731
0.70	97	261	474	732	732
0.80	82	233	437	732	732
0.90	66	208	397	686	737
1.00	48	185	355	652	733
1.10	28	161	309	614	741
1.20		135	261	574	732
1.30		107	241	530	739
1.40		78	223	482	740
1.50		44	206	458	739
1.60		35	189	433	742
1.70		31	171	407	717
1.80			152	381	701
1.90			133	353	698
2.00			112	323	690
2.20			69	262	664
2.40			36	240	637
2.60			31	220	608
2.80				201	578
3.00				181	545
3.20				161	514
3.40				140	482
3.60				117	447
3.80				94	410
4.00				69	372
4.20				39	330
4.40				32	287
4.60				30	254
4.80					234
5.00					214
5.20					195
5.40					175
5.60					155
5.80					133
6.00					110

F14

Time Graphs of Temperature of Combustion Gases. Type F Enclosed Space. $\epsilon_{res} = 0.60$
 Opening Factor $A \cdot \sqrt{H}/A_t = 0.08 \text{ m}^{1/2}$

T	0.1	0.3	0.5	1.0	2.0
q	12.0	36.0	60.0	120.0	240.0
Time h	T e m p e r a t u r e				
0.05	568	568	550	568	568
0.10	840	840	884	741	741
0.15	560	852	845	791	791
0.20	440	854	854	856	856
0.25	324	860	860	855	855
0.30	190	802	862	862	862
0.35	172	732	865	864	864
0.40	160	650	867	866	866
0.45	150	556	869	868	868
0.50	142	509	787	870	870
0.60	125	408	683	872	872
0.65	116	353	621	873	873
0.70	108	294	552	874	874
0.80	92	263	510	875	875
0.90	73	235	460	816	880
1.00	51	206	406	773	877
1.10	27	178	350	727	878
1.20		148	290	676	880
1.30		115	270	621	879
1.40		82	250	560	880
1.50		39	229	532	885
1.60		31	208	501	880
1.70			188	470	852
1.80			167	437	843
1.90			145	402	831
2.00			121	367	819
2.20			70	291	787
2.40			31	269	753
2.60				246	717
2.80				223	679
3.00				200	638
3.20				177	600
3.40				153	560
3.60				127	517
3.80				100	472
4.00				71	424
4.20				34	374
4.40					320
4.60					282
4.80					260
5.00					237
5.20					214
5.40					191
5.60					168
5.80					143
6.00					116

F15

Time Graphs of Temperature of Combustion Gases. Type F Enclosed Space. $\epsilon_{res} = 0.60$
 Opening Factor $A \cdot \sqrt{H}/A_t = 0.12 \text{ m}^{1/2}$

T	0.1	0.3	0.5	1.0	2.0
q	18.0	54.0	90.0	180.0	360.0
Time h	T e m p e r a t u r e				
0.05	613	613	613	613	613
0.10	931	931	931	818	818
0.15	599	933	933	868	867
0.20	468	936	936	940	940
0.25	339	943	943	937	937
0.30	192	870	945	942	941
0.35	177	795	947	946	946
0.40	166	703	948	948	947
0.45	157	596	949	949	949
0.50	148	544	873	950	950
0.60	130	432	752	952	952
0.65	121	371	680	953	952
0.70	112	306	601	953	953
0.80	95	274	547	954	954
0.90	76	244	491	892	955
1.00	52	214	432	845	956
1.10		184	370	793	956
1.20		152	305	735	957
1.30		118	282	672	957
1.40		82	261	604	961
1.50		35	239	568	959
1.60		28	217	534	959
1.70			195	499	926
1.80			173	462	912
1.90			149	424	899
2.00			124	385	885
2.20			70	303	850
2.40			28	280	814
2.60				256	774
2.80				232	732
3.00				207	686
3.20				183	643
3.40				158	598
3.60				130	550
3.80				102	500
4.00				71	448
4.20				30	392
4.40					335
4.60					293
4.80					270
5.00					246
5.20					221
5.40					197
5.60					173
5.80					146
6.00					118

G1

Time Graphs of Temperature of Combustion Gases. Type G Enclosed Space.

Opening Factor $A \cdot \sqrt{H}/A_t = 0.01 \text{ m}^{1/2}$

T	0.1	0.2	0.3	0.5	0.75	1.0	1.5	2.0
q	1.5	3.0	4.5	7.5	11.25	15.0	22.5	30.0
Time h	T e m p e r a t u r e							
0.05	287	287	287	287	287	287	287	287
0.10	473	471	471	471	362	361	361	361
0.15	290	478	478	478	440	440	440	440
0.20	253	456	494	494	498	498	498	498
0.25	199	390	500	500	495	495	495	495
0.30	139	324	467	505	501	501	501	501
0.35	135	305	423	510	507	507	507	507
0.40	128	278	380	514	513	513	513	513
0.45	122	247	350	517	517	517	517	517
0.50	117	217	320	480	521	521	521	521
0.60	108	197	278	422	548	547	547	547
0.65	102	187	254	401	573	573	573	573
0.70	97	178	231	375	553	583	583	583
0.80	88	160	210	355	533	606	606	606
0.90	79	141	191	331	494	584	620	620
1.00	69	121	174	305	448	562	631	631
1.10	59	100	157	276	411	543	649	649
1.20	55	80	140	244	393	527	674	674
1.30	52	79	123	229	376	503	674	692
1.40	49	75	104	215	357	471	673	706
1.50	46	72	86	201	334	453	668	715
1.60	44	69	84	189	309	433	658	726
1.70	42	66	80	176	283	413	645	710
1.80	41	63	78	163	271	392	628	716
1.90	39	60	75	150	260	370	610	711
2.00	38	57	71	136	250	348	590	706
2.20	36	52	65	108	231	302	551	638
2.40	34	48	60	90	213	278	513	648
2.60	32	45	55	86	196	256	472	635
2.80	31	43	52	80	179	237	427	613
3.00	30	40	48	73	162	218	378	587
3.20		38	46	68	144	200	338	560
3.40		37	43	63	125	182	315	530
3.60		35	41	59	107	164	295	499
3.80		34	40	56	93	146	278	466
4.00		33	38	53	89	127	261	431
4.20			37	50	84	107	245	395
4.40			35	48	79	100	229	357
4.60			34	46	74	94	214	324
4.80			33	44	70	90	199	300
5.00			32	43	66	84	184	279
5.20				41	63	79	170	258
5.40				40	60	75	155	238
5.60				39	57	71	139	218
5.80				38	54	67	123	198
6.00				37	52	64	107	179

G2

Time Graphs of Temperature of Combustion Gases. Type G Enclosed Space.

Opening Factor $A \cdot \sqrt{H}/A_t = 0.02 \text{ m}^{1/2}$

T	0.1	0.2	0.3	0.5	0.75	1.0	1.5	2.0			
q	3.0	6.0	9.0	15.0	22.5	30.0	45.0	60.0			
Time h	T	e	m	p	e	r	a	t	u	r	e
0.05	413	413	413	413	413	413	413	413			
0.10	675	676	676	676	676	558	559	559			
0.15	391	654	654	654	602	602	602	602			
0.20	335	606	663	663	674	674	674	674			
0.25	257	513	672	672	668	668	668	668			
0.30	173	417	623	680	677	677	677	677			
0.35	167	376	570	707	684	684	684	684			
0.40	157	344	536	736	730	730	730	730			
0.45	149	301	468	753	745	745	745	745			
0.50	141	258	440	717	766	766	766	766			
0.60	126	243	368	637	796	796	796	796			
0.65	119	228	327	580	808	808	808	808			
0.70	112	213	286	530	783	819	819	819			
0.80	100	187	260	493	747	849	849	849			
0.90	88	161	234	458	698	762	814	814			
1.00	75	134	210	418	631	738	845	845			
1.10	62	106	186	373	572	713	866	866			
1.20	58	76	162	325	538	670	877	877			
1.30	55	75	138	302	501	626	780	807			
1.40	51	70	111	281	464	580	787	834			
1.50	48	67	85	261	425	551	790	856			
1.60	46	62	80	241	386	521	772	876			
1.70	43	59	78	221	345	491	769	814			
1.80	41	55	75	201	326	461	751	853			
1.90	39	53	72	182	310	431	724	856			
2.00	38	50	68	162	295	399	695	847			
2.20	35	46	61	120	270	334	635	821			
2.40	33	42	55	92	245	303	575	790			
2.60	31	40	51	83	222	277	512	756			
2.80	29	37	47	78	199	253	443	719			
3.00	28	35	44	72	176	230	374	681			
3.20	27	34	41	67	153	207	322	645			
3.40	26	32	39	61	128	185	297	607			
3.60	26	31	37	57	103	163	277	569			
3.80		30	36	53	85	139	258	529			
4.00		29	34	50	80	114	241	488			
4.20		28	33	47	73	88	224	444			
4.40		28	32	45	68	81	208	400			
4.60		27	31	43	63	73	193	364			
4.80		27	30	41	59	67	177	342			
5.00		26	30	40	56	62	160	321			
5.20			29	38	53	59	143	301			
5.40			28	37	50	55	126	281			
5.60			28	36	48	52	107	261			
5.80			27	35	46	50	90	241			
6.00			27	34	44	48	73	220			

G3

Time Graphs of Temperature of Combustion Gases. Type G Enclosed Space.
 Opening Factor $A \cdot \sqrt{H}/A_t = 0.04 \text{ m}^{1/2}$

T	0.1	0.2	0.3	0.5	0.75	1.0	1.5	2.0			
q	6.0	12.0	18.0	30.0	45.0	60.0	90.0	120.0			
Time h	T	e	m	p	e	r	a	t	u	r	e
0.05	545	546	546	545	545	546	546	546			
0.10	842	842	842	842	695	695	695	695			
0.15	481	839	839	838	763	763	763	763			
0.20	403	774	852	851	854	854	854	854			
0.25	297	650	876	875	855	855	855	855			
0.30	184	547	838	902	893	891	891	891			
0.35	179	496	770	925	917	915	915	915			
0.40	170	436	693	945	938	938	938	938			
0.45	161	373	595	967	959	959	959	959			
0.50	152	307	548	902	975	975	975	975			
0.60	135	274	443	733	939	939	939	939			
0.65	127	258	387	678	965	965	965	965			
0.70	119	241	331	608	927	982	982	982			
0.80	103	208	297	558	774	912	912	912			
0.90	87	177	268	506	724	885	954	954			
1.00	71	143	238	449	645	858	991	991			
1.10	52	107	208	390	587	821	1013	1013			
1.20	49	69	179	329	546	770	981	981			
1.30	46	65	148	304	504	716	964	1002			
1.40	43	61	114	281	461	648	946	1009			
1.50	40	58	80	259	420	610	926	1011			
1.60	38	55	74	237	376	572	894	1014			
1.70	36	51	68	215	329	535	861	982			
1.80	34	48	67	193	313	496	826	965			
1.90	31	45	62	171	298	457	790	950			
2.00	29	43	59	148	285	417	751	934			
2.20		39	52	99	259	336	677	894			
2.40		36	47	71	233	303	606	852			
2.60		34	43	59	208	276	532	809			
2.80		32	40	52	184	250	455	762			
3.00		30	37	47	159	224	374	712			
3.20			35	43	131	199	320	666			
3.40			33	41	103	174	300	618			
3.60			32	38	75	147	282	569			
3.80			31	36	54	119	265	518			
4.00			30	35	47	92	248	466			
4.20				33	43	61	231	412			
4.40				32	41	53	214	357			
4.60				31	38	48	198	315			
4.80				31	37	45	182	291			
5.00				30	35	42	165	267			
5.20					34	40	147	244			
5.40					33	38	129	219			
5.60					32	37	110	196			
5.80					32	36	92	172			
6.00					31	35	71	147			

G4

Time Graphs of Temperature of Combustion Gases. Type G Enclosed Space.

Opening Factor $A\sqrt{H}/A_t = 0.06 \text{ m}^{1/2}$

T	0.1	0.2	0.3	0.5	0.75	1.0	1.5	2.0
q	9.0	18.0	27.0	45.0	67.5	90.0	135.0	180.0
Time h	T e m p e r a t u r e							
0.05	593	593	593	593	593	593	593	593
0.10	947	947	947	947	780	780	780	780
0.15	532	943	943	943	860	860	860	860
0.20	439	863	955	955	960	960	960	960
0.25	316	759	983	983	973	973	973	973
0.30	187	604	930	1007	998	998	998	998
0.35	184	540	855	1031	1023	1023	1023	1023
0.40	174	474	757	<u>1051</u>	1044	1044	1044	1044
0.45	165	402	645	<u>998</u>	<u>1059</u>	<u>1059</u>	<u>1059</u>	<u>1059</u>
0.50	156	325	588	937	<u>1008</u>	<u>1008</u>	<u>1008</u>	<u>1008</u>
0.60	138	286	472	818	<u>1057</u>	<u>1057</u>	<u>1057</u>	<u>1057</u>
0.65	129	267	411	746	<u>1001</u>	<u>1001</u>	<u>1001</u>	<u>1001</u>
0.70	121	249	347	664	936	1002	1002	1002
0.80	104	213	309	599	885	1045	1045	1045
0.90	86	179	274	535	816	<u>997</u>	<u>1080</u>	<u>1080</u>
1.00	68	143	242	472	714	<u>903</u>	<u>1047</u>	<u>1047</u>
1.10	46	104	208	408	637	861	1074	1074
1.20	43	61	176	341	592	800	<u>1076</u>	<u>1076</u>
1.30	40	58	143	313	544	729		
1.40	37	52	106	288	494	651		
1.50	35	48	68	264	444	611		
1.60	33	45	64	240	391	570		
1.70	31	42	58	217	338	531		
1.80	30	39	57	193	320	491		
1.90	29	37	53	170	304	451		
2.00	28	36	50	145	290	410		
2.20		33	44	92	263	326		
2.40		31	40	62	236	298		
2.60		29	37	51	209	273		
2.80		28	34	45	184	247		
3.00		27	32	41	158	222		
3.20			31	37	129	197		
3.40			29	35	99	173		
3.60			28	33	68	146		
3.80			27	32	46	118		
4.00			26	30	40	89		
4.20				29	37	59		
4.40				29	35	53		
4.60				28	33	51		
4.80				27	32	49		
5.00				27	31	48		
5.20					30	47		
5.40					29	46		
5.60					29	45		
5.80					28	44		
6.00					28	43		

G5

Time Graphs of Temperature of Combustion Gases. Type G Enclosed Space.

Opening Factor $A \cdot \sqrt{H}/A_t = 0.08 \text{ m}^{1/2}$

T	0.1	0.2	0.3	0.5	0.75	1.0	1.5	2.0
q	12.0	24.0	36.0	60.0	90.0	120.0	180.0	240.0
Time h	T e m p e r a t u r e							
0.05	643	640	640	640	641	640	640	640
0.10	1015	1015	1015	1015	840	842	842	842
0.15	574	1009	1009	1009	916	918	918	918
0.20	460	939	1024	1024	1024	1027	1027	1027
0.25	327	802	1049	1049	1036	1038	1038	1038
0.30	188	634	985	1071	1060	1062	1062	1062
0.35	186	566	900	<u>1094</u>	<u>1088</u>	<u>1090</u>	<u>1090</u>	<u>1090</u>
0.40	176	491	797	<u>1047</u>	<u>1044</u>	<u>1046</u>	<u>1046</u>	<u>1046</u>
0.45	167	413	673	1074	1065	1067	1067	1067
0.50	157	330	610	<u>998</u>	<u>1090</u>	<u>1092</u>	<u>1092</u>	<u>1092</u>
0.60	139	290	484	797	1056	1058	<u>1058</u>	<u>1058</u>
0.65	130	271	418	710	1065	1067	1067	1067
0.70	121	252	350	638	1015	<u>1087</u>	<u>1087</u>	<u>1087</u>
0.80	103	215	311	585	945	<u>1069</u>	<u>1069</u>	<u>1069</u>
0.90	85	180	275	527	<u>852</u>	1010	1097	1097
1.00	66	142	241	464	<u>720</u>	961	<u>1117</u>	<u>1117</u>
1.10	41	101	207	397	650	898		
1.20	38	55	173	328	608	828		
1.30	36	49	139	303	559	752		
1.40	34	48	100	280	508	670		
1.50	32	43	60	257	456	627		
1.60		40	56	234	402	584		
1.70		38	51	210	348	543		
1.80		36	50	188	333	501		
1.90		34	46	164	318	459		
2.00		33	43	139	305	416		
2.20			39	84	279	328		
2.40			36	47	254	300		
2.60			33	40	228	274		
2.80			31	35	202	249		
3.00			29	33	176	222		
3.20					149	197		
3.40					120	171		
3.60					91	144		
3.80					74	115		
4.00					72	85		
4.20					70	51		
4.40					69	46		
4.60					69	44		
4.80					68	42		
5.00					67	41		
5.20					67	40		
5.40					66	40		
5.60					66	39		
5.80					65	38		
6.00					65	38		

G6

Time Graphs of Temperature of Combustion Gases. Type G Enclosed Space.

Opening Factor $A \cdot \sqrt{H}/A_t = 0.12 \text{ m}^{1/2}$

T	0.1	0.2	0.3	0.5	0.75	1.0	1.5	2.0			
q	18.0	35.0	54.0	90.0	135.0	180.0	270.0	360.0			
Time h	T	e	m	p	e	r	a	t	u	r	e
0.05	726	723	723	723	726	723	723	723			
0.10	1099	1099	1099	1099	907	907	907	907			
0.15	615	1091	1091	1091	988	988	988	988			
0.20	486	1009	1104	1104	1105	1104	1104	1104			
0.25	340	853	1125	1125	1117	1117	1117	1117			
0.30	188	669	<u>1048</u>	<u>1144</u>	<u>1136</u>	<u>1136</u>	<u>1136</u>	<u>1136</u>			
0.35	187	593	<u>900</u>	<u>1118</u>	<u>1157</u>	<u>1157</u>	<u>1157</u>	<u>1157</u>			
0.40	177	508	796	1134	<u>1120</u>	<u>1120</u>	<u>1120</u>	<u>1120</u>			
0.45	168	422	670	1153	1141	1141	1141	1141			
0.50	159	332	610	<u>1052</u>	<u>1158</u>	<u>1158</u>	<u>1158</u>	<u>1158</u>			
0.60	140	293	477	<u>856</u>	<u>1131</u>	<u>1131</u>	<u>1131</u>	<u>1131</u>			
0.65	131	274	407	772	1147	1147	1147	1147			
0.70	121	255	336	674	<u>1085</u>	<u>1163</u>	<u>1163</u>	<u>1163</u>			
0.80	103	216	301	614	<u>960</u>	<u>1148</u>	<u>1148</u>	<u>1148</u>			
0.90	84	180	267	547	869	<u>1071</u>	<u>1169</u>	<u>1169</u>			
1.00	63	140	233	477	753						
1.10	35	97	200	405	662						
1.20	33	47	167	333	606						
1.30	31	41	130	308	552						
1.40	29	40	92	284	497						
1.50	28	37	46	260	442						
1.60	27	35	44	236	386						
1.70	26	33	40	211	329						
1.80		31	37	187	315						
1.90		30	35	163	301						
2.00		29	33	136	288						
2.20		27	30	79	262						
2.40		25	28	39	235						
2.60			26	34	208						
2.80				31	183						
3.00				28	155						
3.20					126						
3.40					95						
3.60					64						
3.80					38						
4.00					36						
4.20					35						
4.40					34						
4.60					33						
4.80					33						
5.00					32						
5.20					32						
5.40					31						
5.60					31						
5.80					31						
6.00					30						

.....